REGIONAL FREQUENCY ANALYSIS OF SEASONAL RAINFALL AND SNOWFALL FOR THE SOUTHERN INTERIOR OF BRITISH COLUMBIA

by

CLAUDETTE ANNE MARTIN

B.Sc. McGill University, 1992

A THESIS SUBMITTED IN PARTIAL FULFILLMENT OF THE REQUIREMENTS FOR

THE DEGREE OF

MASTER OF SCIENCE IN ENVIRONMENTAL SCIENCES

in the Department of Geography and Environmental Studies

Thesis examining committee:

Darryl Carlyle-Moses (PhD), Associate Professor and Thesis Supervisor, Department of Geography and Environmental Studies

Karl Larsen (PhD), Professor, Department of Natural Resource Sciences

Shane Rollans (PhD), Senior Lecturer, Department of Mathematics and Statistics

Rita Winkler (PhD), Adjunct Faculty Member, Department of Natural Resources Sciences and Research Hydrologist, BC Ministry of Forests and Range

Jonathan Hosking (PhD), External Examiner, Research Staff Member, Statistical Analysis and Forecasting IBM T. J. Watson Research Center, Yorktown Heights, New York, USA

January 2015

Thompson Rivers University

ACKNOWLEDGEMENTS

I would like to thank my supervisor, Dr. Darryl Carlyle-Moses, for his unending patience and support in the completion of this thesis. Thanks to my committee members who helped shape my final report: Drs. Rita Winkler and Karl Larsen. A big thank you to my committee member, Dr. Shane Rollans, who not only answered many, many statistical questions but helped me realize the moment when my analysis was complete. A special thanks to my external advisor, Dr. J.R.M. Hosking who inspired my research and gave me the opportunity to learn from the very best in my field of study.

Thanks to Dr Mari Jones, Christopher Trefry, Caroline Barnes and Giselle Bramwell for answering numerous technical questions. Thanks also to the faculty at Thompson Rivers University who were very supportive during my research project. I would like to thank Andrea Johnstone, Linda Rinaldi and Maggie Hermiston for listening to me chatter nonstop about statistics and for picking up the slack in my life when I got bogged down. Finally a special thank you to Dean, Lance, Megan, Kyla and my parents for encouraging me to go to graduate school and then supporting me non-stop throughout my journey.

This project would not have been possible without the funding support provided by the Discovery Grant awarded to Dr. Darryl Carlyle-Moses.

Thesis Supervisor: Associate Professor Darryl Carlyle-Moses

ABSTRACT

Extreme precipitation events are rare in nature, but they can have a strong impact on society. Canada's adaptation policies for these extreme events require the availability of precise, up-to-date quantile estimates that relate event magnitudes to probabilities of occurrence. This study developed seasonal maximum daily rainfall and snowfall quantile estimates for the southern interior of British Columbia. This area has complex precipitation patterns and proved to be an excellent site for studying extreme rainfall and snowfall. Instead of the more traditional at-site analysis using method of moment estimators, a regional frequency analysis approach based on L-moments was used. Seasonal rainfall and snowfall data were selected to provide a finer delineation of events and examine the variation in extreme precipitation type during the year. A serial dependence analysis done as part of the regional frequency analysis screening process concluded that overall there appeared to be no change in the frequency of seasonal extreme rainfall or snowfall events for the study area. Homogeneous regions were successfully developed using a cluster analysis and extensive manual refinement. These regions were overall geographically cohesive and reflected the local valley systems. A few regions with high elevation stations were geographically dispersive possibly due to the influence of the freezing level on precipitation type. Regional quantiles estimates with associated root mean square errors and 90% error bounds were developed for fall, spring and summer rainfall data and winter snowfall data. A comparison of select regional and at-site estimations showed quantiles for both methods were comparable, but almost all regional estimations had significantly lower root mean square errors by a factor of 1.5 to 5.0 when compared to at-site estimations. This comparison demonstrates that a regional frequency analysis develops quantile estimates more precise than at-site estimates for the southern interior of British Columbia.

Key words: rainfall, snowfall, extreme precipitation, regional frequency analysis, L-moments, index-flood, serial dependence, quantiles

TABLE OF CONTENTS

LIST OF FIGURES

LIST OF TABLES

LIST OF SYMBOLS

B_r — Bias of the rth regional average L-moment ratio

D_i — Discordancy measure for site i in a region

$E(.)$ — Expectation of a random variable

F — Nonexceedance probability

$F(.)$ — Cumulative distribution function

$G(.)$ — Cumulative distribution function

H — Heterogeneity measure for regional data

M — Probability weighted moment

N — Number of sites

n — Record length at a site

p — Probability that data amount is zero

$Q_i(.)$ — Quantile function for site i in a region

$q(.)$ — Regional growth curve

R — Regional value

$RMSE(.)$ — Root mean square error of an estimator

T — Return period

T — Transposition of a matrix

t — L-CV of a data sample

t_r — r^{th} L-moment ratio of a data sample

$x(.)$ — Quantile function

Z^{DIST} — Goodness-of-fit measure for regional data

α_r — r^{th} probability weighted moment of a frequency distribution

β_r — r^{th} probability weighted moment of a frequency distribution

λ_r — r^{th} L-moment of a frequency distribution

μ — Mean of a frequency distribution

$\bar{\rho}$ — Average Spearman rank correlation

σ — Standard deviation of a frequency distribution

τ — L-CV of a frequency distribution

τ_r — r^{th} L-moment ratio of a frequency distribution

LIST OF ABBREVIATIONS

EVT   : Extreme Value Theory

FDR   : False Discovery Rate

PWM   : Probability Weighted Moment

POT   : Peak-Over-Threshold

MK   : Mann-Kendall

ML   : Maximum Likelihood

MSC   : Meteorological Service of Canada

RFA   : Regional Frequency Analysis

CHAPTER 1 – INTRODUCTION

On June 23, 2014 a line of significant convective cells – with intensities up to 150 mm/hour – dropped approximately 25 mm of rain in 20 minutes onto the city of Kamloops, British Columbia. This heavy rainfall event had a magnitude approximately equivalent to 66% of the average total June rainfall for Kamloops. Much of the Kamloops' storm sewer system was overwhelmed resulting in a torrent of water and debris flooding parts of the city. Fire and rescue services were called out to assist people caught in flooded vehicles and significant soil erosion occurred around affected creeks running through Kamloops. Even though this event was short in duration, it illustrates how heavy precipitation events can have a strong impact on communities. Extreme rainfall and snowfall events can affect vulnerable infrastructure such as road systems and power grids that may be located in risk-prone areas, and lead to flooding, soil erosion, landslides and power outages (IPCC, 2007; Henstra and McBean, 2009). Extreme rainfall events have even been linked with waterborne disease outbreaks such as the Walkerton outbreak of waterborne gastroenteritis in May, 2000 (Auld, 2004). The risk of these heavy precipitation events affecting communities are increasing as populations and assets continue to be located in low-lying areas, slopes and other risk-prone regions (IPCC, 2007, City of Toronto Climate Adaptation Steering Group, 2008). Geo-technical and civil engineers, urban planners and governmental emergency response agencies need to have access to precise, up-to-date forecasts of heavy precipitation events' magnitudes and occurrences to support communities' adaptive capacity to extreme weather.

STATISTICAL ANALYSIS THEORY

Extreme value theory

Extreme events by definition are rare and very difficult to forecast based on deterministic methods – that past extreme events can be used to predict precisely even rarer extreme events in the future (WMO, 2009). To estimate the magnitude and occurrence of extreme events that may not yet have been experienced, a model is required that can describe

the probability of events that are more extreme than any that have been observed. For example, suppose a culvert must be designed to hold the maximum capacity of a 100 year return period one day rainfall event. Local rainfall data might be available from the area where the culvert will be installed but for a much shorter period such as 20 years. Extreme value theory (EVT) can be used to estimate the magnitude of a long return period event from a shorter period data set by allowing the stochastic behaviour of a process to be quantitatively described at unusually large or small magnitudes based on historical data (Coles, 2001).

EVT has been used in the applied sciences since the 1940s mostly in areas such as engineering where extreme values can affect the failure of a given system (Castillo, 1988). An early example of EVT application was the estimation of very high wind magnitudes needed to design bridges and buildings able to withstand the extreme forces associated with these rarely experienced winds (Cole, 2001). EVT also became popular in the field of hydrology for forecasting the probability of flood events (Jarvis, 1936; Gumbel, 1941). Over the last 65 years, EVT has been increasingly used in other fields where risk assessment is required. Insurance and financial institutions use EVT as a risk management tool to predict the occurrence of catastrophic losses such as credit default and stock market crashes (Embrechts *et al*., 1999). An important foundation in earthquake prediction is EVT – particularly for estimating the magnitude of long return period earthquakes (Al-Abbasi and Fahmi, 1985). Projection of extreme ocean wave heights derived using EVT are crucial in designing offshore oil platforms and managing coastlines hazards such as floods and wave erosion, and EVT is even being utilized in determining exposure to food chemicals (Cole, 2001; Tressou *et al*., 2004). In climate prediction, EVT is used to forecast the probability of extreme weather events such as heavy rainfall and snowfall, heat waves and droughts. Locations with short weather records which are common in places like Canada benefit from EVT's ability to generate long return period quantiles from short period data sets.

Regional frequency analysis

Frequency analysis is defined as the process of estimating how often a specified event will occur in a particular area (Dalrymple, 1960). Early frequency analysis of extreme precipitation was done from single-site data (Jarvis, 1936). This type of frequency analysis –

known as an at-site frequency analysis – can be used to estimate extreme events for a particular location as long as sufficient data are available (Stedinger *et al*., 1992; Reed *et al*., 1999). Unfortunately, in many parts of the world including Canada, data sets long enough to generate reliable estimations of extreme events with return periods (T) of 50 or 100 years are scarce (Adamowski *et al*., 1996; Klein Tank *et al*., 2009). Another disadvantage for an at-site frequency analysis is being unable to provide quantiles for sites with limited precipitation records.

But if different sites have similar event frequencies for different observed quantities, a pooled frequency analysis can be done instead of an at-site analysis. A regional frequency analysis (RFA) trades space for time; it combines together data from sites with similar event frequencies into homogeneous regions. This increases the effective length of the data set which in turn increases the precision of the estimated quantiles (Cunnane, 1988; Stedinger *et al*., 1992; Hosking and Wallis, 2005). A RFA also allows quantiles to be developed for sites with limited precipitation records.

A set of site variables define the homogeneous regions developed by a RFA. These site characteristics should be physically related to the event frequency distribution but not be the summary statistics that statistically describe the data set. These summary statistics are used instead to test the homogeneity of the regions. A literature review determined that there appeared to be no standard set of site characteristics used in RFA. Site characteristics can be anything that helps define a region's precipitation climate but some of the common characteristics are latitude, longitude, elevation and mean annual precipitation (Hosking and Wallis, 2005).

The index-flood procedure is a convenient method in a RFA to pool summary statistics from different data samples. This procedure assumes homogeneous regions contain sites that have identical frequency distributions apart from a site-specific scaling factor called the index-flood (Stewart *et al*., 1999). The index-flood is a location estimator that is used as an inter-site comparison for a region. It should be a relatively common at-site extreme event magnitude that can be reliably estimated from the data record (Dalrymple, 1960; Stewart *et al*., 1999). The index flood most often used is the sample mean of the site data, but can also be the sample median (Stewart *et al*., 1999; Fowler and Kilsby, 2003).

A regional growth curve is calculated for each region. This curve represents a set of dimensionless factors that specify the magnitude of a rare extreme event relative to the size of a common extreme event (the index-flood). It is also called the quantile function of the regional frequency distribution (Stewart *et al.*, 1999; Hosking and Wallis, 2005). The regional growth curve is described by parameters that are estimated separately at each site and then combined through a weighted average based on each site's record length. The quantile estimates at each site in a region are then obtained by combining the estimates of the index flood with the regional growth curve for that particular region (Stewart *et al.*, 1999).

For a frequency analysis of any type to be theoretically valid, data sets must meet certain statistical criteria such as independence, randomness and stationarity (WMO, 2009). Some of these assumptions are plausible for many types of environmental data while others are unlikely to be satisfied in practice. The index-flood procedure makes five assumptions (Hosking and Wallis, 2005). The first two assumptions are that observations at any given site must be serially independent and identically distributed. These two basic assumptions are quite plausible for extremes since it is assumed that events observed in the past are typical of what will occur in the future for a data set (Dalrymple, 1960). Where these two assumptions may become undermined is when obvious serial dependence is present. While serial dependence can cause a small amount of bias, Hosking and Wallis (2005) have concluded that for a RFA small quantities of serial dependence in annual data series have little effect on the quantile estimates' quality.

The third assumption in the index-flood procedure is that observations at different sites must be independent (e.g. not affected by the same precipitation event). Unfortunately this assumption is unlikely to be satisfied in practice as meteorological events such as frontal precipitation can affect large areas containing more than one site and therefore event magnitudes at neighbouring sites can be correlated (Hosking and Wallis, 2005). However it has been shown that even when inter-site (spatial) dependence is present, RFA is more accurate than at-site analysis (Hosking and Wallis, 1988). The fourth assumption for the index-flood procedure is that different site frequency distributions are identical except for a scale factor (the index-flood); this allows the data from different sites in a homogeneous region to be pooled together into one data set. The fifth assumption is that the regional

growth curve mathematical form is correctly specified. In practice the last two assumptions are never completely valid, but careful selection of regions and frequency distribution allow them to be approximated (Hosking and Wallis, 2005).

Canada's meteorological monitoring network has many surface observing stations with short weather records (Adamowski *et al.*, 1996). These stations can benefit from a RFA as opposed to an at-site analysis. An example is Douglas Lake in British Columbia with a spring maximum daily rainfall data set length of 17 years. When this station's data set is pooled with other spring maximum daily rainfall data sets from weather stations that have similar event frequencies, the effective length of Douglas Lake's data set increases to 439 years; this in turn may increase the precision of the site's estimated quantiles particularly for long return periods.

L-moments

Traditionally, the shape of a probability distribution has been described by the distribution's classic moments (parameters) such as the mean, variance, and coefficient of skewness (Helsel and Hirsch, 1992; Wilks, 2011). The estimates of these moments are considered neither robust nor resilient due to the possibility of the higher estimated moments (e.g. the sample coefficient of skewness) becoming severely biased and unreliable (Wallis *et al*., 1974; Wilks, 2011).

As Cunnane (1988) notes, probability weighted moment (PWM) estimators are preferred over classic moment estimators (also referred to as the method of moments) for a RFA. Greenwood *et al*. (1979) define PWMs to be the quantities:

$$M_{i,j,k} = E\left[X^i F^j \{1 - F\}^k\right] \qquad (1.1)$$

where $E(.)$ is the expectation of a random variable, $F(.)$ is the cumulative distribution function, and i, j and k are real numbers. Since PWMs involve raising values of the function to powers, they are much less susceptible to sample outlier value influences (Dingman, 2002). They also compare favourably to the maximum likelihood (ML) estimation (Landwehr *et al*., 1979; Hosking *et al*., 1985, Dingman, 2002). Considered a general and

flexible method, maximum likelihood estimation selects estimators that maximize the probability of obtaining the observed data under the resulting distribution (Coles, 2001). This method can be problematic for small sample sizes (Madsen *et al.*, 1997; Martins and Stedinger, 2001). A study by Coles and Dixon (1999) demonstrated that if a constraint of a bounded mean is imposed on ML estimators, its performance is comparable and possibly even superior to PWM for small samples. Unfortunately, it is questionable whether it is appropriate to impose a constraint such as a bounded mean for hydrological applications (Katz *et al.*, 2002).

L-moments were developed by Hosking (1990) as an alternative method of estimating a distribution's parameters. They are modifications of the PWMs of Greenwood *et al.* (1979) that are derived by linearly combining the PWMs - hence the "L" in L-moments. In terms of probability weighted moments, L-moments are given in general by:

$$\lambda_{r+1} = (-1)^r \sum_{k=0}^{r} P_{r,k}^* \alpha_k = \sum_{k=0}^{r} P_{r,k}^* \beta_k \tag{1.2}$$

where $\alpha_k = M_{1,0,r}$, $\beta_k = M_{1,r,0}$ and $P_{r,k}^*$ is a set of orthogonal polynomials described by:

$$P_{r,k}^* = (-1)^{r-k} \binom{r}{k} \binom{r+k}{k} = \frac{(-1)^{r-k}(r+k)!}{(k!)^2(r-k)!} \tag{1.3}$$

where $P_{r,k}^*$ is the rth shifted Legendre polynomial (Hosking, 1990).

λ_1 and λ_2 are the L-location (mean) and L-scale respectively of the distribution. Higher-order L-moments are represented for convenience by dimensionless versions called L-moment ratios. These ratios are defined by:

$$\tau_r = \lambda_r / \lambda_2, \qquad r = 3, 4, \dots \tag{1.4}$$

where τ_3 is the L-skewness and τ_4 is the L-kurtosis.

Finally, the dimensionless ratio called the coefficient of L-variation, L-CV is defined as:

$$\tau = \lambda_2/\lambda_1 \qquad (1.5)$$

(Hosking, 1990)

L-moments are much less susceptible to sample outlier value influences and do not have sample-size related bounds. They are also considered easier to compute than ML estimates and more reliable and less biased particularly for small samples (Hosking 1990; Vogel and Fennessey, 1993; Ngongondo *et al*., 2011). Hosking and Wallis (2005) recommend L-moment statistics as a method for fitting a regional frequency distribution.

SEASAONAL MAXIMUM VERSUS PEAK-OVER-THRESHOLD

Most precipitation RFA methods are based on block (e.g. annual or seasonal) maxima (Cunnane, 1988); however, this is in direct contradiction with theoretical guidance that recommends extracting extreme data in a peak-over-threshold (POT) format (Reed et *al*., 1999; Fowler and Kilsby, 2003). An extreme analysis should contain all significant events for the record period. A POT series accomplishes this by setting a threshold that allows the inclusion of all large events and excludes block maxima that can be small and thus misleading (Lang *et al*., 1999; Fowler and Kilsby, 2003). A POT series also has the advantage of producing a larger sample size that is more comprehensive compared to a block maxima series (Fitzgerald, 1989; Reed *et al*., 1999). Unfortunately, the difficulty in extracting POT events can outweigh the theoretical benefits. There is no clear protocol for setting a threshold level and deciding which peaks to exclude from the same rainfall event (Lang *et al*., 1999). POT is also much more demanding when dealing with missing data compared to the block maxima method (Reed *et al*., 1999; Fowler and Kilsby, 2003). It is for these reasons that a block maxima approach was adopted for this study.

METEOROLOGICAL CHARACTERISTICS OF THE STUDY AREA

General weather patterns of British Columbia

The mean upper flow circulation over British Columbia is the result of two semi-permanent synoptic features called the Pacific High and the Aleutian Low. The Pacific High extends from the Pacific Coast of the United States down to just east of Hawaii while the Aleutian Low dominates the Gulf of Alaska and the Aleutian Islands. In the summer, the Pacific High strengthens, shifts north and causes a more northwesterly upper flow. The Aleutian Low is strongest in the winter when it resides in the Gulf of Alaska and causes the upper flow to become more southwesterly. Intertwined with these two synoptic features are upper troughs of low pressure and upper ridges of high pressure that move along with the upper flow and alter the normal mean circulation pattern (Klock and Mullock, 2001).

Upper troughs induce vertical lift that can cause cloud formation and precipitation if sufficient moisture is present. These troughs are strongest in the winter and during that season can create widespread clouds and precipitation that can become further enhanced by orographic lift. During summer months, upper troughs are weaker with their cloud shields narrower and the precipitation more convective. Upper troughs can intensify any pre-existing instability in the atmosphere. If an upper trough moves through an area where the atmosphere is already destabilizing due to strong daytime heating (e.g. Kamloops during a hot summer day) severe thunderstorms can occur. An upper trough passing through a region where strong baroclinicity (temperature gradients) exist can also lead to the development of a low pressure system or frontal wave.

Upper ridges on the other hand produce areas of sinking air in the atmosphere. This sinking area does not usually produce clouds, thus upper ridges are associated with clear skies and no precipitation. In the summer and winter a large north-to-south upper ridge can sit over British Columbia for many days in a row (Klock and Mullock, 2001).

During the winter, low pressure systems can develop in the Gulf of Alaska or just off the British Columbia coastline. These systems weaken as they pass over the Coast Mountains but can still provide steady or intermittent rain or snow for the interior of British Columbia depending on the freezing level. High pressure systems sitting over British Columbia in the

winter can cause a strong low level inversion to form due to cold air pooling in the valleys. This inversion traps moisture from local sources that combined with the low level stability resists any precipitation development.

Cold lows largely influence the weather in early summer for British Columbia. Cold lows are areas of the atmosphere where temperatures get colder toward the center of the low, both at the surface and aloft. They form when cold pools of air break away from the Aleutian Low and take residence off the British Columbia or Washington coast. Cold lows produce wide-spread clouds and precipitation. A cold low sitting off the coast will generate a series of upper cold fronts that rotate counter clockwise across southern British Columbia. The cool unstable air associated with these fronts produce bands of clouds, showers and even thunderstorms if there is enhanced vertical lift (Klock and Mullock, 2001; Pike *et al.*, 2010).

The remainder of summer is dominated by the Pacific High and strong upper ridges. Hot and dry weather with occasional late afternoon convective development is common during this time of the year. Many weeks can pass between significant weather during the months of August and September. When the high or upper ridge does break down, cool and moist air moves in and more significant convective activity can result.

Precipitation patterns of the Thompson and Okanagan regions

British Columbia is considered to have the most difficult weather to forecast in Canada due the interaction of migratory weather systems from the Pacific Ocean with the topography of British Columbia's land surface. Large north-to-south running mountain ranges modify these weather systems as they pass over the province and produce distinctive precipitation patterns that vary with elevation, distance from the coast, season, location and exposure to the prevailing upper flow (Pike *et al.*, 2010). The southern interior of British Columbia is of particular interest when it comes to examining the occurrence and magnitude of extreme rainfall and snowfall. This area consists of the Thompson and Okanagan regions located between two major north-to-south running mountain ranges – the Coast Mountains to the west and the Monashees to the east. The Coast Mountains separate the Pacific coast from the interior of British Columbia and impact significantly on the province's precipitation patterns. A prevailing mean westerly upper flow experiences orographic uplift on the western side of the Coast Mountains. Warm, moist air approaching the coast is lifted rapidly by these

windward slopes resulting in widespread precipitation for the coastal area. On the leeside of the Coast Mountains, air subsides and warms. This sinking air – much drier since a large portion of its moisture was removed during the uplift process – results in a rain shadow effect for the Thompson and Okanagan regions. As the drier air continues to travel eastward it releases further moisture ascending the Monashees. Overall, the Thompson and Okanagan regions have much lower mean annual precipitation compared to coastal locations on the windward side of the Coast Mountains. Tucked up against the lee side of the Coast Mountains, locations such as Ashcroft and Cache Creek have even lower mean annual precipitation when compared to the eastern portion of the Thompson and Okanagan regions.

Summer temperatures in the valleys of the southern interior of British Columbia are generally high; when combined with passing upper troughs or cold fronts, these temperatures can trigger significant convective activity. What is interesting is that due to the orientation of local mountain ranges and deep valleys, this convective precipitation can be quite localized depending on the direction of upper flow and proximity to orographic lift and local bodies of water. For example, in Kamloops it is possible to see severe convective cells move easterly from Kamloops Lake along the north side of the South Thompson Valley leaving the south side of the valley without any significant precipitation. Another example of localized effect is when the Shuswap Lakes area has significant convective buildup while Kamloops (approximately 80 km away) may only experience fair weather cumulus even when both locations are under the same high pressure ridge.

Elevation plays a strong role in the type of precipitation experienced by locations in the Thompson and Okanagan regions – particularly in the spring, fall and winter seasons. The Monashees help moderate the winter climate for the Thompson and Okanagan regions by restricting the western movement of cold arctic air but occasionally an arctic outbreak does occur. When the cold arctic air mass starts to break down and allow weather systems from the Pacific to invade, snow changing to rain can occur. Whether this precipitation occurs as snow, rain or mixed depends on elevation and location, and can vary widely throughout the regions.

It is this complex interaction between synoptic weather features and the topography of the southern interior of British Columbia that make it an ideal study site for examining

extreme rainfall and snowfall events. The Thompson and Okanagan regions also have the advantage of containing a large number of weather stations that are part of the Environment Canada's surface weather station network.

DATA SOURCE – METEOROLOGICAL SERVICE OF CANADA (MSC) SURFACE WEATHER NETWORK

For my study, I used only weather stations that were part of Environment Canada's MSC surface weather station network. Historically this network consisted only of stations where manned surface weather observations were conducted. With the introduction of automated weather observing stations, the network is currently a mix of weather stations that report both human and automated observations. There are approximately 1300 stations in the network across Canada either owned by Environment Canada or other agencies such as NAV Canada and National Defense. A portion of the stations are operated by volunteers. There are many benefits to using MSCs surface weather station network as opposed to provincial or private weather observing networks. MSC's network is part of the World Meteorological Organization climate data and monitoring program. As a result, MSC's weather stations follow strict international standards on observing procedures and protocols. All MSC trained weather observers are certified in providing accurate, timely weather observations and adhering to proper coding and dissemination of meteorological conditions. Automatic weather observing stations are maintained on a regular basis to a high standard. All reported meteorological data are quality controlled at the source and again before becoming part of the National Digital Archive.

Within MSC's weather network, precipitation is measured with a variety of equipment that has changed over time. The official rain gauge currently used at manned weather stations is the Type-B rain gauge which replaced the MSC rain gauge in the 1970s. The MSC rain gauge had been used since about the 1920s; there appears to be no records of what type of rainfall measuring equipment had been used before that time. The Type-B rain gauge is cylindrical in shape with a funnel at the top that channels rainfall inside into a

graduated cylinder that can measure a maximum amount of 25 mm. If more than that amount of rain falls between observations, the overflow is caught in the white outside container.

For manned weather observations, snowfall is measured with an official Environment Canada snow ruler. Prior to 1978, this ruler was 36 inches long with graduations every 0.2 inches (Metcalfe *et al.*, 1994). The current ruler is one meter long and graduated every 0.2 cm. The Nipher shielded snow gauge was introduced in the 1960s to manned weather stations and is a non-recording gauge with an outside shield that looks like an upside-down bell. This shield reduces air flow over the top of the gauge that might otherwise affect the amount of snow captured. Inside the snow gauge is a copper cylinder that is taken inside by the weather observer and the contents melted to determine the water equivalent of the snow. If snowfall occurs without rain and partially or completely melts, the water equivalent obtained from the Nipher gauge is multiplied by 10 and converted to centimeters to obtain an estimated value for the snowfall.

Information on the types of precipitation measuring equipment for automated stations is scarce. The two main types of precipitation gauges used on Environment Canada's automatic weather stations are the Fischer and Porter weighing gauge and the Geonor (Environment Canada, 2013). Each gauge measures the amount of both rainfall and snowfall in mm. Metal pickets around the gauge disrupt the wind flow and help catch precipitation through an opening on top of the cover. The precipitation is then directed into a bucket inside the gauge that sits on a weighing mechanism and measures how much precipitation has fallen.

THESIS GOALS AND STRUCTURE

This thesis is presented in three main chapters. In the current chapter, I have presented the theoretical background on the analysis used in this thesis. My study site's general and local weather patterns with reference to British Columbia topography have been described. I have also explained the rationale for using Environment Canada's MSC surface weather observing network instead of provincial or private weather observing networks, and examined the types and changes to precipitation measuring equipment used for observations.

In Chapter 2, I report on the results of my study – a RFA based on historical seasonal maximum daily rainfall and snowfall for surface weather stations in the Thompson and Okanagan regions of British Columbia. The initial motivation for this study was the need identified by different agencies and governments across Canada to update Canadian extreme precipitation probability distributions (City of Toronto Climate Adaptation Steering Group, 2008; Redding, 2008). While an extreme precipitation probability distribution has commonly been derived from at-site frequency analysis, recent papers from counties like Great Britain, China and United States of America on extreme precipitation events have used regional frequency analysis instead (e.g. Fowler and Kilsby, 2003; Trefry *et al*., 2005; Yang *et al*., 2010). A review of regional frequency analysis papers showed few studies that have examined extreme precipitation events in British Columbia using RFA (Wallis *et al*., 2007). A recent study by Carlyle-Moses (2007) analyzed depth-duration-frequencies for daily maximum rainfall in the southern interior of British Columbia, but this was an at-site analysis involving annual daily maximum rainfall. Due to the abundance of weather stations in the Thompson and Okanagan regions with short precipitation records, using a RFA instead of the more common at-site analysis was deemed a better choice for a frequency analysis.

A review of the literature indicated no RFA studies in British Columbia that used seasonal rainfall and snowfall maxima instead of annual maxima. Seasonal snowfall and rainfall data are desirable for constructing quantiles and return periods for extreme precipitation; it provides a finer scale that allows for a more meaningful interpretation of the occurrence and magnitude of extreme events. For example, extreme rainfall or snowfall events can be experienced in the winter season for the southern interior of British Columbia depending on location and elevation.

There were three objectives for my study:

- Develop acceptably homogeneous regions within the Thompson and Okanagan regions for seasonal extreme rainfall and snowfall events;
- Develop regional quantile functions for each seasonal rainfall and snowfall region;
- Compare regional versus at-site estimation for site quantiles of select stations within the study area.

Chapter 3 presents a more focussed discussion of my research within the larger context of extreme weather adaptation planning. A summary of research findings from Chapter 2 is given with an emphasis on key results. Next, the limitations of the methodology are examined, in particular implications resulting from the lack of available metadata. Finally, I discuss how seasonal regional quantiles can be used to increase the adaptive capacity of communities to extreme precipitation events.

LITERATURE CITED

Adamowski, K., Y. Alila, and P.J. Pilon. 1996. Regional rainfall distribution for Canada. *Atmospheric Research* 42 (1): 75-88.

Al-Abbasi, J. N., and K.J. Fahmi. 1985. Estimating maximum magnitude earthquakes in Iraq using extreme value statistics. *Geophysical Journal International* 82 (3): 535- 548.

Auld, H., D. MacIver, and J. Klaassen. 2004. Heavy rainfall and waterborne disease outbreaks: the Walkerton example. *Journal of Toxicology and Environmental Health, Part A* 67 (20-22): 1879-1887.

Carlyle-Moses, D., 2007. Maximum Daily Rainfall Depth Frequency Analysis for the Southern Interior Forest Region of British Columbia. Kamloops, Canada.

City of Toronto Climate Adaptation Steering Group, Clean Air Patnership, Toronto Environment Office. 2008. "AHEAD OF THE STORM…Preparing Toronto for Climate Change".
http://www.climateneeds.umd.edu/reports/Toronto%20City-Preparing%20Toronto%20for%20Climate%20Change

Castillo, E. 1988. *Extreme value theory in engineering.* San Diego: Academic Press.

Coles, S. 2001. *An introduction to statistical modeling of extreme value.* London: Springer.

Coles, S. G., and M.J. Dixon. 1999. Likelihood-based inference for extreme value models. *Extremes* 2 (1): 5-23.

Cunnane, C. 1988. Methods and merits of regional flood frequency analysis. *Journal of Hydrology* 100 (1): 269-290.

Dalrymple, T. 1960. Flood frequency analyses. *Water Supply Paper* 1543-A, U.S. Geological Survey, Reston, Va.

Dingman, S.L. 2002. *Physical Hydrology* (Second Edition). New Jersey: Prentice-Hall.

Embrechts, P., S.I. Resnick, and G. Samorodnitsky. 1999. Extreme value theory as a risk management tool. *North American Actuarial Journal* 3 (2): 30-41.

Environment Canada. 2013. "All-weather precipitation gauge". https://ec.gc.ca/meteoaloeil-skywatchers/default.asp?lang=En&n=7EF00E34-1

Fitzgerald, D. L. 1989. Single station and regional analysis of daily rainfall extremes. *Stochastic Hydrology and Hydraulics* 3 (4): 281-292.

Fowler, H. J., and C.G. Kilsby. 2003. A regional frequency analysis of United Kingdom extreme rainfall from 1961 to 2000. *International Journal of Climatology* 23 (11): 1313-1334.

Greenwood, J. A., J.M. Landwehr, N.C. Matalas, and J.R. Wallis. 1979. Probability weighted moments: definition and relation to parameters of several distributions expressable in inverse form. *Water Resources Research*, 15 (5): 1049-1054.

Gumbel, E. J. 1941. The Return Period of Flood Flows. *The Annals of Mathematical Statistics* 12 (2): 163-190. http://projecteuclid.org/euclid.aoms/1177731747.

Helsel, D. R., and R. M. Hirsch. 1992. *Statistical Methods in Water Resources*. Amsterdam: Elsevier Science Publishers.

Henstra, D., and G. McBean. 2009. Climate Change Adaptation and Extreme Weather. *Adaptation to Climate Change Team*. http://act-adapt.org/.

Hosking, J. R.M. 1990. L-moments: analysis and estimation of distributions using linear combinations of order statistics. *Journal of the Royal Statistical Society. Series B (Methodological)* 52:105-124.

Hosking, J. R. M., and J. R.Wallis. 1988. The effect of intersite dependence on regional flood frequency analysis. *Water Resources Research* 24 (4): 588-600.

Hosking, J. R. M., and J.R. Wallis. 2005. *Regional frequency analysis: an approach based on L-moments*. Cambridge: Cambridge University Press.

Hosking, J. R. M., J. R. Wallis, and E. F. Wood. 1985. Estimation of the generalized extreme-value distribution by the method of probability-weighted moments. *Technometrics*, 27 (3): 251-261.

IPCC, 2007: *Climate Change 2007: Impacts, Adaptation and Vulnerability. Contribution of Working Group II to the Fourth Assessment Report of the Intergovernmental Panel on Climate Change*, M.L. Parry, O.F. Canziani, J.P. Palutikof, P.J. van der Linden and C.E. Hanson, Eds., Cambridge University Press, Cambridge, UK, 976pp.

Jarvis, C. S., and others. 1936. Floods in the United States, magnitude and frequency. *U.S. Geol. Survey Water-Supply Paper* 771, 497 p.

Katz, R. W., M. B. Parlange, and P. Naveau. 2002. Statistics of extremes in hydrology. *Advances in Water Resources* 25 (8): 1287-1304.

Klein Tank, A. M. G., F. W. Zwiers, and X. Zhang. 2009. Guidelines on analysis of extremes in a changing climate in support of informed decisions for adaptation, climate data and monitoring WCDMP-No. 72, WMO-TD No. 1500, 56 pp.

Klock, R., and J. Mullock. 2001. The weather of British Columbia: graphic area forecast 31. NAV Canada.

Landwehr, J. M., N. C. Matalas, and J. R. Wallis. 1979. Probability weighted moments compared with some traditional techniques in estimating Gumbel parameters and quantiles. *Water Resources Research* 15 (5): 1055-1064.

Lang, M., T. B. M. J. Ouarda, and B. Bobée. 1999. Towards operational guidelines for over-threshold modeling. *Journal of Hydrology* 225 (3): 103-117.

Madsen, H., P. F. Rasmussen, and D. Rosbjerg. 1997. Comparison of annual maximum series and partial duration series methods for modeling extreme hydrologic events: 1. At-site modeling. *Water Resources Research* 33 (4): 747-757.

Martins, E. S., and J. R. Stedinger. 2001. Generalized Maximum Likelihood Pareto-Poisson estimators for partial duration series. *Water Resources Research* 37 (10): 2551-2557.

Metcalfe, J. R., S. Ishida, and B. E. Goodison. 1994. A corrected precipitation archive for the Northwest Territories of Canada. Environment Canada – Mackenzie Basin Impact Study, Interim Report #2.

Ngongondo, C. S., C. Y. Xu, L. M. Tallaksen, B. Alemaw, and T. Chirwa. 2011. Regional frequency analysis of rainfall extremes in Southern Malawi using the index rainfall and L-moments approaches. *Stochastic Environmental Research and Risk Assessment* 25 (7): 939-955.

Pike, G. G., T. E. Redding, R. D. Moore, R. D. Winkler, and K. D. Bladon, eds. 2010. Compendium of forest hydrology and geomorphology in British Columbia. B.C. Min. For. Range, For. Sci. Prog., Victoria, B.C. and FORREX Forum for Research and Extension in Natural Resources, Kamloops, B.C. Land Management Handbook No. 66.
http://www.for.gov.bc.ca/hfd/pubs/Docs/Lmh/Lmh66.htm

Redding, T. 2008. Changing climate, uncertain futures, and evolving practices. *FORREX Link* 10 (2): 15.
http://www.forrex.org/sites/default/files/publications/articles/vol10_no2_art10.pdf

Reed, D. W., D. S. Faulkner, and E. J. Stewart. 1999. The FORGEX method of rainfall growth estimation II: Description. *Hydrology and Earth System Sciences* 3 (2): 197-203.

Ruggiero, P., P. D. Komar, and J. C. Allan. 2010. Increasing wave heights and extreme value projections: The wave climate of the US Pacific Northwest. *Coastal Engineering* 57(5): 539-552.

Stedinger, J. R., R. M. Vogel, E. Foufoula-Georgiu. 1993. Frequency analysis of extreme events. Chapt. 18 in *Handbook of Hydrology*. Ed. by David Maidment. New York: McGraw- Hill.

Stewart, E.J., D. W. Reed, D. S. Faulkner, N. S. Reynard. 1999. The FORGEX method of rainfall growth estimation I: Review of requirement. *Hydrology and Earth System Sciences* 3 (2): 187-195.

Trefry, C. M., D. W. Watkins Jr., and D. L. Johnson. 2005. Regional rainfall frequency analysis for the state of Michigan. *Journal of Hydrologic Engineering* 10 (6): 437-449.

Tressou, J., A. Crépet, P. Bertail, M. H. Feinberg, and J. C. Leblanc. 2004. Probabilistic exposure assessment to food chemicals based on extreme value theory. Application to heavy metals from fish and sea products. *Food and Chemical Toxicology* 42 (8): 1349-1358.

Vogel, R. M., and N. M. Fennessey. 1993. L moment diagrams should replace product moment diagrams. *Water Resources Research* 29 (6): 1745-1752.

Wallis, J. R., N. C. Matalas, and J. R. Slack. 1974. Just a moment! *Water Resources Research*, 10 (2): 211-219.

Wallis, J. R., M. G. Schaefer, B. L. Barker, and G. H. Taylor. 2007. Regional precipitation-frequency analysis and spatial mapping for 24-hour and 2-hour durations for Washington State. *Hydrology & Earth System Sciences* 11 (1): 415-442.

Wilks, D. S. 2011. *Statistical methods in the atmospheric sciences*. 2nd ed. vol. 91. Academic press.

World Meteorological Organization (WMO). 2009. Management of Water Resources and Application of Hydrological Practices. *Guide to Hydrologic Processes* Volume II. WMO Publ. No. 168. 6th ed. Geneva.

Yang, T., Q. Shao, Z. C. Hao, X. Chen, Z. Zhang, C. Y. Xu, and L. Sun. 2010. Regional frequency analysis and spatio-temporal pattern characterization of rainfall extremes in the Pearl River Basin, China. *Journal of Hydrology* 380 (3): 386-405.

CHAPTER 2 – REGIONAL FREQUENCY ANALYSIS OF SEASONAL RAINFALL AND SNOWFALL FOR THE SOUTHERN INTERIOR OF BRITISH COLUMBIA

INTRODUCTION

In 2013, an extreme precipitation event contributed to Canada's costliest natural disaster to date. An intense and slow-moving low pressure system embedded with thunderstorms stalled over southwestern Alberta and produced a series of heavy rainfall events. These rains contributed to landslides and massive flooding that caused the evacuation of up to 100,000 people, and damage and recovery costs exceeding six billion Canadian dollars (Environment Canada, 2014). Extreme precipitation events such as the one that occurred in Alberta can contribute to disasters including floods, erosion, landslides and even waterborne disease outbreaks (Auld, 2004; Henstra and McBean, 2009). Of concern is the growing risk associated with these extreme events as populations and assets are increasingly located in low-lying areas, slopes and other risk-prone regions (IPCC, 2007, City of Toronto Climate Adaptation Steering Group, 2008).

The motivation for this paper is the need identified by different agencies and governments across Canada to update Canadian extreme precipitation probability distributions (City of Toronto Climate Adaptation Steering Group, 2008; Redding, 2008). Precise, up-to-date extreme precipitation quantiles with associated recurrence intervals are needed for civil engineers, urban planners and government emergency response agencies to support communities' adaptive capacity to extreme weather. These extreme precipitation quantiles have commonly been derived from at-site frequency analysis; this method is valid as long as sufficient data are available (Jarvis, 1936; Stedinger *et al*., 1992; Reed *et al*., 1999. Unfortunately, data sets long enough to generate reliable estimations of extreme events with return periods (T) of 50 or 100 years are scarce in many parts of the world, including Canada (Adamowski *et al*., 1996; Klein Tank *et al*., 2009). At-site analysis also has the limitation of being unable to provide quantiles for sites with very short precipitation records.

Recent papers on extreme precipitation events have instead used regional frequency analysis (RFA) (e.g. Fowler and Kilsby, 2003; Trefry *et al*., 2005; Yang *et al*., 2010). If

different sites have similar event frequencies for different observed quantities, a pooled frequency analysis can be utilized rather than a site-only analysis (Stewart *et al*., 1999; Hosking and Wallis, 2005). This trading of space for time pools together data from sites with similar event frequencies into homogeneous regions, thus increasing the length of the data set that in turn increases the precision of the estimated quantiles (Stedinger *et al*., 1992). These quantile estimates produced by a RFA are considered superior to at-site estimates (Cunnane, 1988; Hosking and Wallis, 2005). A review showed few studies have examined extreme precipitation events in British Columbia using RFA (Wallis *et al*., 2007). Carlyle-Moses (2007) analyzed depth-duration-frequencies for annual daily maximum rainfall in the southern interior of British Columbia but this was an at-site analysis. Due to the abundance of weather stations with short precipitation records in the southern interior of British Columbia, it was determined that a better choice for estimating quantiles in this area was using a RFA approach instead.

Seasonal snowfall and rainfall data can be considered more useful than annual data for constructing quantiles and return periods for extreme precipitation by providing a finer scale that allows for a more meaningful interpretation of the occurrence and magnitude of extreme events. It was discovered through a review that there appeared to be no British Columbia RFA studies that used seasonal rainfall and snowfall maxima instead of annual precipitation or rainfall maxima. For the interior of British Columbia, the type of extreme precipitation varies throughout the year; as a result extreme rainfall or snowfall events can be experienced in the winter season depending on location and elevation. Estimated seasonal snowfall and rainfall quantiles help differentiate the times of the year when certain types of extreme precipitation events occur.

This paper presents the findings of a RFA using L-moments for seasonal daily maximum rainfall and snowfall for the southern interior of British Columbia. The specific goals of the study were to:

- develop acceptably homogeneous regions within the Thompson and Okanagan regions for seasonal extreme rainfall and snowfall events;
- develop regional quantile functions for each seasonal rainfall and snowfall region;

- compare regional versus at-site estimation for site quantiles of select stations within the study area.

Index-flood procedure

Homogeneous regions that are developed in a RFA are defined by a set of site characteristic variables physically related to the frequency distribution and are tested by summary statistics (Hosking and Wallis, 2005). A convenient way to develop summary statistics is with the index-flood procedure. This procedure assumes sites form a homogeneous region where the frequency distributions of the sites are identical apart from a site-specific scaling factor called the index-flood (Stewart *et al*., 1999). The index-flood characterises the typical type of extreme event at a site and is used to compare sites from a homogeneous region. A common index-flood is the sample mean of the data at a site, but can also be the median (Stewart *et al*., 1999; Fowler and Kilsby, 2003). For each region, a regional growth curve that represents a set of factors that specify the sizes of rare extreme events relative to the size of a common extreme event is calculated (Stewart *et al*., 1999; Hosking and Wallis, 2005). The quantile estimates at each site within a region is then obtained by combining the site's index-flood with the regional growth curve (Stewart *et al*., 1999).

For a frequency analysis of any type to be theoretically valid, data sets must meet certain statistical criteria such as independence, randomness and stationarity (WMO, 2009). The first two assumptions made by the index-flood procedure are that observations at any given site must be serially independent and identically distributed. While serial dependence can cause a small amount of bias, Hosking and Wallis (2005) have concluded that small quantities of serial dependence in annual data series have little effect on the quantile estimates' quality. The next assumption is that observations at different sites must be independent. This assumption is unlikely to be satisfied due to meteorological events that affect large areas and cause correlation of event magnitudes at neighbouring sites. Even when inter-site (spatial) dependence is present, RFA has been shown to be more accurate than at-site analysis (Hosking and Wallis, 1988). The last two assumptions for the index-flood procedure are that the different site frequency distributions are identical except for a scale

factor, and that the regional growth curve mathematical form is correctly specified. In practice these two assumptions are never exactly valid, but they may be approximately attained by careful selection of regions and frequency distribution (Hosking and Wallis, 2005).

L-moments

L-moments are summary statistics for a data set that are used to derive parameter estimates of frequency distributions. They were developed by Hosking (1990) as modifications of the probability weighted moment (PWM) estimators of Greenwood *et al*. (1979). In terms of PWMs, L-moments are given in general by:

$$\lambda_{r+1} = (-1)^r \sum_{k=0}^{r} P_{r,k}^* \alpha_k = \sum_{k=0}^{r} P_{r,k}^* \beta_k \tag{2.1}$$

where $\alpha_{k=} M_{1,0,r}$, $\beta_k = M_{1,r,0}$ and $P_{r,k}^*$ is a set of orthogonal polynomials described by:

$$P_{r,k}^* = (-1)^{r-k} \binom{r}{k} \binom{r+k}{k} = \frac{(-1)^{r-k}(r+k)!}{(k!)^2 (r-k)!} \tag{2.2}$$

where $P_{r,k}^*$ is the rth shifted Legendre polynomial (Hosking, 1990).

λ_1 and λ_2 are the L-location (mean) and L-scale respectively of the distribution. Higher-order L-moments are represented by dimensionless versions called L-moment ratios. These ratios are defined by:

$$\tau_r = \lambda_r / \lambda_2, \qquad r = 3, 4, ... \tag{2.3}$$

where τ_3 is the L-skewness and τ_4 is the L-kurtosis.

Finally, the dimensionless ratio called the coefficient of L-variation, L-CV is defined as:

$$\tau = \lambda_2/\lambda_1 \qquad\qquad (2.4)$$

(Hosking, 1990)

L-moments are much less susceptible to the influences of sample outlier values and do not have sample size related bounds. They are also considered more reliable and less biased particularly for small samples, and are easier to compute than maximum likelihood estimates (Hosking 1990; Vogel and Fennessey, 1993; Ngongondo *et al.*, 2011).

METHODOLOGY

Computer software

Data organization and graphing were performed using Microsoft[©] Office Excel 2007 and 2010 (Microsoft Corporation, Redmond, WA, USA) software packages. XLSTAT[©] 2012 (Addinsoft, New York, NY, USA) software package was used for the three serial dependence tests: Pettitt's Test for Change, Mann-Kendall trend test and Spearman's rho rank correlation test. All regional frequency and at-site analyses were performed using R[©] version 3.0.2 (R Foundation for statistical computing, Vienna, Austria). Three software packages were used with R[©]: lmomRFA version 3.0, lmom version 2.2 and Kendall version 2.2.

Data collection and screening

Study area

The Thompson River Basin District and the Okanagan River Basin District (hereafter referred to as the Thompson and Okanagan regions) were selected as the study area (Figure 2.1, Table 2.1). These two regions located in the southern interior of British Columbia were chosen due to their complex precipitation patterns. British Columbia is considered to have some of the most difficult weather to accurately forecast in Canada due to the interaction between migratory weather systems from the Pacific Ocean and the province's complex topography of high mountains, ocean coastline, interior plateaus and deep valleys. Large north-to-south running mountain ranges modify these weather systems as they pass over
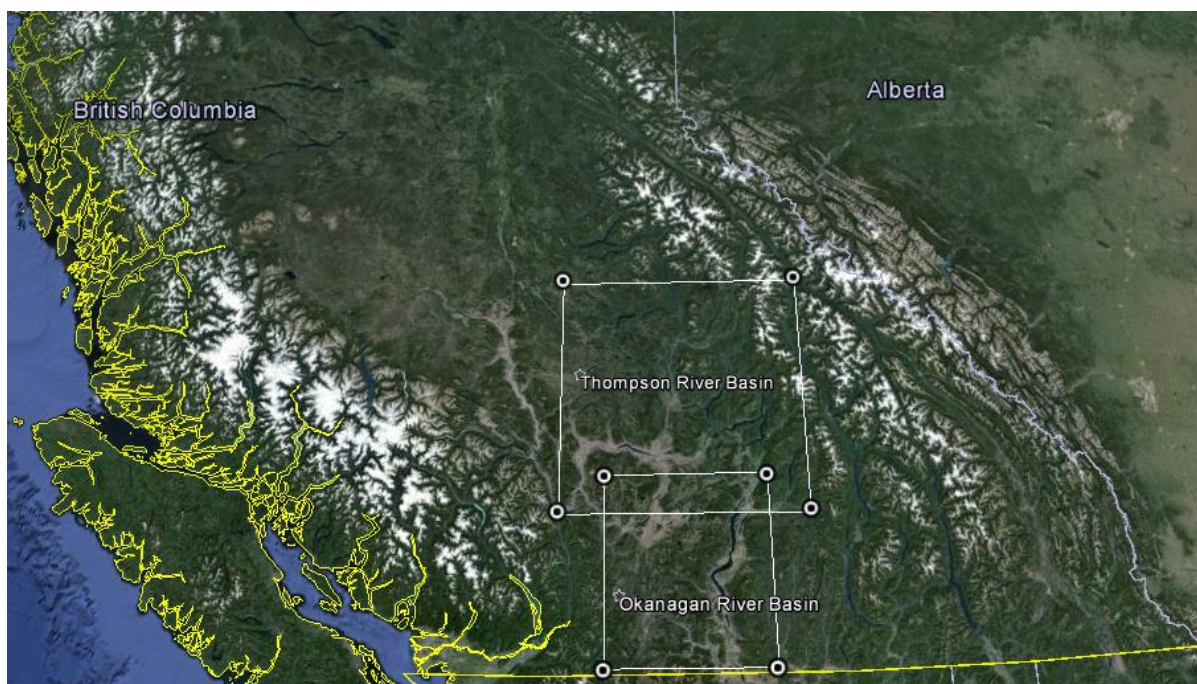
Figure 2.1. Thompson River Basin District (upper white polygon) and Okanagan River Basin District (lower white polygon) defined in Table 2.1 (Source: Google Earth).

Table 2.1. General characteristics of the study area: Thompson River Basin District and the Okanagan River Basin District.

	Thompson River Basin	Okanagan River Basin
Maximum Latitude	52°09´N	50°30´N
Minimum Latitude	50°13´N	49°01´N
Maximum Longitude	121°35´W	121°01´W
Minimum Longitude	118°30´W	119°01´W
Maximum Elevation (m)	2030	1890
Minimum Elevation (m)	232	280
Number of Weather Sites	140	113
Overall Data Range (yrs)	1873-2007	1878-2007

British Columbia; this produces distinctive precipitation patterns that vary with season, elevation, distance from the coast and exposure to the prevailing upper flow ((Pike *et al.*, 2010). The southern interior of British Columbia is bordered to the west by the Coast

Mountains and to the east by the Monashees, a subset of the Columbia Mountains. The Coast Mountains in particular are a strong weather controller for this area. A prevailing mean westerly upper flow passing over the Coast Mountains experiences subsidence on the lee side that results in a significant rain shadow effect and low annual precipitation amounts for the interior compared to the coast of British Columbia. The result is that a weather system from the Pacific Ocean is weakened as it moves easterly over the province though widespread precipitation can still occur inland if the system is strong enough. High summer temperatures in the interior valleys can combine with passing upper troughs or cold fronts to trigger significant convective activity. The location and movement of these convective cells are influenced by orientation of valleys, proximity of water bodies, and prevailing surface winds.

Elevation in the Thompson and Okanagan region has a strong role in the type of precipitation experienced by different locations – particularly in the spring, fall and winter seasons. While the Monashees help moderate the winter climate for the southern interior of British Columbia by restricting the western movement of cold arctic air, occasionally an arctic outbreak does occur. When the cold arctic air mass starts to break down, weather systems from the Pacific invade and bring precipitation. Whether a location in the Thompson and Okanagan regions experiences this precipitation as snow, rain or mixed can depend on its elevation.

Data extraction and compilation

Historical monthly maximum 24-hour (daily) rainfall and snowfall data for the 253 stations located in the Thompson and Okanagan regions were extracted from the Climate Information Branch Meteorological Service of Canada (MSC) 2000 Canadian Daily Climate Data CD (CDCD V1.02). A station was included if it had a data range ≥ 10 years (Smithers and Schulze, 2001; Hosking and Wallis, 2005). Monthly data were rejected if there was greater than three days missing in that month; this criterion is considered stringent compared to other research (e.g. Dales and Reed, 1989), however it is prudent when lack of meteorological stations make it difficult to validate maxima (Jones *et al*., 2013). Estimated data were accepted into the study as MSC use these data to calculate normals (C. Barnes, personal communication, February 14, 2011). All other flagged data as described in

Appendix 2.A were rejected. MSC has a quality control program for meteorological data but it is uncertain whether the data used in this study were fully corrected for spatial and temporal inhomogeneities as described in the World Meteorological Organization (WMO) Guide to Meteorological Instruments and Methods of Observation (2008). Regardless, as part of WMO's international surface weather network with the associated standards and quality control program, MSC meteorological data are still considered more reliable and accurate when compared to other government or industry weather observation networks.

Out of the 253 extracted stations, 138 stations remained viable after the initial screening process. A summary of all initial stations with the viable stations in bold are listed in Appendix 2.B. All remaining rainfall and snowfall data were then seasonally sorted with the seasons defined as March-May for spring, June-August for summer, September-November for fall, and December-February (following year) for winter (Zhang *et al*., 2001; Meteorological Service of Canada, 2014). Finally, seasonal maxima were extracted from years with no missing data. A block maxima approach was used for the data extraction instead of peak-over-threshold (POT) due to ease of use and lack of protocols for setting a threshold level and deciding which peaks to exclude from the analysis (Lang *et al*., 1999; Reed *et al*., 1999; Fowler and Kilsby, 2003). Over most of southern Canada, snowfall is uncommon during the summer months; therefore snowfall maxima were excluded from any further analysis (Zhang *et al*., 2001).

Metadata

Metadata are a station's history from establishment to decommission, and typically includes frequency and type of observations, observing irregularities, and equipment descriptions, defects, changes and relocation. This history is important in determining whether variations present in a data sample are due to changes in the circumstances under that the data were collected, or actual climate variability and change (Aguilar *et al*., 2003; Hosking and Wallis, 2005). While metadata recorded by MSC (2013) do not cover every scenario that could affect a weather station's microclimate (e.g. nearby land-use changes) they are a valuable quality control tool to ensure the maximum accuracy of the meteorological data for statistical analysis (Kundzewicz and Robson, 2000).

Unfortunately due to the cost recovery policy of MSC, metadata information such as station equipment and weather observing procedural changes were not available for almost all the stations used in this study except at a substantial cost well beyond the available research funding. Three stations within the study region did have very limited metadata available on the internet in the form of a climate summary publication (Canadian Climate Program, 1984a; Canadian Climate Program, 1984b; Canadian Climate Program, 1984c). These publications did not provide enough detail to be useful in determining if any changes in observing procedures or equipment were significant enough to affect the quality of the data; therefore, an assumption was made that all data used were deemed a true representation of the quantity being measured.

Serial dependence

Serial dependence was examined using three non-parametric (distribution-free) rank-based tests that were chosen due to their robustness and simplicity of use (Kundzewicz and Robson 2000). These tests looked at two different types of series changes: step-change and trend. Step-change was examined with a Pettit's Test for Change that looks for a change in the median with the exact time of change unknown (Pettitt, 1979). This test is robust to distributional form changes, and is considered powerful compared to the Wilcoxon-Mann-Whitney Test that assumes that the time of change is known (Kundzewicz and Robson 2000).

Spearman's rho and Mann-Kendall (MK) tests examined trend. Both of these statistical tests are used in hydrological studies for detecting monotonic trends in time series data (Yue *et al*., 2002; WMO, 2009). Spearman's rho is a test for correlation between two variables (Spearman, 1904). It is a rank-based version of its classical parametric counterpart – the Pearson product moment (Berenson and Levine, 1988). The MK test is similar to Spearman's rho however uses a different measure of correlation that has no parametric equivalent (Mann, 1945; Kendall, 1975; Kundzewicz and Robson, 2000). Since publication of a paper by Hirsch *et al*. (1982), this test has been used more widely than the Spearman's rho test for trends in hydrological times series; the reason that the MK test is more popular than the Spearman's rho test is unknown considering that both tests have demonstrated

similar power in detecting a trend (Yue *et al*., 2002). Research using the MK test includes Adamowski and Bougadis (2003), Kwarteng *et al*. (2009) and Yang *et al*. (2010).

An increase in Type I errors for trend analysis can occur if the data has significant autocorrelation (e.g. Storch and Navarra, 1995) or if there is test multiplicity. Since the quality of the quantile estimates developed by a regional frequency analysis is not sensitive to trend, it was appropriate to utilize a Bonferroni correction and a false discovery rate (FDR) procedure to evaluate the overall significance of the three trend tests and reduce Type I errors (Bland and Altman, 1995; Wilks, 2006).

Spatial dependence

With respect to the regional L-moment algorithm, spatial dependence in a regional frequency analysis can have a small effect on the bias of estimated quantiles and theoretically increase the average L-moment ratios' and the estimated regional growth curve's variability. As long as the spatial dependence is not too strong, its effect on variability should be minimal (Hosking and Wallis, 1988). One method to reduce the effect of spatial dependence is to reduce the pooling group of independent sites. This allows the regional growth curve to shift a fixed distance to the right to account for spatial dependence (Dales and Reed, 1989). This method however has not been extensively validated as noted by Fowler and Kilsby (2003) and was not used. Fowler and Kilsby (2003) determined that a definitive methodology to account for dependence with respect to actual quantiles amounts was unavailable; therefore, this study chose instead to incorporate spatial dependence into the quantiles' confidence intervals using a simulation algorithm developed by Hosking and Wallis (2005).

Discordancy measure

A convenient way of checking whether data meet the conditions for a regional frequency analysis is to compare sample L-moments for different sites. Hosking and Wallis (2005) have developed a single statistic called a discordancy measure that amalgamates the L-moment ratios and allows a comparison between the L-moment ratios of a site with the average L-moment ratios of a group of similar sites.

With *N* sites in a group, let:

$$\mathbf{u}_i = \begin{bmatrix} t^{(i)} & t_3^{(i)} & t_4^{(i)} \end{bmatrix}^{\mathrm{T}} \tag{2.5}$$

be a vector of a sample data's L-CV, L-skewness and L-kurtosis respectively for site *i*.
Defining the unweighted group average as:

$$\overline{\mathbf{u}} = N^{-1} \sum_{i=1}^{N} \mathbf{u}_i \tag{2.6}$$

and the matrix of sums of squares and cross-products as:

$$\mathbf{A} = \sum_{i=1}^{N} (\mathbf{u}_i - \overline{\mathbf{u}})(\mathbf{u}_i - \overline{\mathbf{u}})^{\mathrm{T}} \tag{2.7}$$

the discordancy measure for site *i* is given by:

$$D_i = \frac{1}{3} N (\mathbf{u}_i - \overline{\mathbf{u}})^T \mathbf{A}^{-1} (\mathbf{u}_i - \overline{\mathbf{u}}) \tag{2.8}$$

Hosking and Wallis (2005) suggest a site be regarded as discordant if its D_i value exceeds the critical value given in Table 2.2.

Hosking and Wallis (2005) recommend two uses for the discordancy measure. First, that it be used to screen the data for inclusion in a RFA. Any sites flagged as discordant at the screening stage should be examined for gross errors such as transcription errors, possible human-induced site changes, or an unusual rainfall or snowfall event that cannot be explained by known historical weather events.

Later the discordancy measure can be used during the cluster analysis to determine if any sites within a proposed region are discordant and should be moved out of that region. In

Table 2.2. Critical values for the discordancy statistic D_i.

Number of sites in region	Critical value	Number of sites in region	Critical value
5	1.333	11	2.632
6	1.648	12	2.757
7	1.917	13	2.869
8	2.140	14	2.971
9	2.329	≥ 15	3.000
10	2.491		

practice, the variation of L-moment ratios between apparently similar sites can be quite large for precipitation data or a site's L-moments may differ by chance alone from those of other physically similar sites; therefore, caution must be exercised when examining a discordant site.

During the initial screening of data, the Thompson region and the Okanagan region were treated as two single regions and the discordancy measure calculated for each station within the two regions. Any data sets with a $D > 3.00$ were further examined with an exploratory data analysis using graphs such as time series plots and L-moment ratio plots (Kundzewicz and Robson, 2000; Hosking and Wallis, 2005).

Identification of homogeneous regions by cluster analysis

Identifying homogeneous regions involves creating groups of sites that satisfy the homogeneity condition of the sites' frequency distributions being identical apart from a site-specific factor, the index-flood (Stewart *et al*., 1999). These regions are formed using site characteristics with at-site statistics used only to test homogeneity (Hosking and Wallis, 2005). Cluster analysis using Ward's minimum variance hierarchical was chosen as a practical method for forming regions (Smithers and Schulze, 2001; Hosking and Wallis, 2005; Trefry *et al*., 2005).

There appears to be no preferred methodology for determining characteristics most important in defining a site's precipitation climate. Four station characteristics utilized in other studies, (e.g. Trefry *et al*., 2005; Yang *et al*., 2010; Ngongondo *et al*., 2011) were chosen: latitude, longitude, elevation and mean seasonal rainfall or snowfall. A scale

transformation of these site characteristics was required for the cluster analysis. While there is benefit to identifying and weighing accordingly the site characteristics that are more likely to be influential for the development of extreme rainfall or snowfall, a detailed analysis to choose appropriate weights was difficult and beyond the scope of this study; it is also not required for a successful cluster analysis since the validity of the final regions is tested (Kjeldsen *et al*., 2002; Hosking and Wallis, 2005). A review determined that there was no standard transformation method used for RFA (e.g. Yang *et al*., 2010; Ngongondo *et al*., 2011). Smithers and Schulze (2001) evaluated a number of different transformations and their final transformation method which assigned equal weight to each characteristic was chosen for this study (Table 2.3).

Table 2.3. Transformation of site characteristics (Source: Smithers and Schulze, 2001)

Site characteristic (X)	Cluster variable (Y)
Latitude (°)	$\dfrac{X - X_{min}}{X_{max} - X_{min}} * 100$
Longitude (°)	$\dfrac{X - X_{min}}{X_{max} - X_{min}} * 100$
Elevation (m)	$\dfrac{X}{X_{max}} * 100$
Mean seasonal rainfall/snowfall (mm/cm)	$\dfrac{X}{X_{max}} * 100$

Once the clustering analysis was completed, the proposed regions were tested by a heterogeneity measure developed by Hosking and Wallis (2005) that estimates the degree of heterogeneity in a group of sites. The heterogeneity measure compares the between-site variations in sample L-moments for a proposed group of sites with what would be expected for a homogeneous region. The heterogeneity measure also allows for greater variability of L-moment ratios in small samples by weighting averages proportionally to the sites' record lengths.

Let a proposed region have N sites with site i having record length n_i and sample L-moments ratios $t^{(i)}, t_3^{(i)}, \text{and } t_4^{(i)}$. Denote the regional average L-CV, L-skewness and L-kurtosis by $t^R, t_3^R, \text{and } t_4^R$ respectively, with each average weighted proportionally to the sites' record length; for example:

$$t^R = \sum_{i=1}^{N} n_i t^{(i)} \Big/ \sum_{i=1}^{N} n_i \qquad (2.9)$$

The weighted standard deviation of the at-site sample L-CVs is given by:

$$V = \left\{ \sum_{i=1}^{N} n_i \big(t^{(i)} - t^R\big)^2 \Big/ \sum_{i=1}^{N} n_i \right\}^{1/2} \qquad (2.10)$$

A kappa distribution is fitted to the regional average L-moment ratios and used to simulate a large number of homogeneous regions each with N sites, no spatial or serial correlation, and the sites having the same record lengths as their real world counterparts. For each simulated region, V is calculated, and the mean μ_V and standard deviation σ_V are determined.

Thus, the heterogeneity measure is defined by:

$$H = \frac{(V - \sigma_V)}{\sigma_V} \qquad (2.11)$$

Hosking and Wallis (2005) suggest that proposed region be declared acceptably homogeneous if $H < 1$, possibly homogeneous if $1 \leq H \leq 2$ and definitely heterogeneous if $H \geq 2$. It is possible to have negative values of H that indicate dispersion among the at-site sample L-CV values are less than what would be expected of a homogeneous region with complete independence between at-site frequency distributions (Hosking and Wallis, 2005). A strong effort was made to ensure that there were no negative H values associated with the

final regions to reduce the effect of any serial dependence on the bias of estimated quantiles. The regions derived from the initial cluster analysis were not considered to be final. Numerous subjective adjustments were made to improve the geographical coherence of the regions and to ensure as many of the regions as possible were acceptably homogeneous with no negative H values.

Homogeneous regions were independently developed for maximum daily rainfall and snowfall for each of the four seasons with the exception of summer maximum daily snowfall. The regions were restricted in size from 5 to 20 sites. Five sites are the minimum number of sites within a region that can be tested with the discordancy measure and there is no gain in the accuracy of quantile estimates by using more than 20 sites in a region (Hosking and Wallis, 2005).

Development of estimated quantiles

Frequency distribution choice using the goodness-of-fit measure

Hosking and Wallis (2005) recommend that distributions with three to five parameters should be used with a RFA as these distributions – when estimated accurately – will yield less biased estimates of quantiles in the tails as compared to distributions with only two parameters. Five three-parameter distributions were tested as possible fits: Generalized Logistic (GLO), Generalized Extreme Value (GEV), Generalized Normal (GNO), Generalized Pareto (GPA) and Pearson type III (PE3).

A goodness-of-fit measure developed by Hosking and Wallis (2005) assesses which of the candidate distributions best fit the data. Each candidate three-parameter distribution is fitted to the regional average L-moments 1, t^R and t_3^R. The L-kurtosis of the fitted distribution is denoted by τ_4^{DIST}; the DIST can be any of the candidate three-parameter distributions.

A kappa distribution is then fitted to the regional average L-moment ratios 1, $t^R, t_3^R,$ and t_4^R. Using the same computations and assumptions for the simulated region as the heterogeneity measure, a large number of simulations of kappa regions are generated.

Let $t_3^{(m)},$ and $t_4^{(m)}$ be the regional average L-skewness and L-kurtosis respectively of the mth kappa simulated region.

The bias of t_4^R is calculated as:

$$B_4 = N_{\text{sim}}^{-1} \sum_{m=1}^{N_{\text{sim}}} \left(t_4^{(m)} - t_4^R \right) \qquad (2.12)$$

the standard deviation of t_4^R as:

$$\sigma_4 = \left[(N_{\text{sim}} - 1)^{-1} \left\{ \sum_{m=1}^{N_{\text{sim}}} \left(t_4^{(m)} - t_4^R \right)^2 - N_{sim} B_4^2 \right\} \right]^{1/2} \qquad (2.13)$$

And the goodness-of-fit measure for each distribution:

$$Z^{\text{DIST}} = \left(\tau_4^{\text{DIST}} - t_4^R + B_4 \right) / \sigma_4 \qquad (2.14)$$

The candidate fit is declared to be adequate if $\left| Z^{\text{DIST}} \right| \leq 1.64$ (Hosking and Wallis, 2005). Note that while the Z statistic has the form of a significance test of goodness of fit and the criterion $\left| Z^{\text{DIST}} \right| \leq 1.64$ corresponds roughly to a confidence level of 90%, the assumption of Z having a standard Normal cannot be satisfied in practice; therefore Z cannot be considered a formal test.

The Z statistic was calculated for all three-parameter candidate distributions for each acceptably homogeneous region. The Z statistic was not calculated if a region was not acceptably homogeneous; instead, the Wakeby distribution was automatically chosen as the best fit (Hosking and Wallis, 2005). All distributions that had $|Z| \leq 1.64$ were flagged as acceptable. If more than one candidate distribution were acceptable, the one with the lowest $|Z|$ value was chosen. Along with the Z statistic, L-moment ratio plots were also used to verify the best fitted distribution.

There were regions where none of the three-parameter candidates meet the Z criterion. In these circumstances, the L-moment ratio plot was examined to determine where the regional average (t_3^R, t_4^R) point was located. If the regional average point fell between two

distributions, both distributions were chosen. If the regional average point did not lie between two distributions, the Wakeby distribution was used since this five-parameter distribution is considered more robust to misspecification of the frequency distribution of a homogeneous region than the other three-parameter candidate distributions (Hosking and Wallis, 2005).

Exact zero data values

Certain seasonal rainfall and snowfall data sets contained a number of zero values. Distributions fitted to such data sets can take negative values in the lower tail of the distribution unless the distribution is explicitly constrained to have a lower bound of zero. Guttman et al (1993) rectified this problem by fitting to the regional data a mixed distribution having the form:

$$F(x) = \begin{cases} 0, & x < 0 \\ p + (1 - p)G(x), & x \geq 0 \end{cases} \tag{2.15}$$

where $F(.)$ is the cumulative distribution function of precipitation amounts, p is the probability that the precipitation amount is zero and $G(.)$ is the cumulative distribution function of nonzero precipitation amounts. For this study, a variation of the Guttman *et al.* (1993) algorithm for data sets containing exact zero values was utilized as given in Figure 2.2.

Assessment of the estimated quantile's precision

In traditional statistics, the magnitude of the uncertainty associated with the results of a statistical analysis is determined with confidence intervals for the estimated parameters and quantiles. It is possible to construct similar confidence intervals for a RFA using the regional L-moment algorithm, except that all the assumptions for the index-flood procedure are rarely satisfied in practice. Indeed, Hosking and Wallis (2005) note that one of the strengths of the regional L-moment algorithm is its usefulness even when some of its assumptions are not satisfied.

A Monte Carlo simulation algorithm as outlined in Table 6.1 of Hosking and Wallis (2005) was used to determine the accuracy of the estimated quantiles. This simulation

START

Is region acceptably homogeneous? ──────────────────────────→

YES ↓   **NO**

Is three-parameter candidate distribution acceptable? ──────→

YES ↓   **NO**

Fit three-parametre candidate distribution

Fit Wakeby

Proportion of zeroes
in data less than 0.02? ──────────────────────────────────→

YES ↓   **NO**

Estimate of 0.02
quantile less than 0?

Lower bound of fitted
distribution less than 0?

NO   **YES** ↓   **YES** ↓   **NO**

Fit Wakeby as a mixed
distribution with lower
bound
constrained to be zero

END

Figure 2.2. Algorithm for choosing a distribution when the data set contains exact zero values (variation of Guttman *et al*., 1993).

 matched the particular characteristics of the data used to estimate the quantiles: number of sites, record lengths at each site and regional average L-moment ratios. To account for any intersite dependence within an actual region, the simulation algorithm was modified using a correlation matrix **R** that considers sites from a region as equicorrelated and estimates the average spearman rank correlation value ρ by the average cross-correlation of all pairs of sites within a region (Hosking and Wallis, 2005).

For fitted distributions that can take on negative values the lower error bound may become very small or even negative, and the upper error bound can become very large or infinite. In these circumstances, the regional average relative RMSE of the estimated quantiles becomes a more reliable measure of accuracy (Hosking and Wallis, 2005).

The accuracy that the error bounds and RMSEs can be estimated increases with the number of repetitions of the simulation procedure. Even though 100 repetitions can give a useful indication of the magnitude of errors, 10,000 repetitions were used for each simulation to ensure that the error estimates were as precise as possible.

Comparison of select regional and at-site estimations

One station from each seasonal maximum daily rainfall and snowfall region was selected based on population or data set size for a comparison between regional and at-site estimation. The regionally derived site quantile estimates were obtained by combining the regional growth curve with the individual site's mean extreme rainfall or snowfall value (index-flood). The at-site quantiles were estimated using the method of L-moments, and fitting the preferred regional distribution and/or a GEV distribution. For the at-site quantiles, RMSEs and error bounds were generated using the Monte Carlo simulation algorithm as outlined in Table 6.1 of Hosking and Wallis (2005).

RESULTS

Serial dependence

Table 2.4 summarizes results of the three serial dependence tests. Appendix 2.C gives the full results of the three tests. P-values were examined at the 5% and 1 % significance level, and with a Bonferroni correction and FDR procedure. One hundred and five data sets were rejected at the 5% significance level by the Pettitt, Mann-Kendall and/or Spearman's rho tests; this was lowered to 32 rejected data sets at the 1% significance level. The Bonferroni correction and FDR procedure further reduced the number of rejected data sets to 8: Kamloops A and Westwold spring maximum daily rainfall, Hedley and Westbank summer

Table 2.4. Number of data sets rejected by the Pettitt, MK and/or Spearman's rho tests at the 5%, 1% significance level and with a Bonferroni and/or FDR correction (B/FDR).

	Number of Rejected Sites		
	$\alpha = 0.05$	$\alpha = 0.01$	B/ FDR
Fall Rainfall	11	2	1
Spring Rainfall	14	8	2
Summer Rainfall	21	5	2
Winter Rainfall	15	4	1
Fall Snowfall	10	0	0
Spring Snowfall	22	8	1
Winter Snowfall	12	5	1

maximum daily rainfall, Keremous fall maximum daily rainfall, Kelowna MWSO winter maximum daily rainfall, Summerland CDA spring maximum daily snowfall, and Mt Kobau Observatory winter maximum daily snowfall.

These 8 data sets showed either a strong trend or step change and were excluded from any further analysis. Figure 2.3A is the Mt Kobau Observatory winter maximum daily snowfall time series. It graphically demonstrates the step change serial dependence. There was an overall increase in the magnitude of winter maximum daily snowfall per year from 1967 to 1973 with Pettitt's test determining that a step change occurred in 1974. After 1982 there was an overall decrease in the magnitude of winter maximum daily snowfall per year. Figures 2.3B and 2.3C are two time series for Summerland CDA spring maximum daily snowfall and Hedley summer maximum daily rainfall, respectively. Summerland CDA had a statistically significant overall decrease in spring maximum daily snowfall per year while Hedley had a statistically significant overall increase in summer maximum daily rainfall. It is interesting to note that out of the 8 rejected stations, only Hedley summer maximum daily rainfall had a decreasing trend; the rest of data sets had either step changes or increasing trends. A likely cause of the step changes detected in the rejected data sets is an instrument change or relocation, or a sudden adjacent land-use change. The causes of the trend serial dependence are more difficult to determine. These detected trends could be due to the aforementioned reasons or natural long-term climate variability or change. Without access to
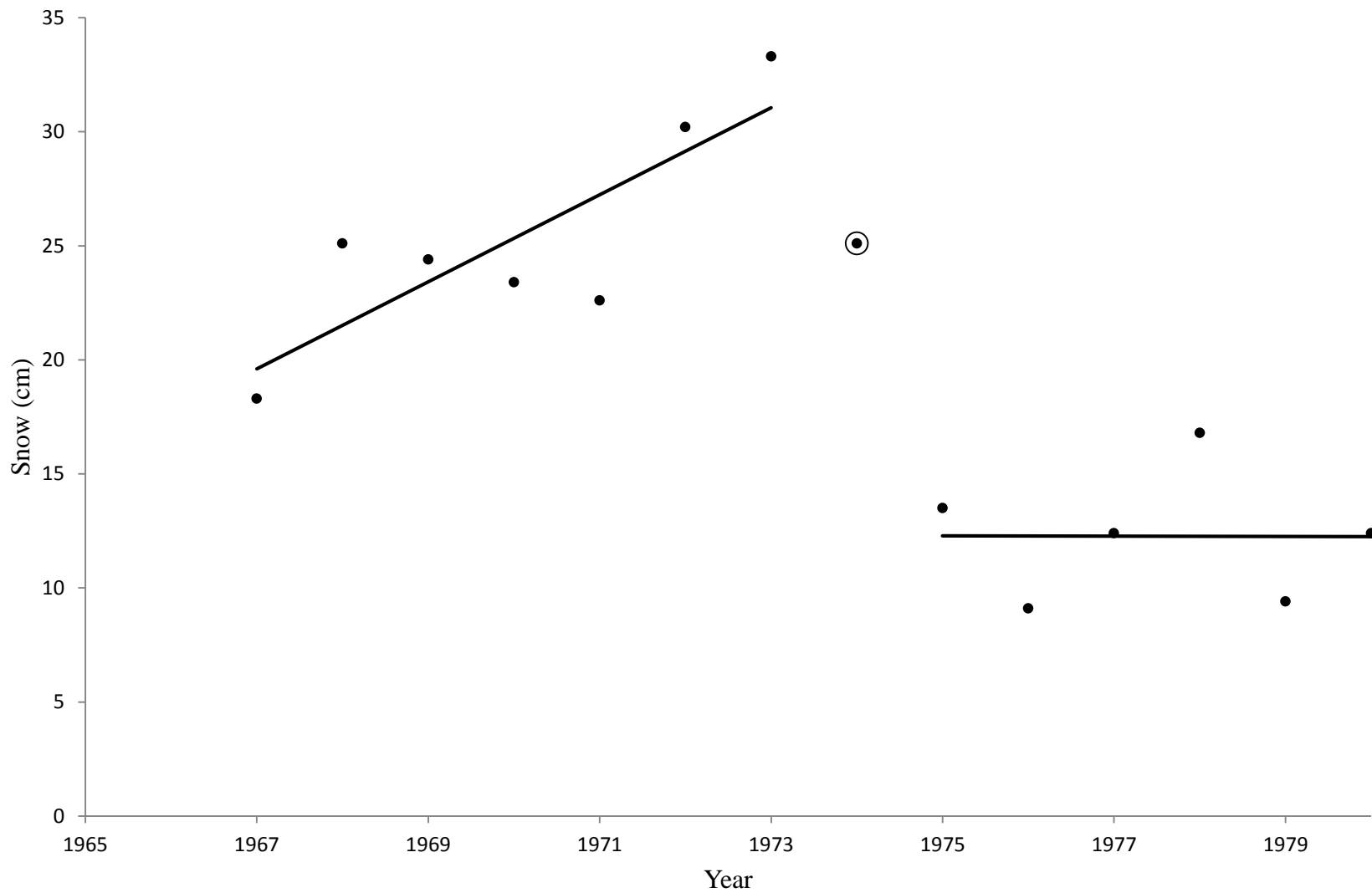
Figure 2.3.A. Mt Kobau Observatory winter maximum daily snowfall time series showing step change serial dependence. A trendline (solid line) is shown for data points before and after the step change time (circled point).
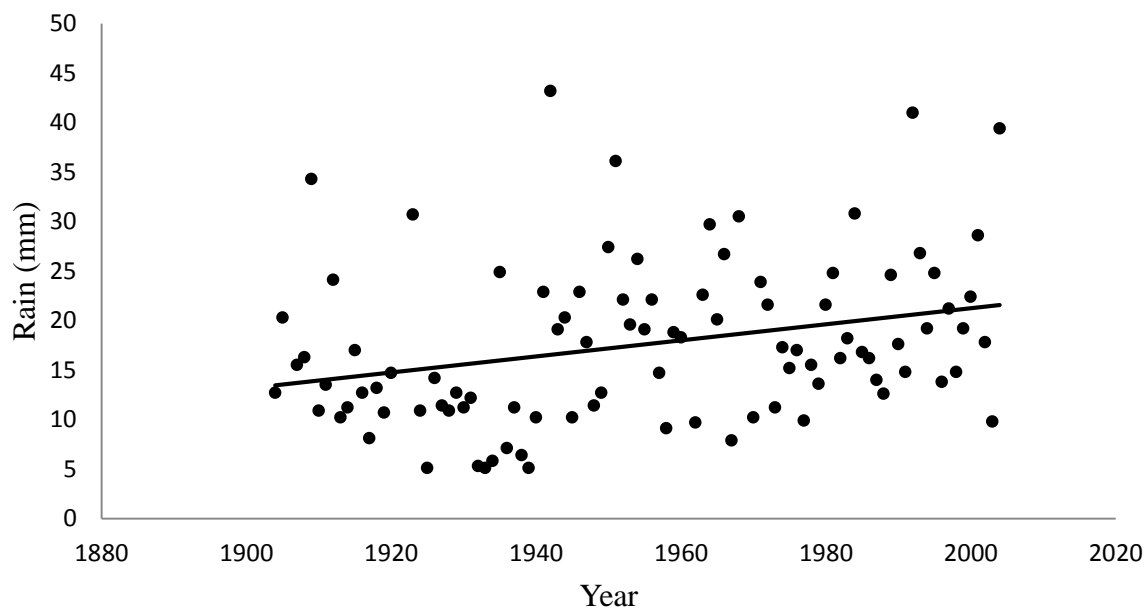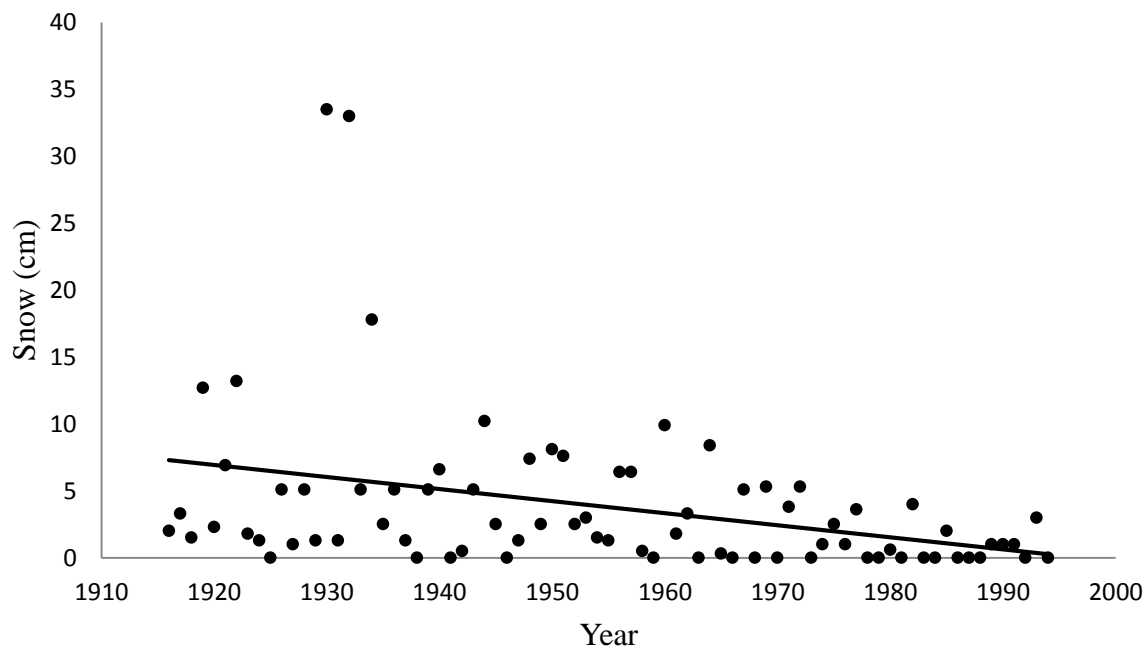
Figures 2.3.B and 2.3C. Summerland CDA spring maximum daily snowfall time series (top) and Hedley summer maximum daily rainfall (bottom) time series both showing trend serial dependence (solid line).

the accompanying metadata for these sites it is impossible to determine for certain the reason(s) for any of the detected serial dependence.

Discordancy measure

As part of the initial screening process, D_i was calculated for each seasonal rainfall and snowfall data set for the two regions: Thompson region and Okanagan region. Figures 2.4A and 2.4B show the 29 rainfall data sets and 19 snowfall data sets identified as having D_i > 3.00. Appendix 1.1 lists the discordant data sets along with their discordancy measures and associated L-moments. These 48 discordant data sets were re-examined and four data sets were corrected for transcription errors: Logan Lake summer maximum daily rainfall, Hedley NP Mine and Kamloops Mission Flats fall maximum daily snowfall, and Pinantan Lake winter maximum daily snowfall. New L-moments and discordancy measures were then calculated for the affected data sets and those with D_i > 3.00 were further examined using time series and L-moment ratio plots (see Appendix 2.D). The time series plots detected no gross errors. Visually, there appear to be some trends in certain data sets, but it was decided to retain these stations due to the lack of metadata and because a thorough serial dependence analysis had already been done. The L-moment plots showed on average data sets flagged as discordant had an unusually high or low L-moment or combination thereof compared to the rest of the group. However, this in itself may only indicate that the Thompson region and the Okanagan region are very heterogeneous regions. Elevation of weather stations in the Thompson and Okanagan regions vary widely due to mountain ranges and deep valleys located in the area. For example, Mt. Lolo Kamloops winter rainfall data set has a D_i of 12.38. This discordancy may be explained by the high elevation of this particular station that recorded only one winter maximum daily rainfall from 1965 to 1977. Besides the effect from the diverse topography of the Thompson and Okanagan regions, the rest of the sites with a high discordancy measure could be explained by single large outliers; therefore, all stations with a D_i > 3.00 were retained.
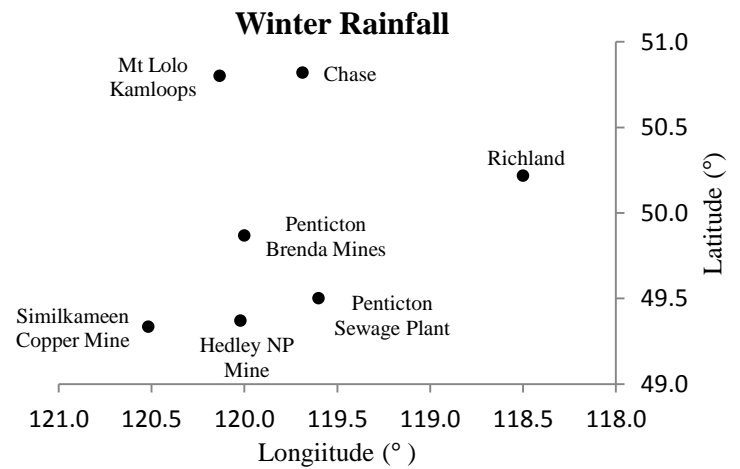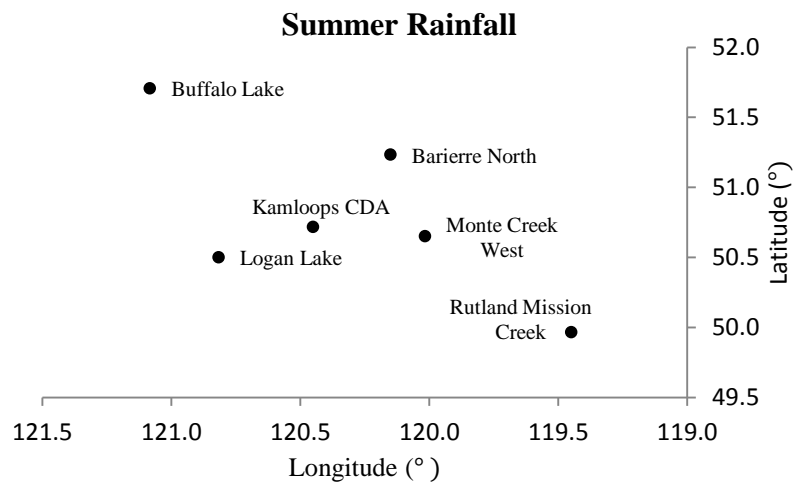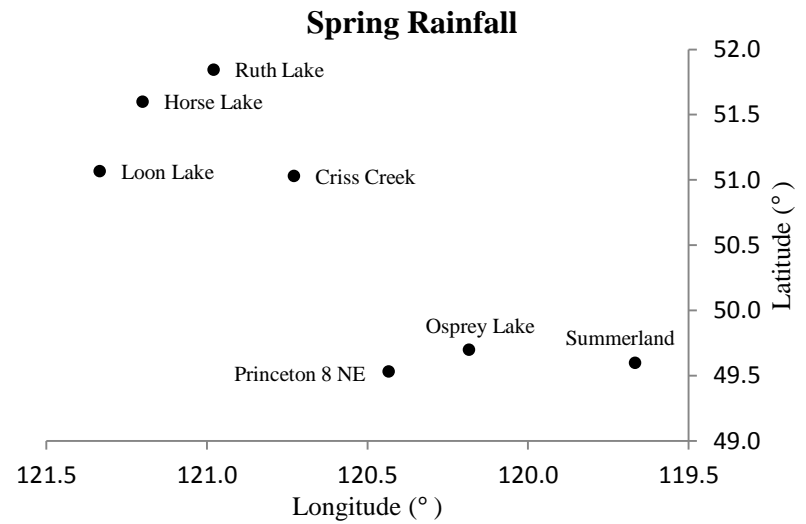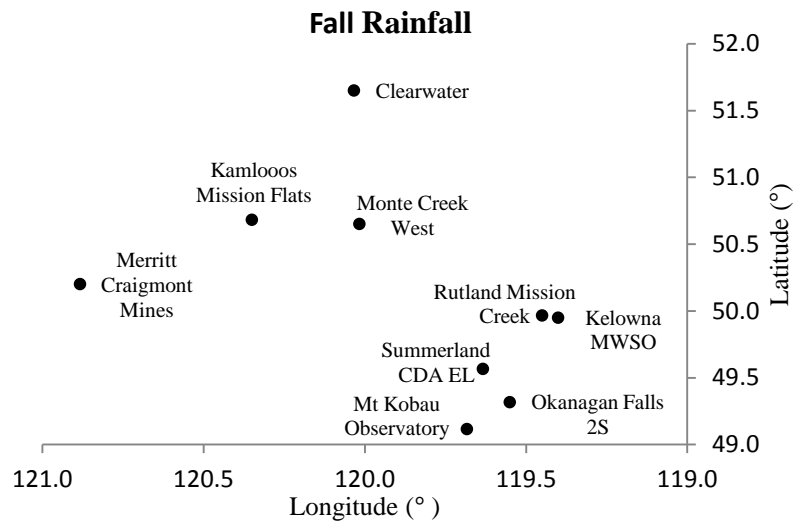
Figure 2.4.A. Seasonal maximum daily rainfall data sets with initial screening discordancy measure > 3.00.
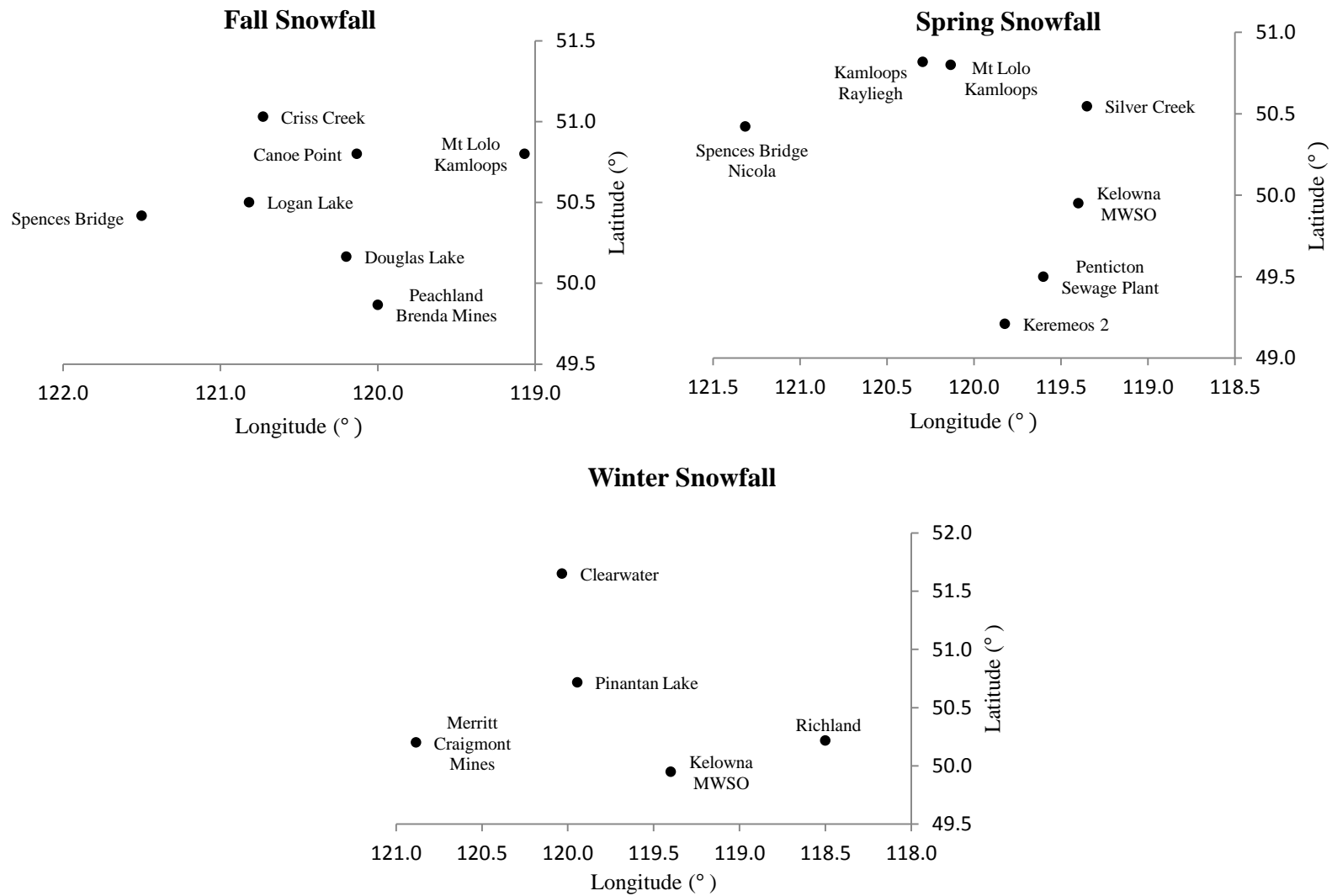
Figure 2.4.B. Seasonal maximum daily snowfall data sets with initial screening discordancy measure > 3.00.

Identification of homogeneous regions

Initial regions were formed to identify eight to ten clusters per seasonal rainfall or snowfall data set. These regions were then tested with the homogeneity measure H. Initial results were quite varied and depended on the data set. Almost all the spring snowfall and winter rainfall initial regions had H values greater than 2, indicating definite heterogeneity. An explanation for the lack of homogeneity is that spring snowfall and winter rainfall can be temperature dependant and therefore quite localised. Approximately half of the spring rainfall, summer rainfall and snow winter initial regions had H values between zero and negative one, indicating the possible presence of positive correlation between data values at different stations. An increase in frontal precipitation during the spring and winter seasons may explain the presence of correlation for those seasons. Correlation of stations in the summer season could be due to widespread convection caused by the passage of an upper cold front.

Extensive manual refinement of the regions was conducted using local knowledge of topography and weather patterns. The majority of weather stations in the southern interior of British Columbia are located in valleys that are separated from each other by high plateaus and mountain ranges; thus many of the regions graphically reflected the local valley systems. While most of the regions were physically cohesive, a few select regions were geographically dispersed. Examination of these regions showed the dispersion of stations seemed to be due to the influence of elevation over the other site characteristics. Four stations were not able to be fit into a region: Horse Lake spring maximum daily rainfall, Canoe Point fall maximum daily snowfall, Mt. Lolo Kamloops spring maximum daily snowfall and Blue River North winter maximum daily snowfall. Due to their unique frequency distributions, these sites would benefit most from an at-site analysis. All final regions were acceptably homogeneous with positive H values and all D measures less than the region's critical D measure value. Figures 2.5A – 2.5G graphically display the regions for each seasonal rainfall and snowfall data set along with a listing of all stations within each region. Appendix 2.E lists the attributes of all the stations for each region.

Nine acceptably homogeneous regions were developed for the fall maximum daily rainfall data set (Figure 2.5A). The regions overall were geographically cohesive with the
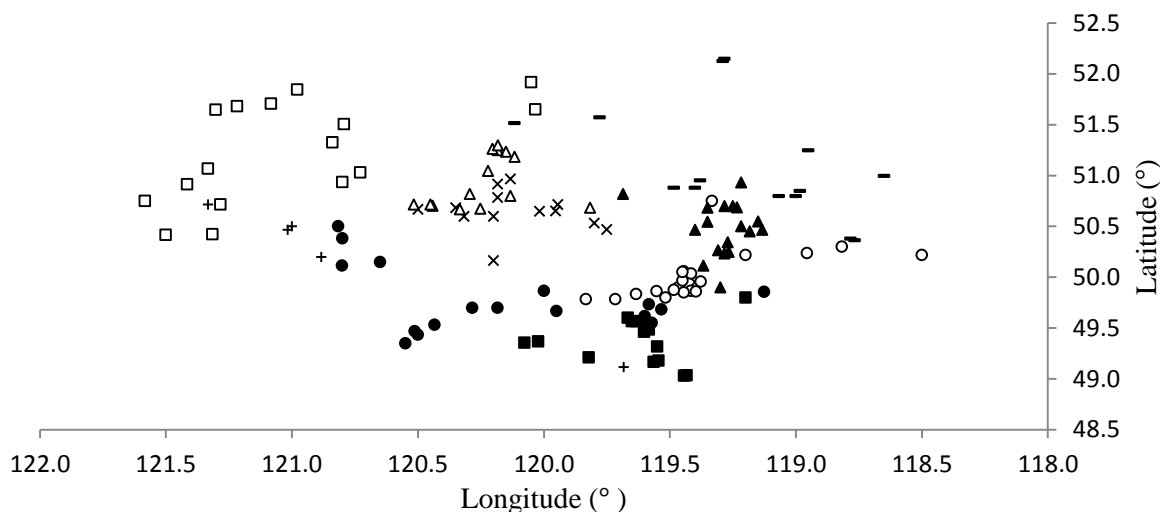
Princeton A Region: Adra, Bankier Chain Lake, Chute Lake, Joe Rich Creek, Kirton, Logan Lake, Mamit Lake, Merritt STP, Naramata (1924-1936), Naramata (1971-2004), Nicola Lake, Osprey Lake, Peachland Brenda Mines, Princeton, Princeton 8 NE, Princeton A, Similkameen Mine

Monte Creek Region: Douglas Lake, Heffley Creek, Kamloops Afton Mines, Kamloops Mission Flats, Kamloops Pratt Road, Kelowna MWSO, Knouff Lake, Knutsford 2S, Monte Creek, Monte Creek West, Monte Lake Paxton Valley, Mt Lolo Admin Kamloops, Pinantan Lake, Westwold

Kelowna A Region: Kelowna, Kelowna A, Kelowna CDA, Kelowna Dav-Spiers Road, Kelowna East, Kelowna Lakeview, Kelowna PC Burnetts Nurs, Lumby, Okanagan Centre, Okanagan Mission, Peachland, Peachland Trepanier Cr, Richland, Rutland Mission Creek, Shuswap Falls, Tappen, Vernon Coldstream Ranch, Westbank, Winfield, Woods Lake

Penticton A Region: Hedley, Hedley NP Mine, Keremeos 2, McCulloch, Okanagan Falls 2S, Oliver, Oliver STP, Osoyoos, Osoyoos West, Penticton, Penticton A, Penticton Sewage Plant, Summerland, Summerland CDA, Summerland CDA EL

Cache Creek 16 Mile Region: 100 Mile House, 100 Mile House 6 NE, Ashcroft (1912-1970), Bridge Lake 2, Buffalo Lake, Cache Creek 16 Mile, Clearwater, Criss Creek, Hat Creek, Hemp Creek Clearwater, Loon Lake, Red Lake, Ruth Lake, Spences Bridge, Spences Bridge Nicola, Vidette Lake Sharpe Lake

Merritt Region: Ashcroft M, Highland Valley BCCL, Highland Valley Lornex, Merritt, Merritt Craigmont Mines, Mt Kobau Observatory

Salmon Arm A Region: Armstrong, Armstrong Hullcar, Armstrong North, Chase, Eagle Bay, Enderby, Falkland Salmon Valley, Kelowna Bankhead, Oyama, Salmon Arm, Salmon Arm 2, Salmon Arm 3, Salmon Arm A, Silver Creek, Vernon, Vernon (1971-1994), Vernon Bella Vista, Vernon North

Kamloops A Region: Barriere, Barriere North, Chinook Cove, Chinook Cove Posby Lake, Darfield, Kamloops, Kamloops A, Kamloops CDA, Kamloops Rayleigh, Kamloops Valleyview, McLure, Mt Lolo Kamloops, Pritchard, Tranquille

Blue River A Region: Blue River A, Blue River North, Canoe Point, Celista, Clearwater Axel Crk, Lumby Sigalet Rd, Mabel Lake, Malakwa Eagle R Hatchery, Seymour Arm, Sicamous, Sicamous 2, Sorrento, Sorrento East, Vavenby

Figure 2.5A. Final homogeneous regions for fall maximum daily rainfall.

Figure 2.5.B. Final homogeneous regions for spring maximum daily rainfall.
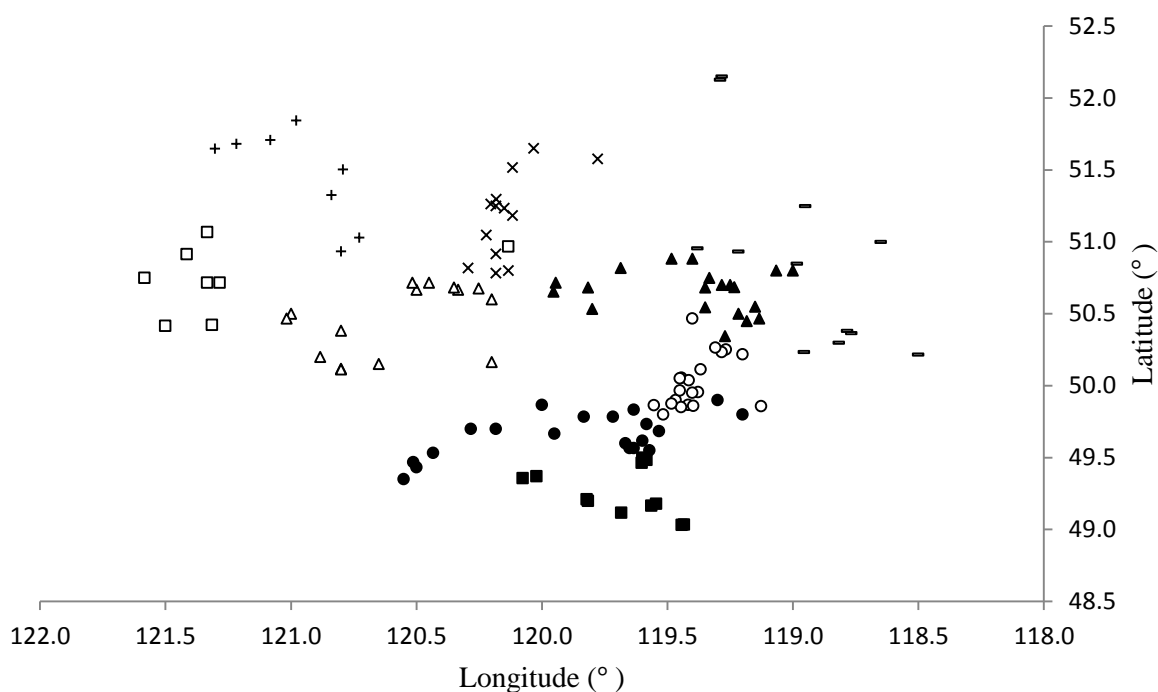
- ● **Princeton A Region:** Adra, Bankier Chain Lake, Chute Lake, Kelowna Bankhead, Kirton, McCulloch, Naramata (1924-1936), Naramata (1971-2004), Osprey Lake, Peachland, Peachland Brenda Mines, Peachland Trepanier Cr, Princeton, Princeton 8 NE, Princeton A, Similkameen Mine, Summerland, Summerland CDA, Summerland CDA EL, Westbank
- ■ **Penticton A Region:** Hedley, Hedley NP Mine, Keremeos, Keremeos 2, Mt Kobau Observatory, Oliver, Oliver STP, Osoyoos, Osoyoos West, Penticton, Penticton A, Penticton Sewage Plant
- ○ **Kelowna A Region:** Falkland Salmon Valley, Joe Rich Creek, Kelowna, Kelowna A, Kelowna CDA, Kelowna Dav-Spiers Road, Kelowna East, Kelowna Lakeview, Kelowna MWSO, Kelowna PC Burnetts Nurs, Okanagan Centre, Okanagan Mission, Oyama, Rutland Mission Creek, Vernon, Vernon (1971-1994), Vernon Bella Vista, Vernon Coldstream Ranch, Winfield, Woods Lake
- ▲ **Salmon Arm A Region:** Armstrong, Armstrong Hullcar, Armstrong North, Canoe Point, Chase, Enderby, Monte Creek, Monte Lake Paxton Valley, Pinantan Lake, Pritchard, Salmon Arm, Salmon Arm 2, Salmon Arm 3, Salmon Arm A, Sicamous, Silver Creek, Sorrento, Sorrento East, Tappen, Vernon North
- − **Blue River A Region:** Blue River A, Blue River North, Celista, Eagle Bay, Lumby, Lumby Sigalet Rd, Mabel Lake, Malakwa Eagle R Hatchery, Richland, Seymour Arm, Shuswap Falls, Sicamous 2
- × **Clearwater Region:** Barriere, Barriere North, Chinook Cove, Chinook Cove Posby Lake, Clearwater, Clearwater Axel Crk, Darfield, Heffley Creek, Kamloops Rayleigh, McLure, Mt Lolo Admin Kamloops, Mt Lolo Kamloops, Vavenby
- □ **Cache Creek 16 Mile Region:** Ashcroft M, Ashcroft (1912-1970), Cache Creek 16 Mile, Hat Creek, Knouff Lake, Loon Lake, Spences Bridge, Spences Bridge Nicola
- + **100 Mile House Region:** 100 Mile House, 100 Mile House 6 NE, Bridge Lake 2, Buffalo Lake, Criss Creek, Red Lake, Ruth Lake, Vidette Lake Sharpe Lake
- △ **Kamloops Region:** Douglas Lake, Highland Valley BCCL, Highland Valley Lornex, Kamloops, Kamloops Afton Mines, Kamloops CDA, Kamloops Mission Flats, Kamloops Pratt Road, Kamloops Valleyview, Mamit Lake, Merritt, Merritt Craigmont Mines, Merritt STP, Nicola Lake, Tranquille
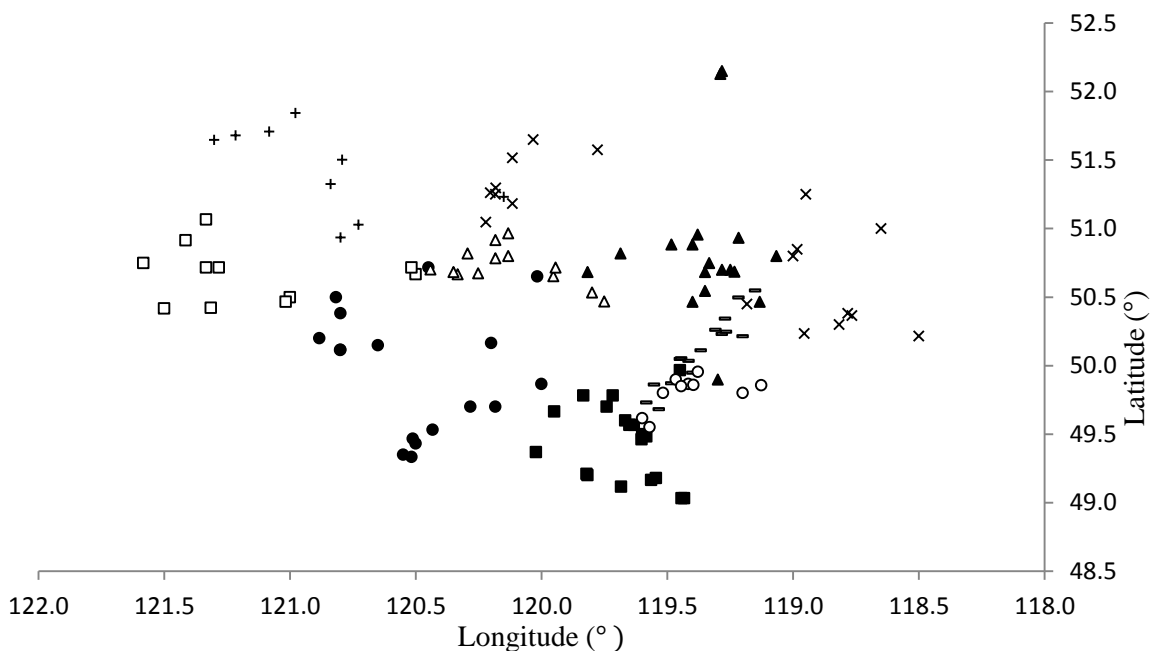
+ **100 Mile House Region:** 100 Mile House, 100 Mile House 6 NE, Barriere North, Bridge Lake 2, Buffalo Lake, Criss Creek, Red Lake, Ruth Lake, Vidette Lake Sharpe Lake

■ **Penticton A Region:** Hedley NP Mine, Keremeos, Keremeos 2, Kirton, Mt Kobau Observatory, Oliver, Oliver STP, Osoyoos, Osoyoos West, Peachland, Peachland Greata Ranch, Peachland Trepanier Cr, Penticton, Penticton A, Penticton Sewage Plant, Rutland Mission Creek, Summerland, Summerland CDA, Summerland CDA EL

– **Vernon Region:** Adra, Armstrong Hullcar, Chute Lake, Enderby, Kelowna Lakeview, Kelowna MWSO, Kelowna PC Burnetts Nurs, Okanagan Centre, Oyama, Vernon, Vernon (1971-1994), Vernon Bella Vista, Vernon Coldstream Ranch, Vernon North, Winfield, Woods Lake

□ **Cache Creek 16 Mile Region:** Ashcroft M, Ashcroft (1912-1970), Cache Creek 16 Mile, Hat Creek, Highland Valley BCCL, Highland Valley Lornex, Kamloops Afton Mines, Loon Lake, Spences Bridge, Spences Bridge Nicola, Tranquille

● **Princeton A Region:** Bankier Chain Lake, Douglas Lake, Kamloops CDA, Logan Lake, Mamit Lake, Merritt, Merritt Craigmont Mines, Merritt STP, Monte Creek West, Nicola Lake, Osprey Lake, Peachland Brenda Mines, Princeton, Princeton 8 NE, Princeton A, Similkameen Copper Mtn, Similkameen Mine

△ **Kamloops A Region:** Heffley Creek, Kamloops, Kamloops A, Kamloops Mission Flats, Kamloops Rayleigh, Kamloops Valleyview, Knouff Lake, Monte Creek, Monte Lake Paxton Valley, Mt Lolo Admin Kamloops, Mt Lolo Kamloops, Pinantan Lake, Westwold

× **Clearwater Region:** Armstrong, Barriere, Chinook Cove, Chinook Cove Posby Lake, Clearwater, Clearwater Axel Crk, Darfield, Lumby, Lumby Sigalet Rd, Mabel Lake, Malakwa Eagle R Hatchery, McLure, Richland, Seymour Arm, Shuswap Falls, Sicamous, Sicamous 2, Vavenby

▲ **Salmon Arm A Region:** Armstrong North, Blue River A, Blue River North, Canoe Point, Celista, Chase, Eagle Bay, Falkland Salmon Valley, Kelowna Bankhead, Pritchard, Salmon Arm, Salmon Arm 2, Salmon Arm 3, Salmon Arm A, Silver Creek, Sorrento, Sorrento East, Tappen

○ **Kelowna A Region:** Joe Rich Creek, Kelowna, Kelowna A, Kelowna CDA, Kelowna Dav-Spiers Road, Kelowna East, McCulloch, Naramata (1924-1936), Naramata (1971-2004), Okanagan Mission

Figure 2.5.C. Final homogeneous regions for summer maximum daily rainfall.
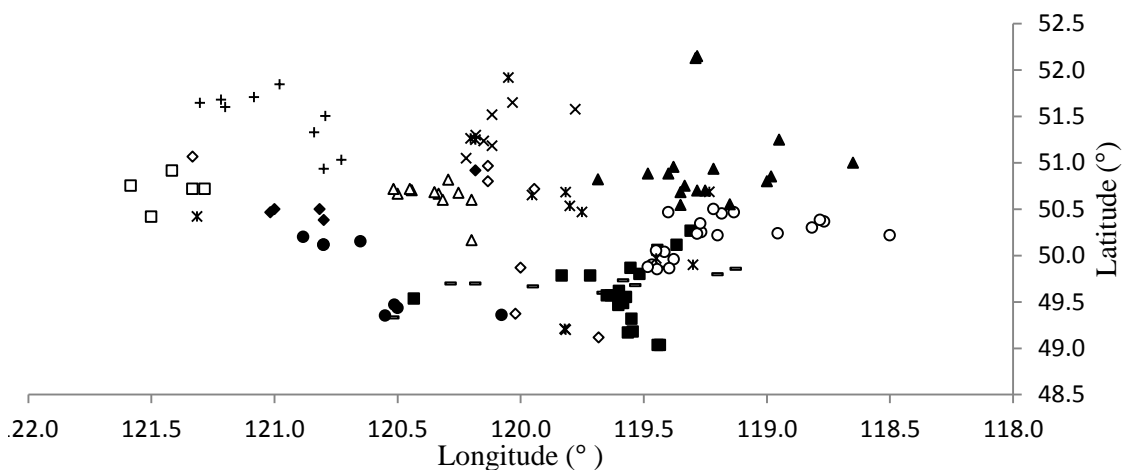
- **Summerland Region:** Adra, Bankier Chain Lake, Chute Lake, Joe Rich Creek, Kelowna CDA, Kirton, McCulloch, Osprey Lake, Similkameen Copper Mtn, Summerland
- **Kamloops A Region:** Douglas Lake, Kamloops, Kamloops A, Kamloops Afton Mines, Kamloops CDA, Kamloops Mission Flats, Kamloops Pratt Road, Kamloops Rayleigh, Kamloops Valleyview, Knutsford 2S, Tranquille
- **Penticton A Region:** Kelowna Lakeview, Naramata (1924-1936), Naramata (1971-2004), Okanagan Centre, Okanagan Falls 2S, Okanagan Mission, Oliver, Oliver STP, Osoyoos, Osoyoos West, Oyama, Peachland, Peachland Trepanier Cr, Penticton, Penticton A, Penticton Sewage Plant, Princeton 8 NE, Summerland CDA, Summerland CDA EL, Vernon Bella Vista
- **100 Mile House Region:** 100 Mile House, 100 Mile House 6 NE, Bridge Lake 2, Buffalo Lake, Criss Creek, Horse Lake, Red Lake, Ruth Lake, Vidette Lake Sharpe Lake
- **Kelowna A Region:** Armstrong, Armstrong Hullcar, Armstrong North, Falkland Salmon Valley, Kelowna, Kelowna A, Kelowna Dav-Spiers Road, Kelowna East, Kelowna PC Burnetts Nurs, Lumby, Lumby Sigalet Rd, Mabel Lake, Richland, Shuswap Falls, Vernon, Vernon (1971-1994), Vernon Coldstream Ranch, Vernon North, Winfield, Woods Lake
- **Princeton A Region:** Hedley, Merritt, Merritt Craigmont Mines, Merritt STP, Nicola Lake, Princeton, Princeton A, Similkameen Mine
- **Cache Creek 16 Mile Region:** Ashcroft M, Ashcroft (1912-1970), Cache Creek 16 Mile, Hat Creek, Spences Bridge
- **Clearwater Region:** Barriere, Barriere North, Clearwater, Clearwater Axel Crk, Darfield, McLure, Vavenby
- **Salmon Arm Region:** Blue River A, Blue River North, Celista, Chase, Eagle Bay, Enderby, Malakwa Eagle R Hatchery, Salmon Arm, Salmon Arm 2, Salmon Arm 3, Seymour Arm, Sicamous, Sicamous 2, Silver Creek, Sorrento, Sorrento East, Tappen
- **Monte Creek Region:** Chinook Cove, Chinook Cove Posby Lake, Hemp Creek Clearwater, Kelowna Bankhead, Keremeos, Keremeos 2, Monte Creek, Monte Lake Paxton Valley, Pritchard, Rutland Mission Creek, Salmon Arm A, Spences Bridge Nicola, Westwold
- **Logan Lake Region:** Heffley Creek, Highland Valley BCCL, Highland Valley Lornex, Logan Lake, Mamit Lake
- **Mt Kobau Observatory Region:** Hedley NP Mine, Knouff Lake, Loon Lake, Mt Kobau Observatory, Mt Lolo Kamloops, Peachland Brenda Mines, Pinantan Lake

Figure 2.5.D. Final homogeneous regions for winter maximum daily rainfall.
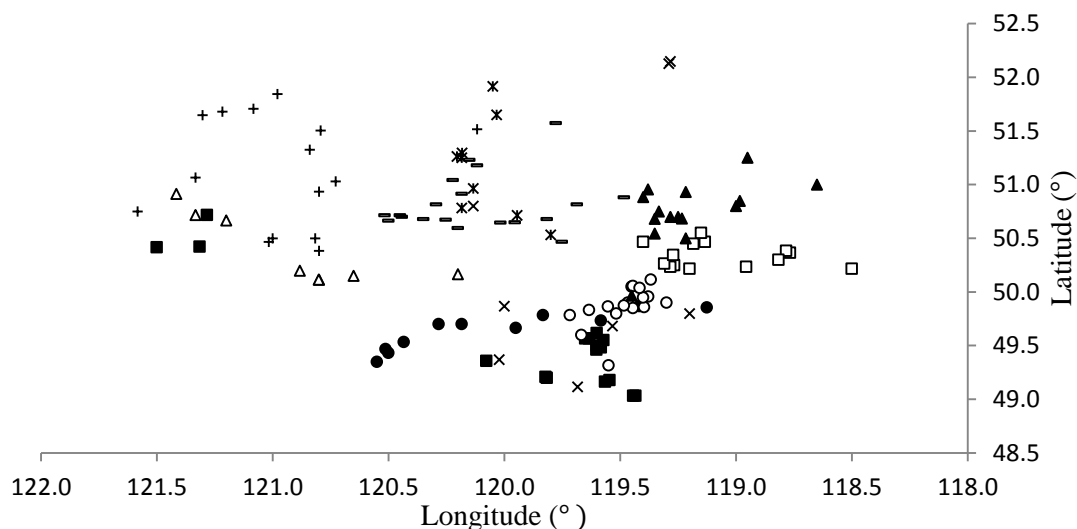
- **Princeton A Region:** Adra, Bankier Chain Lake, Joe Rich Creek, Kelowna CDA, Kirton, Osprey Lake, Peachland Trepanier Cr, Princeton, Princeton 8 NE, Princeton A, Similkameen Mine, Woods Lake
- **Mt Kobau Observatory Region:** Blue River A, Blue River North, Chute Lake, Hedley NP Mine, McCulloch, Mt Kobau Observatory, Mt Lolo Kamloops, Peachland Brenda Mines
- **Cache Creek 16 Mile Region:** Ashcroft M, Cache Creek 16 Mile, Douglas Lake, Kamloops, Merritt, Merritt, Craigmont Mines, Merritt STP, Nicola Lake
- **Penticton A Region:** Ashcroft (1912-1970), Hedley, Keremeos, Keremeos 2, Naramata (1924-1936), Naramata (1971-2004), Oliver, Oliver STP, Osoyoos, Osoyoos West, Penticton, Penticton A, Penticton Sewage Plant, Spences Bridge, Spences Bridge Nicola, Summerland CDA, Summerland CDA EL
- **Kelowna A Region:** Kelowna, Kelowna A, Kelowna Bankhead, Kelowna Dav-Spiers Road, Kelowna East, Kelowna Lakeview, Kelowna MWSO, Kelowna PC Burnetts Nurs, Okanagan Centre, Okanagan Falls 2S, Okanagan Mission, Oyama, Peachland, Summerland, Westbank, Winfield
- **Logan Lake Region:** 100 Mile House, 100 Mile House 6 NE, Bridge Lake 2, Buffalo Lake, Clearwater Axel Crk, Criss Creek, Hat Creek, Highland Valley BCCL, Highland Valley Lornex, Logan Lake, Loon Lake, Mamit Lake, Red Lake, Ruth Lake, Vidette Lake Sharpe Lake
- **Vernon Region:** Armstrong, Armstrong North, Enderby, Falkland Salmon Valley, Lumby, Lumby Sigalet Rd, Mabel Lake, Richland, Shuswap Falls, Vernon, Vernon (1971-1994), Vernon Bella Vista, Vernon Coldstream Ranch, Vernon North
- **Salmon Arm A Region:** Armstrong Hullcar, Celista, Eagle Bay, Malakwa Eagle R Hatchery, Rutland Mission Creek, Salmon Arm, Salmon Arm 2, Salmon Arm 3, Salmon Arm A, Seymour Arm, Sicamous, Sicamous 2, Silver Creek, Sorrento East, Tappen
- **Kamloops A Region:** Barriere, Barriere North, Chase, Heffley Creek, Kamloops A, Kamloops Afton Mines, Kamloops CDA, Kamloops Mission Flats, Kamloops Pratt Road, Kamloops Rayleigh, Kamloops Valleyview, McLure, Monte Creek, Monte Creek West, Pritchard, Sorrento, Tranquille, Vavenby, Westwold
- **Clearwater Region:** Chinook Cove, Chinook Cove Posby Lake, Clearwater, Darfield, Hemp Creek Clearwater, Knouff Lake, Monte Lake Paxton Valley, Mt Lolo Admin Kamloops, Pinantan Lake

Figure 2.5.E. Final homogeneous regions for fall maximum daily snowfall.
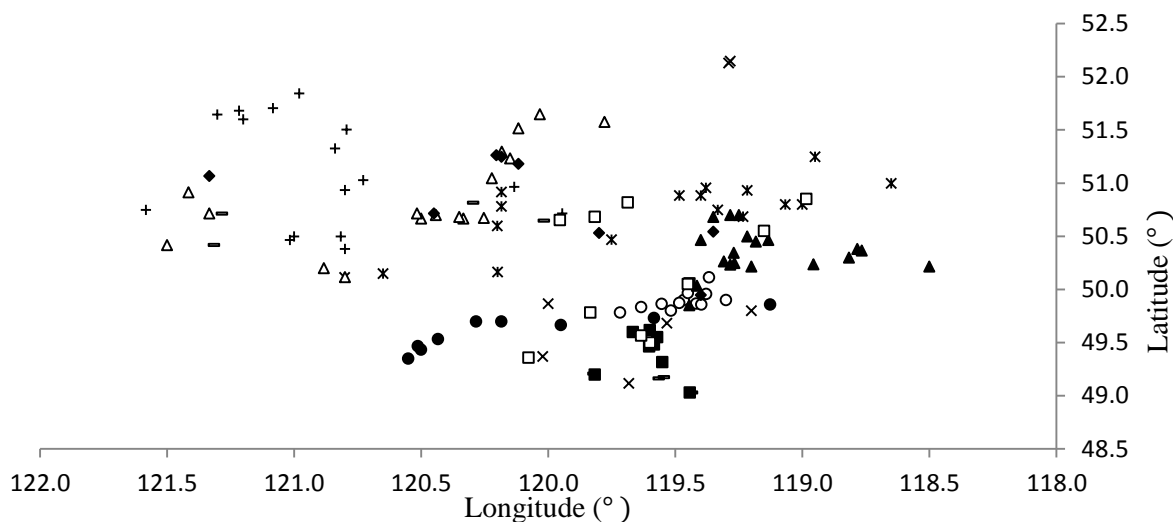
- **Princeton A:** Adra, Bankier Chain Lake, Joe Rich Creek, Kirton, Osprey Lake, Princeton, Princeton 8 NE, Princeton A, Similkameen Mine
- **Mt Kobau Observatory Region:** Blue River A, Blue River North, Chute Lake, Hedley NP Mine, McCulloch, Mt Kobau Observatory, Peachland Brenda Mines
- **Salmon Arm A Region:** Canoe Point, Celista, Douglas Lake, Eagle Bay, Heffley Creek, Kamloops Pratt Road, Malakwa Eagle R Hatchery, Merritt STP, Mt Lolo Admin Kamloops, Nicola Lake, Salmon Arm A, Seymour Arm, Sicamous, Sorrento, Sorrento East, Tappen, Westwold
- **Kamloops A Region:** Ashcroft M, Barriere North, Cache Creek 16 Mile, Clearwater, Clearwater Axel Crk, Darfield, Kamloops, Kamloops A, Kamloops Afton Mines, Kamloops Mission Flats, Kamloops Valleyview, McLure, Merritt, Merritt Craigmont Mines, Spences Bridge, Tranquille, Vavenby
- **Logan Lake Region:** 100 Mile House, 100 Mile House 6 NE, Bridge Lake 2, Buffalo Lake, Criss Creek, Hat Creek, Highland Valley BCCL, Highland Valley Lornex, Horse Lake, Knouff Lake, Logan Lake, Mamit Lake, Pinantan Lake, Red Lake, Ruth Lake, Vidette Lake Sharpe Lake
- **Penticton A Region:** Keremeos, Naramata (1924-1936), Naramata (1971-2004), Okanagan Falls 2S, Osoyoos West, Penticton, Penticton A, Summerland
- **Kelowna A Region:** Kelowna, Kelowna A, Kelowna Bankhead, Kelowna CDA, Kelowna East, Kelowna Lakeview, Kelowna PC Burnetts Nurs, Okanagan Mission, Oyama, Peachland, Rutland Mission Creek, Westbank
- **Vernon Region:** Armstrong, Armstrong Hullcar, Armstrong North, Falkland Salmon Valley, Kelowna Dav-Spiers Road, Lumby, Lumby Sigalet Rd, Mabel Lake, Richland, Salmon Arm, Salmon Arm 2, Salmon Arm 3, Shuswap Falls, Vernon, Vernon (1971-1994), Vernon Bella Vista, Vernon Coldstream Ranch, Vernon North, Winfield
- **Monte Creek Region:** Chase, Enderby, Hedley, Monte Creek, Okanagan Centre, Peachland Trepanier Cr, Penticton Sewage Plant, Pritchard, Sicamous 2, Summerland CDA EL, Woods Lake
- **Oliver Region:** Ashcroft (1912-1970), Kamloops Rayleigh, Keremeos 2, Monte Creek West, Oliver, Oliver STP, Osoyoos, Spences Bridge
- **Kamloops CDA Region:** Barriere, Chinook Cove, Chinook Cove Posby Lake, Kamloops CDA, Kelowna MWSO, Loon Lake, Monte Lake Paxton Valley, Silver Creek

Figure 2.5.F. Final homogeneous regions for spring maximum daily snowfall.
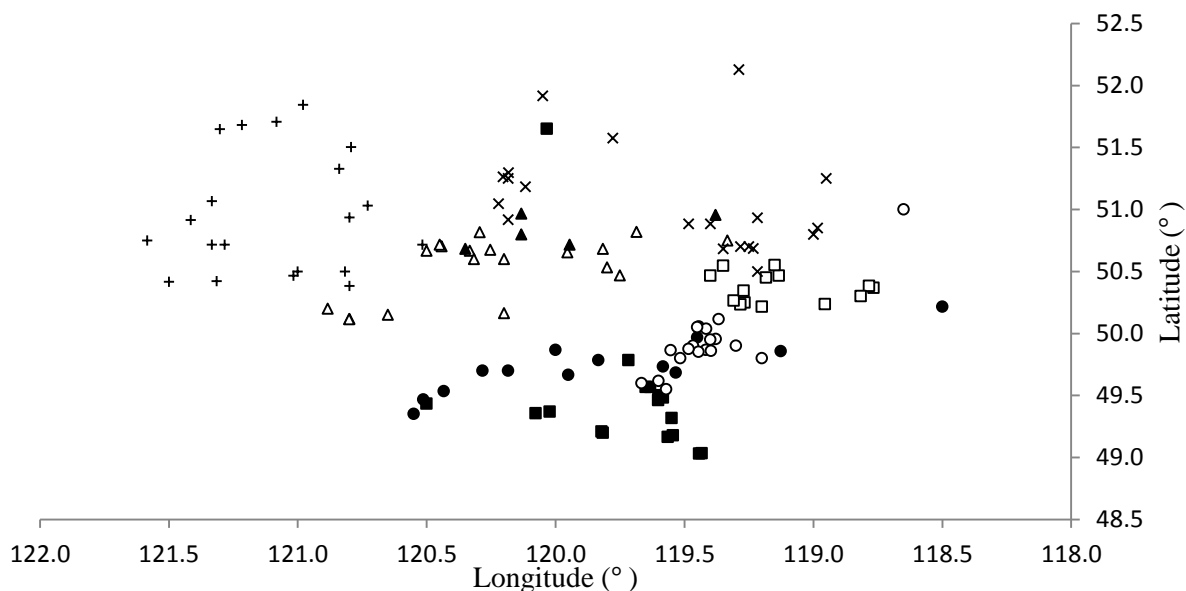
- **Princeton A Region:** Adra, Bankier Chain Lake, Chute Lake, Joe Rich Creek, Kirton, Osprey Lake, Peachland Brenda Mines, Peachland Trepanier Cr, Princeton 8 NE, Princeton A, Richland, Rutland Mission Creek, Similkameen Mine
- **Kamloops A Region:** Chase, Douglas Lake, Kamloops, Kamloops A, Kamloops Afton Mines, Kamloops CDA, Kamloops Pratt Road, Kamloops Rayleigh, Kamloops Valleyview, Knutsford 2S, Merritt, Merritt Craigmont Mines, Merritt STP, Monte Creek, Monte Lake Paxton Valley, Nicola Lake, Pritchard, Tappen, Westwold
- **Penticton A Region:** Clearwater, Hedley, Hedley NP Mine, Keremeos, Keremeos 2, Okanagan Falls 2S, Oliver, Oliver STP, Osoyoos, Osoyoos West, Peachland, Penticton, Penticton A, Penticton Sewage Plant, Princeton, Summerland CDA, Summerland CDA EL
- **Kelowna A Region:** Kelowna, Kelowna A, Kelowna Bankhead, Kelowna CDA, Kelowna Dav-Spiers Road, Kelowna East, Kelowna Lakeview, Kelowna MWSO, Kelowna PC Burnetts Nurs, Malakwa Eagle R Hatchery, McCulloch, Naramata (1924-1936), Naramata (1971-2004), Okanagan Centre, Okanagan Mission, Oyama, Summerland, Winfield, Woods Lake
- **Cache Creek 16 Mile Region:** 100 Mile House, 100 Mile House 6 NE, Ashcroft M, Ashcroft (1912-1970), Bridge Lake 2, Buffalo Lake, Cache Creek 16 Mile, Criss Creek, Hat Creek, Highland Valley BCCL, Highland Valley Lornex, Logan Lake, Loon Lake, Mamit Lake, Red Lake, Ruth Lake, Spences Bridge, Spences Bridge Nicola, Tranquille, Vidette Lake Sharpe Lake
- **Vernon Region:** Armstrong, Armstrong North, Enderby, Falkland Salmon Valley, Lumby, Lumby Sigalet Rd, Mabel Lake, Shuswap Falls, Silver Creek, Vernon, Vernon (1971-1994), Vernon Bella Vista, Vernon Coldstream Ranch, Vernon North
- **Salmon Arm A Region:** Armstrong Hullcar, Barriere, Blue River A, Chinook Cove, Chinook Cove Posby Lake, Darfield, Eagle Bay, Heffley Creek, Hemp Creek Clearwater, McLure, Salmon Arm, Salmon Arm 2, Salmon Arm 3, Salmon Arm A, Seymour Arm, Sicamous, Sicamous 2, Sorrento, Sorrento East, Vavenby
- **Knouff Lake Region:** Celista, Kamloops Mission Flats, Knouff Lake, Mt Lolo Kamloops, Pinantan Lake

Figure 2.5.G. Final homogeneous regions for winter maximum daily snowfall.

exception of Merritt and Cache Creek 16 Mile regions. These two regions were dispersed due to different factors. Merritt region had the majority of its stations near the Nicola Valley / Logan Lake area but also included Mt. Kobau Observatory (located between Keremeos and Osoyoos). Cache Creek 16 Mile region consisted of three distinct side-by-side groups of stations extending from Spences Bridge to Clearwater.

Nine acceptably homogeneous regions were also developed for the spring maximum daily rainfall data set (Figure 2.5B). Overall the 9 regions were similar to the fall maximum daily rainfall regions except for the grouping of the far west stations. The large fall maximum daily rainfall Cache Creek 16 Mile region split into a much smaller Cache Creek 16 Mile region and a new 100 Mile House region for the spring maximum daily rainfall. This could be due to a higher average elevation and mean spring rainfall for 100 Mile House region compared to Cache Creek 16 Mile region.

Summer maximum daily rainfall's 9 regions (Figure 2.5C) were almost identical to the spring maximum daily rainfall's regions with the exception of the north Okanagan area. This area split into two regions; Kelowna A region was made up mostly by stations located around the northern and middle Okanagan Lake area, while Vernon region had stations extending from Armstrong down the valley to Kelowna. Vernon region had higher mean summer rainfall compared to Kelowna A region, possibly due to the influence of three area lakes: Okanagan Lake, Swan Lake and Kalamalka Lake.

Winter maximum daily rainfall's precipitation patterns for the Thompson and Okanagan regions were very different from the other seasonal rainfall. While the rest of the seasonal rainfall data sets had 9 regions, winter rainfall data's regions increased to 12 (Figure 2.5D). Overall, elevation appeared to influence grouping of stations more than the other site characteristics; this is a plausible explanation since freezing level – which determines whether a station receives rain or snow as precipitation – varies the most during the winter season for different locations in the southern interior of British Columbia. Monte Creek region was the most geographically dispersed, extending from Hemp Creek Clearwater to Keremeos.

Fall maximum daily snowfall had 10 regions (Figure 2.5E) that were overall geographically cohesive with the exception of Mt Kobau Observatory region. This region extended from Blue River A to Mt Kobau Observatory and contained the stations with the highest mean fall snowfall (either due to a northern location or high elevation). These different regions reflected the wide variation in mean fall snowfall for the southern interior of British Columbia. The lowest average mean fall snowfall was in the Penticton A and Cache Creek regions; these regions are the most westerly and southerly for the Thompson and Okanagan regions and perhaps the most influenced by warm temperatures during this season.

Spring maximum daily snowfall had 11 regions (Figure 2.5F) similar to fall maximum daily snowfall with the exception of the southern Okanagan area. This area split into two regions: Penticton A and Oliver. Oliver region contained the most southerly stations in the Thompson and Okanagan regions and had the lowest mean spring snowfall.

Winter maximum daily snowfall had the least amount of regions for all the seasonal rainfall and snowfall data sets (Figure 2.5G). This is reflective of the frontal precipitation that is common during the winter months. These 8 regions were overall geographically cohesive with the exception of Penticton A and Kelowna A. These two regions each had a station outside of their general area. Interestingly, these stations – Malakwa Eagle R Hatchery and Clearwater – both had similar elevations to the rest of the stations in their respective regions, but significantly higher mean winter snowfall.

Development of estimated quantiles

Frequency distribution choice

The goodness-of-fit measure was computed for each of the seasonal rainfall and snowfall regions (see Appendix 2.F). Since all the regions were acceptably homogeneous, five three-parameter candidate distributions were tested: GLO, GEV, GNO, GPA and PE3. L-moment plots displayed in Appendix 2.F were generated to verify the best fitted distribution. Most regions had more than one acceptable candidate distribution; if that case, the distribution with the lowest $|Z|$ value was chosen. One region had two candidate distributions with equal lowest $|Z|$ values. Both distributions were chosen for this region.

There were six regions where none of the candidate distributions were accepted by the *Z* criterion: summer maximum daily rainfall Princeton A region, fall maximum daily snowfall Penticton A, Kelowna A and Vernon regions, and spring maximum daily snowfall Kelowna A and Vernon regions. Examination of the L-moment plots showed that for summer maximum daily rainfall Princeton A region, fall maximum daily snowfall Penticton A and Kelowna A regions, and spring maximum daily snowfall Kelowna A region the regional average point laid above GLO; therefore, Wakeby distribution was selected for those regions. The regional average point for fall maximum daily snowfall and spring maximum daily snowfall Vernon regions lay between two distributions; in this situation, both distributions were accepted. Frequency distribution choice is summarized in Tables 2.5A and 2.5B.

Exact zero data values

Certain seasonal data had a large amount of exact zero values. Using the algorithm from Figure 2.2, it was discovered that the majority of winter maximum daily rainfall, fall maximum daily snowfall and spring maximum daily snowfall regions needed to use a Wakeby mixed model distribution with the lower bound constrained to zero. Further investigation of the mixed model paradigm showed that constructing quantiles and the associated RMSEs and error bounds for data sets with exact zeroes was a complicated and time-consuming endeavour. Thus, it was decided to set aside any further analysis of these three seasonal data sets for future research.

Regional quantile estimates

The quantiles (growth curves) of the regional frequency distributions were obtained by fitting the final chosen frequency distributions to each region's data using the regional L-moment algorithm. The regional quantile estimates for the 1, 2, 5, 10, 20, 50 and 100 year return periods along with the final fitted distribution parameters are shown in Appendix 1.2. These regional quantile estimates can be graphically displayed as a regional quantile function. An example is Figure 2.6 showing the regional quantile function of spring

Table 2.5. A Summary of acceptable frequency distributions (Generalized Logistic: GLO, Generalized Extreme Value: GEV, Generalized Normal: GNO, Pearson Type III: PE3, Generalized Pareto: GPA, Wakeby: WAK) for seasonal maximum daily rainfall data sets. Acceptable fitted distributions with lowest $|Z|$ are bolded.

Season	Region	Acceptable fitted distribution					Final chosen distribution
Fall	Princeton A		**GEV**	GNO	PE3		GEV
	Monte Creek		GEV	GNO	**PE3**		PE3
	Kelowna		GEV	**GNO**	PE3		GNO
	Penticton A		GEV	**GNO**	PE3		GNO
	Cache Creek 16 Mile	GLO	GEV	**GNO**	PE3		GNO
	Merritt	**GLO**	GEV	GNO		GPA	GLO
	Salmon Arm A		GEV	**GNO**	PE3		GNO
	Kamloops A	GLO	**GEV**	GNO			GEV
	Blue River A		**GEV**	GNO	PE3		GEV
Spring	Princeton A	**GLO**					GLO
	Penticton A	**GLO**					GLO
	Kelowna A		GEV	**GNO**	PE3		GNO
	Salmon Arm A		**GEV**	GNO	PE3		GEV
	Blue River A		**GEV**	GNO	PE3		GEV
	Clearwater	**GLO**	GEV	GNO			GLO
	Cache Creek 16 Mile	GLO	**GEV**	GNO	PE3		GEV
	100 Mile House	**GLO**					GLO
	Kamloops	**GLO**	GEV				GLO
Summer	100 Mile House	GLO	**GEV**	GNO	PE3		GEV
	Penticton A		**GEV**	GNO			GEV
	Vernon		GEV	GNO	**PE3**		PE3
	Cache Creek 16 Mile		GEV	GNO	**PE3**		PE3
	Princeton A	none *					WAK
	Kamloops A	GLO	**GEV**	GNO	PE3		GEV
	Clearwater		**GEV**	GNO			GEV
	Salmon Arm A	**GLO**					GLO
	Kelowna A	GLO	**GEV**	GNO	PE3		GEV

Season	Region	Acceptable fitted distribution					Final chosen distribution
Winter	Summerland				PE3	**GPA**	WAK ***
	Kamloops A		**GEV ****	**GNO ****	PE3		WAK ***
	Penticton A	**GLO**	GEV				GLO
	100 Mile House	GLO	GEV	**GNO**	PE3	GPA	WAK ***
	Kelowna A	**GLO**	GEV				GLO
	Princeton A	**GLO**	GEV	GNO			WAK ***
	Cache Creek 16 Mile	GLO	**GEV**	GNO	PE3		WAK ***
	Clearwater	**GLO**					GLO
	Salmon Arm	**GLO**					GLO
	Monte Creek	GLO	**GEV**	GNO	PE3		GEV
	Logan Lake	GLO	**GEV**	GNO	PE3	GPA	WAK ***
	Mt Kobau Observatory	GLO	GEV	GNO	**PE3**	GPA	WAK ***

* no acceptable candidate distributions. Regional average point lies above GLO (Appendix 2.F) therefore Wakeby used. ** two |Z| minimum acceptable candidate distributions. *** Wakeby with fixed lower bound $\xi = 0$

maximum daily rainfall Penticton A region. From these regional quantile functions, site quantiles for a particular station are calculated by combining the regional quantile estimates (growth curve value) for the region in which the station is located with the station's index-flood. For example, the spring maximum daily rainfall 1 year return period site quantile for Osoyoos can be derived by using the regional quantile function given in Figure 2.6. From this regional quantile function, the 100 year return period growth curve is determined to be 2.982. Combined with the spring rainfall Osoyoos' index-flood listed in Appendix 2.E as 77.2 mm, the Osoyoos spring maximum daily rainfall 100 year return period site quantile is calculated to be 230.2 mm. This demonstrates that once a regional quantile function is generated, site quantiles for any station within that region can be easily calculated as long as the station index-flood is available.

Table 2.5.B. Summary of acceptable frequency distributions (Generalized Logistic: GLO, Generalized Extreme Value: GEV, Generalized Normal: GNO, Pearson Type III: PE3, Generalized Pareto: GPA, Wakeby: WAK) for seasonal maximum daily snowfall data sets. Acceptable fitted distributions with lowest $|Z|$ are bolded.

Season	Region	Acceptable fitted distribution				Final chosen distribution
Fall	Princeton A		GEV	**GNO**	PE3	GNO
	Mt Kobau Observatory	**GLO**	GEV	GNO		GLO
	Cache Creek		GEV	GNO	**PE3** GPA	WAK ***
	Penticton A	none *				WAK ***
	Kelowna A	none *				WAK ***
	Logan Lake	GLO	**GEV**	GNO		GEV
	Vernon	none **				WAK ***
	Salmon Arm A		GEV	GNO	**PE3**	WAK ***
	Kamloops A				**PE3** GPA	WAK ***
	Clearwater		GEV	GNO	**PE3**	WAK ***
Spring	Princeton A	**GLO**	GEV	GNO		WAK ***
	Mt Kobau Observatory	**GLO**	GEV	GNO	PE3	GLO
	Salmon Arm A				**PE3**	WAK ***
	Kamloops A				PE3 **GPA**	WAK ***
	Logan Lake		GEV	**GNO**	PE3	GNO
	Penticton A				**PE3**	WAK ***
	Kelowna A	none *				WAK ***
	Vernon	none **				WAK ***
	Monty Creek				**PE3**	WAK ***
	Oliver				**PE3**	WAK ***
	Kamloops CDA				PE3 **GPA**	WAK ***
Winter	Princeton A		GEV	**GNO**	PE3	GNO
	Kamloops A		GEV	**GNO**	PE3	GNO
	Penticton A	**GLO**				GLO
	Kelowna A	**GLO**	GEV			GLO
	Cache Creek 16 Mile	**GLO**	GEV			GLO
	Vernon	**GLO**	GEV			GLO
	Salmon Arm A	**GLO**				GLO
	Knouff Lake	**GLO**				GLO

* no acceptable candidate distributions. Regional average point lies below GPA (Appendix F) therefore Wakeby used. ** none of candidate distributions are acceptable. Regional average point lies between two distributions (Appendix 2.F). *** Wakeby with fixed lower bound $\xi = 0$
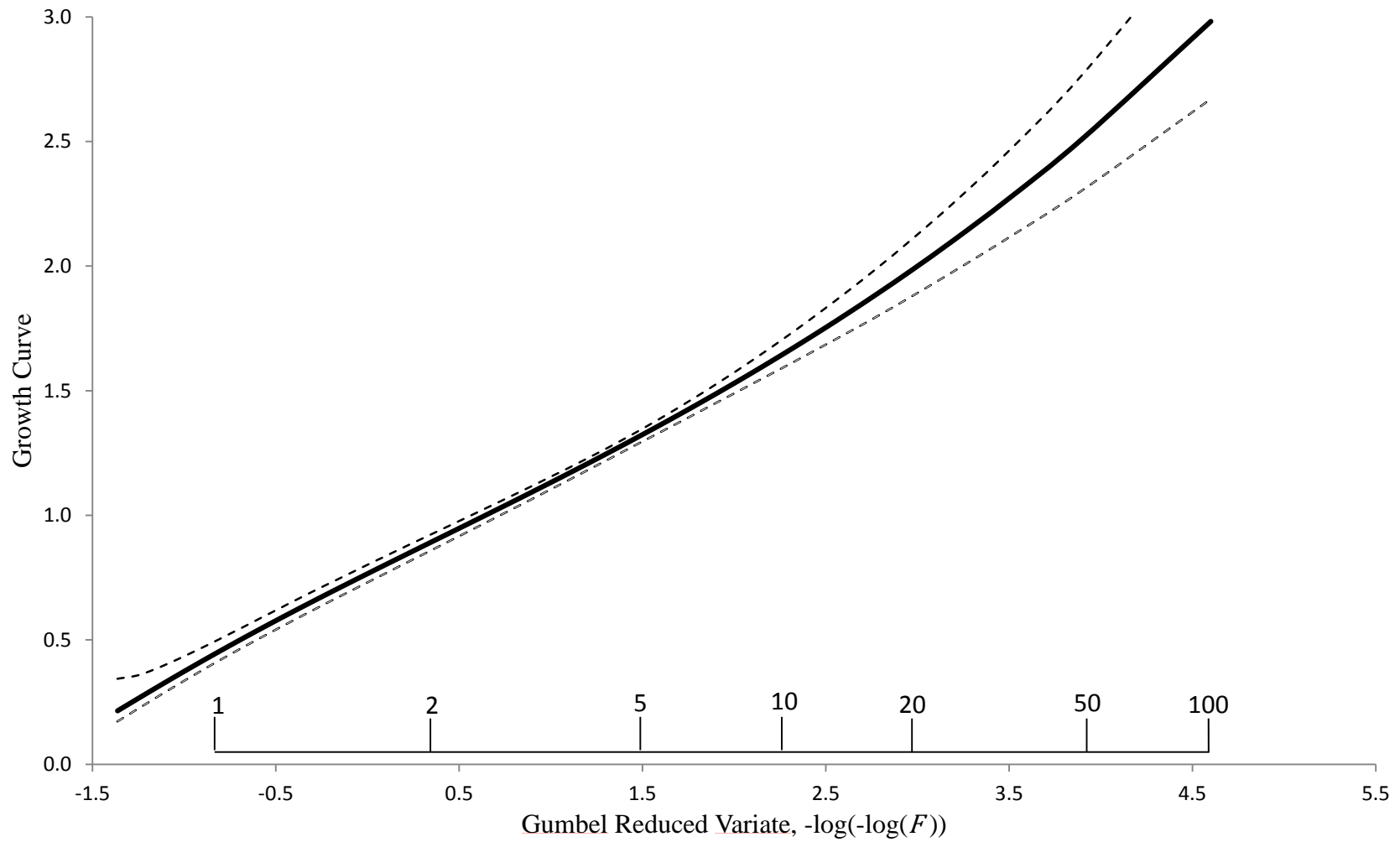
Figure 2.6. Penticton A region spring maximum daily rainfall regional growth curve (regional quantile estimates) as a function of Gumbel reduced variation of non-exceedance probability (F) (solid line) with 90% error bounds (dotted lines).

Precision of estimated regional quantiles

A Monte Carlo simulation generated RMSEs and error bounds at the 90% significance level to determine the precision of the estimated regional quantiles. The simulations assumed homogeneous regions and were tailored for each region's different fitted distribution. A Spearman rank correlation matrix was developed to account for any intersite dependence within an actual region and included in the simulation algorithm. Appendix 2.G shows the matrixes of the 7 seasonal rainfall and snowfall data sets. A full list of regional quantile estimates with associated RMSEs and error bounds from non-exceedance probabilities 0.02 to 0.99 is given in Appendix 2.H.

Comparison of regional and at-site estimation

A reason for using a RFA over an at-site analysis is to generate more precise quantiles for a particular site. This is exemplified by a comparison of regional and at-site estimations. Appendix 2.I gives the results of regional and at-site frequency analyses for select stations. Overall, the estimated quantiles were similar with no systematic differences, even for the higher non-exceedance probabilities or when comparing number of data points per site. The RMSEs and error bounds for both associated RFA and the GEV distribution at-site analyses were also very similar. However, there was a large difference between the RFA and at-site estimators' RMSEs and error bounds. For a couple of stations, the RMSEs associated with lower non-exceedance probabilities (0.1 to 0.8) were the same for RFA and at-site estimator. For the vast majority of stations, the RMSE of the RFA was lower than that of the at-site estimator, sometimes by a large amount. At the more extreme quantile estimates, regional estimation produced a very large reduction in the RMSE of the estimates for some stations. Appendix 1.3 compares site quantile estimates for regional frequency analysis versus at-site analysis fitting the same distribution. On average, the RMSE of the RFA quantile was lower by a factor of 1.5 to 2.0 when compared to the corresponding at-site quantile. A few station data sets had a 100 year return period RFA RMSE lower by a factor of 5.0 compared to the corresponding at-site quantile. Figure 2.7 graphically shows the difference between the RFA RMSE and at-site RMSE for winter maximum daily snowfall One Hundred Mile House. This RMSE difference detected in the comparison could be due to the fact that RFA uses data from several or many sites that in turn can lower the variability of
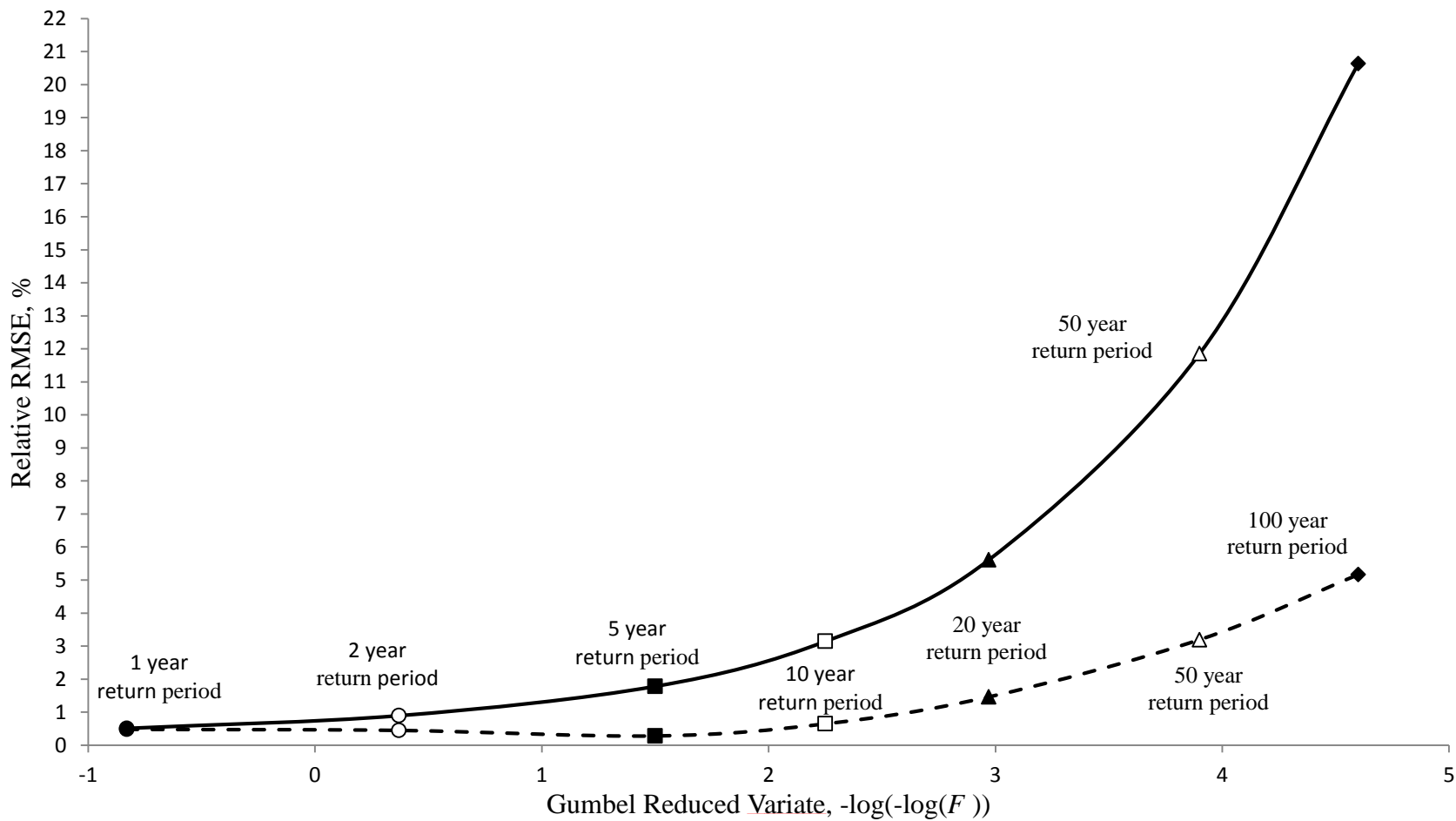
Figure 2.7. 100 Mile House winter maximum daily snowfall relative root mean square errors, RMSEs of estimated quantiles for associated return periods and Gumbel reduced variation of non-exceedance probability, *F*. Estimation method: at-site (solid line) and regional (dashed line).

the regional growth curve compared to the variability of the growth curve estimated from at-site data. It is this reduction in error bounds particularly at higher return periods that makes RFA a preferable method over an at-site analysis.

DISCUSSION AND CONCLUSIONS

A RFA using L-moments was used to calculate seasonal maximum daily rainfall and snowfall quantiles for the Thompson and Okanagan region. This method is both labour and computer intensive. The labour is devoted to constructing acceptably homogeneous regions. While a cluster analysis method was utilized to develop initial regions, extensive manual refinement using local weather knowledge was needed to achieve the final homogenous regions. There is a large amount of computational analysis also required for RFA using L-moments. Extensive use of computer code was needed to use the analysis software associated with $R^{©}$, and multiple Monte Carlo simulations were required for calculating heterogeneity measures, goodness-of-fit measures and error bounds. Regardless, RFA using L-moments was shown to be preferable to at-site analysis due to the reduction in quantile estimates' error bounds/RMSEs.

The extraction of the seasonal data from the Canadian Daily Climate Data CD was very time-consuming. The available meteorological data could only be accessed as batch files via the computer's command line interpreter. This meant that monthly data had to be transcribed from the batch files before seasonal data could be extracted. Daily rainfall and snowfall also had to be examined for flagged data. Even with the difficulties in collecting the required data, there are benefits in using seasonal versus annual meteorological data. Seasonal data are highly desired by industry and government agencies because it offers specific information about extreme events during particular times of the year. For example, agriculture would benefit from seasonal data. There is a need to know about the probability of springtime extreme precipitation events because heavy rainfall during the start of the growing season can hurt young plants. A seasonal delineation of extreme rainfall and snowfall events also helps with the forecast models of time-specific disaster occurrences such as spring flooding and winter avalanches.

It could be argued that using fixed seasons does not give a true representation of seasonal maxima, in particular for Canadian seasons that vary in length depending on location. Seasons are traditionally determined by the position of the sun; perhaps defining parameters and meteorological conditions that determine the occurrence of a particular season would be more appropriate. This would also be useful in examining if the start or duration of a season is changing.

Fall and spring maximum daily snowfall and winter maximum daily rainfall data sets had a large number of exact zero values. These data sets were successfully grouped into acceptably homogeneous regions and fitted with a Wakeby mixed model distribution with the lower bound constrained to zero. Unfortunately there were difficulties in developing regional quantile functions with associated error bounds for these data sets. The $R^{©}$ software package, lmomRFA version 3.0 that was used for this study's methodology currently does not have functions for mixed distributions; it was possible to manually develop regional quantile estimates, but the Monte Carlo simulations needed for calculating error bounds and RMSEs were impossible to run without the software package. Future versions of the lmomRFA package will hopefully include functions for mixed zero inflated models since the quantiles associated with these mixed models represent extremely rare extreme precipitation events.

For the remainder of the seasonal rainfall and snowfall data sets, regional quantile functions with associated error bounds and RMSEs were successfully developed. Site quantiles for stations within a region could be easily found by combining the regional growth curve values with a station's index-flood. A convenient way to present site quantiles developed by a RFA is with a regional quantile function graph and a list of associated regional stations with their average seasonal maximum daily rainfall or snowfall. It is also interesting to note that theoretically it is possible that quantiles could be estimated for a location with a known mean that was not used to calculate a regional growth curve but has a precipitation climate similar to the region.

This study examined daily extreme precipitation events. These events reflect short-term rainfall or snowfall that can be destructive in their intensity. However, there is scientific and practical merit in looking at multi-day consecutive extreme precipitation events. Significant rainfall and snowfall events occur with frontal precipitation; if a weather system stalls – as occurred over southwestern Alberta in 2013 – intense precipitation can last for

many days resulting in saturated ground and landslides, flooding, and collapse of buildings from snow accumulation. Quantile estimates developed from multi-day maxima could help predict the impact of heavy rainfall on already saturated ground, and the risk of failure from dams and spillways.

An interesting and unexpected result of this study was the statistical lack of any temporal trends or step changes detected in the serial dependence analyses; there was no overall change in the frequency of seasonal extreme rainfall or snowfall events for the Thompson and Okanagan regions. Many papers report a general world-wide increase in extreme weather events (e.g. Tencer *et al.*, 2014, Coumou and Rahmstorf, 2012, Fowler and Kilsby, 2003) but the Fifth Assessment Report of the Intergovernmental Panel on Climate Change advises that while increases in heavy precipitation have probably occurred since the mid-20th century, it varies from region to region (IPCC, 2013). This indicates that changes in the magnitude and frequency of heavy precipitation must be considered on a local and not global scale. Care should be used in interpreting the results from this study's serial dependence analyses as there are a number of reasons that could explain why trends and step changes were not detected. Only strong trends were investigated since the quality of the quantile estimates generated by a RFA is not sensitive to weak trends. If an objective of the study was to detect serial dependence in the data, utilizing the Bonferroni correction and FDR procedure to reduce Type 1 errors would have been inappropriate. Other explanations for the lack of serial dependence detected could be insufficient data or natural variability that perhaps would preclude any long-term temporal change in the precipitation data sets.

To the best of my knowledge, this study is the first RFA of seasonal rainfall and snowfall maxima for the Thompson and Okanagan regions. These regions have complex precipitation patterns and proved to be an excellent site for studying extreme rainfall and snowfall. Using seasonal instead of annual data gave insight into how precipitation varies from rain to snow throughout the year for the southern interior of British Columbia. It also brought into sharp focus the often-overlooked rare seasonal precipitation such as winter rainfall that is very important to consider when examining extreme events. Finally, RFA was shown to develop quantile estimates that are more precise than at-site estimates for the Thompson and Okanagan regions. Future research should build on these findings,

particularly examining seasonal multi-day extreme rainfall and snowfall events for high-risk areas prone to flooding, landslides and avalanches.

LITERATURE CITED

. Adamowski, K., Y. Alila, and P.J. Pilon. 1996. Regional rainfall distribution for Canada. *Atmospheric Research* 42 (1): 75-88.

Adamowski, K., and J. Bougadis, 2003. Detection of trends in annual extreme rainfall. *Hydrological Processes* 17 (18): 3547-3560.

Aguilar, E., I. Auer, M. Brunet, T. C. Peterson, and J. Wieringa. 2003. Guidance on metadata and homogenization. World Climate Programme Data and Monitoring WCDMP-No.53. WMO-TD No. 1186. Geneva: World Meteorological Organization.

Auld, H., D. MacIver, and J. Klaassen. 2004. Heavy rainfall and waterborne disease outbreaks: the Walkerton example. *Journal of Toxicology and Environmental Health, Part A* 67 (20-22): 1879-1887.

Berenson, M. L., and D. M. Levine. 1988. *Applied statistics: a first course*. Englewood Cliffs, New Jersey: Prentice-Hall.

Bland, J. M., and D. G. Altman. 1995. Multiple significance tests: the Bonferroni method. *BMJ* 310 (6973): 170.

Canadian Climate Program (1984a). *Principle Station Data Kamloops A* (PSD/DSP-36). Ottawa: Canadian Government Publishing Centre

Canadian Climate Program (1984b). *Principle Station Data Kelowna A* (PSD/DSP-37). Ottawa: Canadian Government Publishing Centre

Canadian Climate Program (1984c). *Principle Station Data Penticton A* (PSD/DSP-64). Ottawa: Canadian Government Publishing Centre

Carlyle-Moses, D., 2007. Maximum Daily Rainfall Depth Frequency Analysis for the Southern Interior Forest Region of British Columbia. Kamloops, Canada.

City of Toronto Climate Adaptation Steering Group, Clean Air Patnership, Toronto Environment   Office. 2008. "AHEAD OF THE STORM…Preparing Toronto for Climate Change".
http://www.climateneeds.umd.edu/reports/Toronto%20City-Preparing%20Toronto%20for%20Climate%20Change

Coumou, D., and S. Rahmstorf. 2012. A decade of weather extremes. *Nature Climate Change* 2 (7): 491-496.

Cunnane, C. 1988. Methods and merits of regional flood frequency analysis. *Journal of Hydrology* 100 (1): 269-290.

Dales, M. Y., and D. W. Reed. 1989. *Regional flood and storm hazard assessment*. Institute of Hydrology Report 102. Wallingford, Oxfordshire.

Environment Canada. 2014. Canada's Top Ten Weather Stories for 2013: 1. Alberta's Flood of Floods
http://ec.gc.ca/meteo-weather/default.asp?lang=En&n=5BA5EAFC-&offset=2&toc=show.

Fowler, H. J., and C.G. Kilsby. 2003. A regional frequency analysis of United Kingdom extreme rainfall from 1961 to 2000. *International Journal of Climatology* 23 (11): 1313-1334.

Greenwood, J. A., J.M. Landwehr, N.C. Matalas, and J.R. Wallis. 1979. Probability weighted moments: definition and relation to parameters of several distributions expressable in inverse form. *Water Resources Research*, 15 (5): 1049-1054.

Guttman, N. B., J. R. M. Hosking, and J. R. Wallis, 1993. Regional precipitation quantile values for the continental United States computed from L-moments. *Journal of Climate* 6 (12): 2326-2340.

Henstra, D., and G. McBean. 2009. Climate Change Adaptation and Extreme Weather. *Adaptation to Climate Change Team*.
http://act-adapt.org/.

Hirsch, R. M., J. R. Slack, and R. A. Smith. 1982. Techniques of trend analysis for monthly water quality data. *Water Resources Research* 18 (1): 107-121.

Hosking, J. R.M. 1990. L-moments: analysis and estimation of distributions using linear combinations of order statistics. *Journal of the Royal Statistical Society. Series B (Methodological)* 52:105-124.

Hosking, J. R. M., and J. R.Wallis. 1988. The effect of intersite dependence on regional flood frequency analysis. *Water Resources Research* 24 (4): 588-600.

Hosking, J. R. M., and J.R. Wallis. 2005. *Regional frequency analysis: an approach based on L-moments*. Cambridge: Cambridge University Press.

IPCC, 2013: *Climate Change 2013: The Physical Science Basis. Contribution of Working Group I to the Fifth Assessment Report of the Intergovernmental Panel on Climate Change*, T. F. Stocker, D. Qin, G. K. Plattner, M. Tignor, S. K. Allen, J. Boschung, A. Nauels, Y. Xia, V. Bex and P. M. Midgley, eds., Cambridge University Press, Cambridge, UK and New York, NY, 1535 pp.

IPCC, 2007: *Climate Change 2007: Impacts, Adaptation and Vulnerability. Contribution of Working Group II to the Fourth Assessment Report of the Intergovernmental Panel on Climate Change*, M. L. Parry, O. F. Canziani, J. P. Palutikof, P. J. van der Linden and C. E. Hanson, eds., Cambridge University Press, Cambridge, UK, 976pp.

Jarvis, C. S., and others. 1936. Floods in the United States, magnitude and frequency. *U.S. Geol. Survey Water-Supply Paper* 771, 497 p.

Jones, M. R., H. J. Fowler, C. G. Kilsby, and S. Blenkinsop. 2013. An assessment of changes in seasonal and annual extreme rainfall in the UK between 1961 and 2009. *International Journal of Climatology* 33 (5): 1178-1194.

Kendall, M. G. 1975. Rank correlation measures. London: Charles Griffin.

Kjeldsen, T. R., J. C. Smithers and R. E. Schulze. 2002. Regional flood frequency analysis in the KwaZulu-Natal province, South Africa, using the index-flood method. *Journal of Hydrology* 255 (1): 194-211.

Klein Tank, A. M. G., F. W. Zwiers, and X. Zhang. 2009. Guidelines on analysis of extremes in a changing climate in support of informed decisions for adaptation, climate data and monitoring WCDMP-No. 72, WMO-TD No. 1500, 56 pp.

Kundzewicz Z. W., and A. J. Robson AJ. 2000. Detecting Trend and Other Changes in Hydrological Data. World Climate Programme – Data and Monitoring. Geneva: World Meteorological Organisation.

Kwarteng, A. Y., A. S. Dorvlo, and G. T. Vijaya Kumar. 2009. Analysis of a 27-year rainfall data (1977–2003) in the Sultanate of Oman. *International Journal of Climatology* 29 (4): 605-617.

Lang, M., T. B. M. J. Ouarda, and B. Bobée. 1999. Towards operational guidelines for over-threshold modeling. *Journal of Hydrology* 225 (3): 103-117.

Mann, H. B. 1945. Nonparametric tests against trend. *Econometrica: Journal of the Econometric Society* no. 1:245-259.

Meteorological Service of Canada. 2014. Skill of the Deterministic Forecast System. http://weather.gc.ca/saisons/skill_e.html

Meteorological Service of Canada. 2013. *MANOBS: Manual of Surface Weather Observations*. 7th ed. 18th amd.

Ngongondo, C. S., C. Y. Xu, L. M. Tallaksen, B. Alemaw, and T. Chirwa. 2011. Regional frequency analysis of rainfall extremes in Southern Malawi using the index rainfall and L-moments approaches. *Stochastic Environmental Research and Risk Assessment* 25 (7): 939-955.

Pettitt, A. N. 1979. A non-parametric approach to the change-point problem. *Applied statistics* 28:126-135.

Pike, G. G., T. E. Redding, R. D. Moore, R. D. Winkler, and K. D. Bladon, eds. 2010. Compendium of forest hydrology and geomorphology in British Columbia. B.C. Min. For. Range, For. Sci. Prog., Victoria, B.C. and FORREX Forum for Research and Extension in Natural Resources, Kamloops, B.C. Land Management Handbook No. 66. http://www.for.gov.bc.ca/hfd/pubs/Docs/Lmh/Lmh66.htm

Redding, T. 2008. Changing climate, uncertain futures, and evolving practices. *FORREX Link* 10 (2): 15. http://www.forrex.org/sites/default/files/publications/articles/vol10_no2_art10.pdf

Reed, D. W., D. S. Faulkner, and E. J. Stewart. 1999. The FORGEX method of rainfall growth estimation II: Description. *Hydrology and Earth System Sciences* 3 (2): 197-203.

Smithers, J. C., and R. E. Schulze. 2001. A methodology for the estimation of short duration design storms in South Africa using a regional approach based on L-moments. *Journal of Hydrology* 241 (1): 42-52.

Spearman, C. 1904. The proof and measurement of association between two things. *The American Journal of Psychology* 15 (1): 72-101.

Stedinger, J. R., R. M. Vogel, E. Foufoula-Georgiu. 1993. Frequency analysis of extreme events. Chapt. 18 in *Handbook of Hydrology*. Ed. by David Maidment. New York: McGraw- Hill.

Stewart, E.J., D. W. Reed, D. S. Faulkner, N. S. Reynard. 1999. The FORGEX method of rainfall growth estimation I: Review of requirement. *Hydrology and Earth System Sciences* 3 (2): 187-195.

Tencer, B., A. Weaver, and F. Zwiers. 2014. Joint occurrence of daily temperature and precipitation extreme events over Canada. *Journal of Applied Meteorology and Climatology* 53 (9): 2148-2162.

Trefry, C. M., D. W. Watkins Jr., and D. L. Johnson. 2005. Regional rainfall frequency analysis for the state of Michigan. *Journal of Hydrologic Engineering* 10 (6): 437-449.

von Storch, H., and A. Navarra, eds. 1995. Analysis of Climate Variability: Applications of statistical techniques. New York: Springer.

Wallis, J. R., M. G. Schaefer, B. L. Barker, and G. H. Taylor. 2007. Regional precipitation-frequency analysis and spatial mapping for 24-hour and 2-hour durations for Washington State. *Hydrology & Earth System Sciences* 11 (1): 415-442.

Wilks, D. S. 2006. On "field significance" and the false discovery rate. *Journal of Applied Meteorology and Climatology* 45 (9): 1181-1189.

World Meteorological Organization (WMO). 2009. Management of Water Resources and Application of Hydrological Practices. *Guide to Hydrologic Processes* Volume II. WMO Publ. No. 168. 6th ed. Geneva.

World Meteorological Organization, (WMO). 2008. Guide to Meteorological Instruments and Methods of Observation. WMO Publ. No. 8. 8th ed. Geneva.

Yang, T., Q. Shao, Z. C. Hao, X. Chen, Z. Zhang, C. Y. Xu, and L. Sun. 2010. Regional frequency analysis and spatio-temporal pattern characterization of rainfall extremes in the Pearl River Basin, China. *Journal of Hydrology* 380 (3): 386-405.

Vogel, R. M., and N. M. Fennessey. 1993. L moment diagrams should replace product moment diagrams. *Water Resources Research* 29 (6): 1745-1752.

Yue, S., P. Pilon, and G. Cavadias. 2002. Power of the Mann–Kendall and Spearman's rho tests for detecting monotonic trends in hydrological series. *Journal of Hydrology* 59 (1): 254-271.

Zhang, X., W. D. Hogg, and É. Mekis. 2001. Spatial and temporal characteristics of heavy precipitation events over Canada. *Journal of Climate* 14 (9): 1923-1936.

CHAPTER 3 – CONCLUSION

The purpose of the study presented in Chapter 2 was to help fulfill the need for up-to-date Canadian extreme precipitation probability distributions (City of Toronto Climate Adaptation Steering Group, 2008; Redding, 2008). These distributions are required for designing extreme weather adaptation strategies for communities across Canada. Initially, my methodology was going to use an at-site frequency analysis approach; this is a common method among engineers and hydrologists for analyzing extreme events and was used by Carlyle-Moses (2007) to develop maximum daily rainfall depth frequency distributions for the southern interior of British Columbia. A review – in particular a paper by Fowler and Kilsby (2003) – showed that increasingly regional frequency analysis (RFA) is being used world-wide as it has the ability to develop more precise quantile estimates compared to at-site estimates. Based on this review, RFA was adopted for my research methodology. It was also decided early on in the research to collect both seasonal rainfall and snowfall data. It is uncommon for seasonal as opposed to annual extreme rainfall and/or snowfall data to be developed into quantile estimates. This could possibly be due to the increased amount of data collection or analysis that must take place for seasonal data. However, there are advantages within a management context to having seasonal quantile estimates.

SUMMARY AND KEY CONTRIBUTIONS OF RESEARCH FINDINGS

In this study, a RFA approach based on L-moments developed by Hosking and Wallis (2005) was used to successfully produce seasonal rainfall and snowfall regional quantile estimates for surface weather stations in the Thompson and Okanagan regions of British Columbia. Seasonal maxima daily rainfall and snowfall were extracted from historical meteorological records and examined for serial dependence before being included in the RFA. Three serial dependence tests were utilized: Pettitt's Test for Change, Spearman's rho test and Mann-Kendall's test. Since a small amount of serial dependence would have little effect on the quality of the quantile estimates, a Bonferroni correction and false discovery rate procedure were applied to reduce Type 1 errors. Eight data sets that had strong trends or step changes were rejected at this stage from further analysis.

The overall statistical lack of any temporal trends in the tested data sets contradicts the popular perception that the frequency and magnitude of extreme precipitation events are increasing. Caution must be taken not to generalize changes in extreme precipitation, particularly over large areas; in fact, this is supported by the Fifth Assessment Report of the Intergovernmental Panel on Climate Change that indicates increases in heavy precipitation will vary from region to region (IPCC, 2013). Topography modifies weather systems, and it is this interaction that can make accurately forecasting changes in meteorological conditions very difficult. While the serial dependence tests concluded that overall there appeared to be no change in the frequency of seasonal extreme rainfall or snowfall events for the Thompson and Okanagan regions, this could be the result of natural variability or inadequate data set lengths. It must also be noted that the testing for serial dependence may not have detected weak trends.

It would be interesting to conduct more sensitive serial dependence tests – particularly examining step changes – on the data sets utilized in this study. Most if not all of these surface weather stations had changes in weather reporting procedures and/or precipitation measuring equipment. It has been noted in other papers that these changes can lead to inhomogeneities in the precipitation data (Groisman and Easterling, 1994; Akinremi *et al.*, 1999). If metadata for each station were available, then any step changes detected could be further investigated and corroborated with the station's history.

Acceptably homogeneous regions were successfully developed for 179 out of 183 seasonal rainfall and snowfall station data sets. Each homogeneous region contained stations that had a similar precipitation climate and identical seasonal maximum daily precipitation frequency distributions aside from a scaling factor (the mean seasonal maximum daily rainfall or snowfall for this study). Seasonal groups of rainfall and snowfall data sets (e.g. fall rainfall) each had between 8 and 12 regions with each region having between 5 and 20 seasonal station rainfall or snowfall data sets. Overall, regions were geographically cohesive and reflected the local climate. A graphic depiction of regions showed a tendency of the regions to reflect the local valley systems. From a meteorological point of view, this is logical as local higher terrain can impact the magnitude and duration of precipitation from valley to valley. A few regions were geographically dispersed. Examination of the site characteristics within these regions showed that higher elevation stations throughout the

study area tended to group together for seasonal precipitation more sensitive to freezing levels, such as winter rainfall.

An unexpected result of using seasonal data was the number of data sets that contained a large amount of exact zero values. These types of data sets are usually not analyzed for maximum daily precipitation – though they are common for drought frequency analysis. It was determined that specific computer code would need to be written for constructing quantile estimates and associated uncertainties for these zero inflated data sets. Since this was outside the scope of the study, the affected data sets consisting of spring and fall maximum daily snowfall and winter maximum daily rainfall were set aside for future research.

Regional quantile estimates with associated RMSEs and 90% error bounds were developed for fall, spring and summer maximum daily rainfall data and winter maximum daily snowfall data. These regional quantile estimates are best displayed graphically as regional quantile functions. Site quantiles for any station within a region can easily be calculated from that region's quantile function as long as the station index-flood is available. The RMSEs and error bounds were generated using a simulation algorithm developed by Hosking and Wallis (2005). This simulation algorithm included a modification for spatial dependence because of the substantial correlation between sites in most of the regions. This correlation was not unexpected; some stations over time were relocated to adjacent sites in close proximity to the original site. Other stations were simply located close to each other. These stations had a high likelihood of having similar precipitation climates and being grouped together into regions.

A comparison of select regional and at-site estimations showed quantiles estimates for both methods were comparable. There appeared to be no pattern in the small differences between the regional and at-site estimates even for different return periods. However, almost all regional quantile estimations had significantly lower RMSEs by a factor of 1.5 to 5.0 when compared to at-site estimations. This difference was particularly noticeable for the higher return periods. This precision of the quantile estimates is highly desirable as it aids in the cost-benefit analysis associated with extreme weather adaptation planning.

LIMITATIONS AND FUTURE RESEARCH DIRECTION

Data for this study came from the Climate Information Branch Meteorological Service of Canada (MSC) 2000 Canadian Daily Climate Data CD (CDCD V1.02). These data could only be accessed as batch files via the computer's command line interpreter. There was no method to electronically extract the data from the files, so approximately 120,000 monthly rainfall and snowfall values had to be transcribed and manually entered into a data management program. A program to extract the required information would have made it easier to collect the data. There are data scrapping programs being developed for R$^{©}$, and they hold the promise of being able to extract specific information from large amounts of digitalized raw meteorological data with relative ease.

Metadata represent the history of a weather station and contains critical information about the station's frequency and type of observations, observing irregularities, and equipment descriptions, defects, changes and relocation. This information is recorded as a monthly summary on the 63-2325 surface weather record form and archived only in hard copy at MSC Downsview. Metadata are highly desirable as a quality control tool to ensure the maximum accuracy of the meteorological data for statistical analysis (Kundzewicz and Robson, 2000). Unfortunately due to massive downsizing within MSC Climate Services, it is unlikely that all the stored metadata will ever be digitalized and freely available to the public. Without this metadata, it is very difficult to determine if any trends or step changes detected in the data are caused by changes in the surface weather program or from another cause such as climate change. It would behove MSC to allow academic researchers free access to their stored metadata; unfortunately, this would still require a labour-extensive examination and extraction of the required information from the stored 63-2325 record forms.

Constructing homogeneous regions was a difficult and time-consuming stage of the regional frequency analysis. Even though a cluster analysis method was utilized, the initial regions still needed extensive manual refinement to achieve the final homogenous regions. Developing appropriate weights for site characteristics to reduce the amount of manual refinement needed in the cluster analysis would be desirable for future research. The cluster analysis process would also benefit from the inclusion of other site characteristics useful for

describing a precipitation climate such as proximity of water bodies, direction of prevailing wind, and slope and aspect data.

One of the main reasons for using a regional versus at-site frequency analysis was to develop more precise quantile estimates. While a comparison between select station quantile estimates and associated RMSEs showed that regionally generated quantiles estimates were more precise than at-site generated quantiles estimates, it did not prove whether these estimates were more accurate. It would be very interesting to develop a study that could verify and compare the accuracy of both regionally and at-site developed quantile estimates.

IMPLICATIONS FOR EXTREME WEATHER ADAPTATION PLANNING

There has recently been an increased public awareness of the impact and future risks of extreme weather events on Canadians; this has resulted in a concerted effort by different levels of government and stakeholders to develop adaptation policies that are designed to reduce communities' vulnerabilities to the effects of extreme weather and strengthen their capacity to cope with the impacts of these events. A key component to increasing the adaptive capacity of communities is to first have access to historical meteorological data and then have the expertise to collect, analyze and translate the data into meaningful policy (Henstra and McBean, 2009). This is particularly important for heavy precipitation events, as populations and assets are increasingly becoming located in low-lying areas prone to floods, and slopes susceptible to landslides (IPCC, 2007, City of Toronto Climate Adaptation Steering Group, 2008).

The quantile estimates developed in my study help provide this key information for the Thompson and Okanagan regional governments to use in extreme weather adaptation policy. The seasonal quantile estimates in particular are beneficial as these estimates allow adaptation planners to develop specific responses to seasonal extreme precipitation events. By using a RFA rather than an at-site analysis, the quantiles that this study developed were more precise; this precision is important in terms of costs and benefits for formulating adaptation strategies.

Extreme weather adaptation planning is inevitably linked to the general perception that extreme weather is increasing (Henstra and McBean, 2009). The serial dependence tests

done for my study showed an overall lack of statistical proof of any temporal trends in the seasonal extreme rainfall and snowfall data for the Thompson and Okanagan regions. This does not necessarily mean that the frequency and magnitude of seasonal extreme rainfall and snowfall for this area is not changing. An insufficient amount of data or natural variability that precludes any long-term temporal changes could also account for the lack of serial dependence. Regardless of any conclusion taken from these tests, the focus must remain that extreme precipitation events will still occur in the Thompson and Okanagan regions and these events can have a significant negative impact on the local communities. As previously mentioned, population and assets are expanding into higher-risk areas and communities must be pro-active to mitigate the effects of extreme weather events.

The results from this study support the recommendation that high quality Canadian meteorological data must be collected and developed into accessible and up-to-date extreme precipitation probability distributions to help focus national attention on weather related hazards and assist adaptation planning ((Henstra and McBean, 2009). With current technology, RFA is still a time-consuming endeavour; however, this approach is gaining popularity world-wide (e.g. Fowler and Kilsby, 2003; Trefry *et al*., 2005; Yang *et al*., 2010) and should be further investigated to determine if it can be used as a standard model for developing quantile estimates.

LITERATURE CITED

Akinremi, O. O., S. M. McGinn, and H. W. Cutforth. 1999. Precipitation Trends on the Canadian Prairies*. *Journal of Climate* 12 (10): 2996-3003.

Carlyle-Moses, D., 2007. Maximum Daily Rainfall Depth Frequency Analysis for the Southern Interior Forest Region of British Columbia. Kamloops, Canada.

City of Toronto Climate Adaptation Steering Group, Clean Air Patnership, Toronto Environment Office. 2008. "AHEAD OF THE STORM…Preparing Toronto for Climate Change". http://www.climateneeds.umd.edu/reports/Toronto%20City-Preparing%20Toronto %20for%20Climate%20Change

Fowler, H. J., and C.G. Kilsby. 2003. A regional frequency analysis of United Kingdom extreme rainfall from 1961 to 2000. *International Journal of Climatology* 23 (11): 1313-1334.

Henstra, D., and G. McBean. 2009. Climate Change Adaptation and Extreme Weather. *Adaptation to Climate Change Team*. http://act-adapt.org/.

Hosking, J. R. M., and J.R. Wallis. 2005. *Regional frequency analysis: an approach based on L-moments*. Cambridge: Cambridge University Press.

Groisman, P. Y., and D. R. Easterling. 1994. Variability and trends of total precipitation and snowfall over the United States and Canada. *Journal of Climate* 7 (1): 184-205.

IPCC, 2013: *Climate Change 2013: The Physical Science Basis. Contribution of Working Group I to the Fifth Assessment Report of the Intergovernmental Panel on Climate Change*, T. F. Stocker, D. Qin, G. K. Plattner, M. Tignor, S. K. Allen, J. Boschung, A. Nauels, Y. Xia, V. Bex and P. M. Midgley, eds., Cambridge University Press, Cambridge, UK and New York, NY, 1535 pp.

IPCC, 2007: *Climate Change 2007: Impacts, Adaptation and Vulnerability. Contribution of Working Group II to the Fourth Assessment Report of the Intergovernmental Panel on Climate Change*, M. L. Parry, O. F. Canziani, J. P. Palutikof, P. J. van der Linden and C. E. Hanson, eds., Cambridge University Press, Cambridge, UK, 976pp.

Kundzewicz Z. W., and A. J. Robson AJ. 2000. Detecting Trend and Other Changes in Hydrological Data. World Climate Programme – Data and Monitoring. Geneva: World Meteorological Organisation.

Redding, T. 2008. Changing climate, uncertain futures, and evolving practices. *FORREX Link* 10 (2): 15. http://www.forrex.org/sites/default/files/publications/articles/vol10_no2_art10.pdf

Trefry, C. M., D. W. Watkins Jr., and D. L. Johnson. 2005. Regional rainfall frequency analysis for the state of Michigan. *Journal of Hydrologic Engineering* 10 (6): 437-449.

Yang, T., Q. Shao, Z. C. Hao, X. Chen, Z. Zhang, C. Y. Xu, and L. Sun. 2010. Regional frequency analysis and spatio-temporal pattern characterization of rainfall extremes in the Pearl River Basin, China. *Journal of Hydrology* 380 (3): 386-405.

APPENDIX 1.A. Seasonal maximum daily rainfall and snowfall data sets with initial screening discordancy measure, $D_i > 3.00$ and associated L-moments ($t - t_4$).

Okanagan Region Rain

Season	Site Name	Site ID	t	t_3	t_4	D_i
Fall	Kelowna MWS0	11239R0	0.2505	0.4140	0.5438	4.72
	Merritt Craigmont Mines	1125075	0.4377	0.6297	0.4148	5.16
	Mt Kobau Observatory	1125223	0.4289	0.4096	0.5089	7.12
	Okanagan Falls 2S	1125G0A	0.3855	0.3241	-0.0059	3.48
	Rutland Mission Creek	1126915	0.1972	-0.1660	0.1853	6.50
	Summerland CDA EL	1127830	0.3448	0.0897	-0.0686	3.38
Spring	Osprey Lake	1125880	0.2900	0.4528	0.4621	3.54
	Princeton 8 NE	1126514	0.3196	0.5151	0.4476	3.72
	Summerland	1127798	0.1991	-0.1466	0.1540	4.40
Summer	Logan Lake	1124668	0.3491	0.1487	0.1322	3.92
	Rutland Mission Creek	1126915	0.3402	0.4810	0.2845	3.45
Winter	Hedley NP Mine	1123390	0.9268	0.8599	0.6895	5.99
	Peachland Brenda Mines	1126077	0.9113	0.8244	0.6038	4.54
	Penticton Sewage Plant	1126160	0.2727	0.4999	0.3779	3.77
	Similkameen Copper Mtn	1127358	0.6029	0.3293	-0.0154	3.07

Thompson Region Rain

Season	Site Name	Site ID	t	t_3	t_4	D_i
Fall	Clearwater	1161655	0.1891	-0.1253	0.2756	5.57
	Kamloops Mission Flats	1163840	0.3755	0.0974	-0.0137	4.03
	Monte Creek West	116NJRF	0.3040	-0.0179	-0.1552	4.33
Spring	Criss Creek	1162177	0.1862	0.0785	0.3477	3.01
	Horse Lake	1163595	0.1441	0.4311	0.2668	3.69
	Loon Lake	1164717	0.4152	0.4860	0.5266	5.58
	Ruth Lake	1166912	0.1726	-0.0434	0.2649	3.72
Summer	Barriere North	1160673	0.3429	0.4387	0.1515	4.16
	Buffalo Lake	1161104	0.2370	0.4754	0.1657	4.77
	Kamloops CDA	1163810	0.2953	0.3150	0.4088	3.05
	Monte Creek West	116NJRF	0.2087	0.5181	0.3537	4.59

Thompson Region Rain

Season	Site Name	Site ID	t	t_3	t_4	D_i
Winter	Chase	1161470	0.2622	-0.0227	0.2761	3.10
	Mt Lolo Kamloops	1165225	1.0000	1.0000	1.0000	12.38
	Richland	1166760	0.2368	-0.0303	0.2830	3.14

Okanagan Region Snow

Season	Site Name	Site ID	t	t_3	t_4	D_i
Fall	Douglas Lake	1122541	0.6264	0.6441	0.5953	7.87
	Logan Lake	1124668	0.4768	0.5718	0.4447	3.70
	Peachland Brenda Mines	1126077	0.2883	0.3324	0.2050	3.16
Spring	Kelowna MWS0	11239R0	0.3409	-0.2904	-0.0272	11.04
	Keremeos 2	1124112	0.8653	0.7686	0.5699	4.25
	Penticton Sewage Plant	1126160	0.5942	0.1755	-0.2039	3.66
Winter	Kelowna MWS0	11239R0	0.1571	-0.1494	0.0554	3.35
	Merritt Craigmont Mines	1125075	0.3616	0.2130	-0.0477	4.36

Thompson Region Snow

Season	Site Name	Site ID	t	t_3	t_4	D_i
Fall	Canoe Point	1161312	0.5534	0.4706	0.0971	3.09
	Criss Creek	1162177	0.2425	0.3215	0.2643	3.60
	Mt Lolo Kamloops	1165224	0.4780	0.4982	0.4238	4.35
	Spences Bridge	1167635	0.6455	0.2919	-0.1212	4.36
Spring	Kamloops Rayleigh	116L87J	0.8930	0.7942	0.5628	5.86
	Mt Lolo Kamloops	1165225	0.1606	0.0686	0.3961	3.67
	Silver Creek	1167337	0.2943	-0.0590	0.2261	4.02
	Spences Bridge Nicola	1167637	0.8302	0.6877	0.4057	3.16
Winter	Clearwater	1161655	0.0947	-0.2387	-0.0799	5.00
	Pinantan Lake	1166JFR	0.0989	0.2736	0.4635	4.99
	Richland	1166760	0.1994	0.1493	-0.1405	5.33

APPENDIX 1.B. Final fitted distribution parameters (location: ξ, scale: α, shape: κ, γ, δ) and regional quantile estimates, $\hat{q}(F)$ (dimensionless) corresponding to different non-exceedance probabilities (recurrence periods) for seasonal maximum daily rainfall and snowfall regions.

Fall Rainfall

Region	Distribution parameters			Non-exceedance probability, F(return period)						
	ξ	α	κ	0.10	0.50	0.80	0.90	0.95	0.98	0.99
				1 year	2 year	5 year	10 year	20 year	50 year	100 year
Princeton A	0.773	0.345	-0.077	0.494	0.901	1.321	1.620	1.923	2.341	2.675
Monte Creek	1.000	0.498	1.355	0.476	0.891	1.354	1.666	1.962	2.339	2.616
Kelowna A	0.928	0.413	-0.337	0.499	0.928	1.330	1.590	1.835	2.150	2.386
Penticton A	0.890	0.455	-0.460	0.449	0.890	1.357	1.684	2.008	2.444	2.783
Cache Creek 16 Mile	0.954	0.376	-0.243	0.540	0.954	1.305	1.519	1.714	1.955	2.129
Merritt	0.819	0.273	-0.348	0.399	0.819	1.305	1.720	2.221	3.076	3.920
Salmon Arm A	0.919	0.389	-0.399	0.529	0.919	1.308	1.569	1.823	2.156	2.410
Kamloops A	0.794	0.327	-0.052	0.527	0.915	1.303	1.574	1.843	2.206	2.490
Blue River A	0.822	0.284	-0.048	0.589	0.927	1.264	1.498	1.730	2.042	2.285

Spring Rainfall

Region	Parameters			Non-exceedance probability F(return period)						
	ξ	α	κ	0.10	0.50	0.80	0.90	0.95	0.98	0.99
				1 year	2 year	5 year	10 year	20 year	50 year	100 year
Princeton A	0.927	0.248	-0.172	0.473	0.927	1.316	1.591	1.880	2.304	2.668
Penticton A	0.899	0.262	-0.220	0.443	0.899	1.324	1.640	1.985	2.513	2.982

Spring Rainfall

Region	Parameters				Non-exceedance probability F(return period)						
	ξ	α	κ		0.10 1 year	0.50 2 year	0.80 5 year	0.90 10 year	0.95 20 year	0.98 50 year	0.99 100 year
Kelowna A	0.915	0.378	-0.428		0.542	0.915	1.299	1.561	1.819	2.161	2.425
Salmon Arm A	0.801	0.300	-0.079		0.559	0.913	1.279	1.541	1.807	2.174	2.468
Blue River A	0.837	0.298	0.032		0.585	0.946	1.274	1.485	1.682	1.931	2.113
Clearwater	0.913	0.207	-0.238		0.560	0.913	1.253	1.510	1.795	2.239	2.639
Cache Creek 16 Mile	0.718	0.430	-0.075		0.371	0.878	1.400	1.771	2.147	2.664	3.076
100 Mile House	0.922	0.223	-0.203		0.528	0.922	1.278	1.538	1.818	2.240	2.611
Kamloops	0.906	0.272	-0.200		0.422	0.906	1.341	1.658	1.998	2.510	2.957

Summer Rainfall

Region	Parameters					Non-exceedance probability F(return period)						
	ξ	α	κ	γ	δ	0.10 1 year	0.50 2 year	0.80 5 year	0.90 10 year	0.95 20 year	0.98 50 year	0.99 100 year
100 Mile House	0.804	0.279	-0.114			0.581	0.908	1.260	1.520	1.791	2.176	2.492
Penticton A	0.790	0.365	0.002			0.485	0.924	1.337	1.610	1.872	2.210	2.463
Vernon	1.000	0.405	0.932			0.538	0.938	1.310	1.542	1.754	2.016	2.205
Cache Creek 16 Mile	1.000	0.445	0.999			0.499	0.927	1.337	1.596	1.834	2.130	2.343
Princeton A	0.274	2.319	4.532	0.254	0.172	0.496	0.951	1.256	1.503	1.780	2.201	2.567
Kamloops A	0.791	0.357	-0.009			0.494	0.922	1.330	1.603	1.866	2.209	2.468
Clearwater	0.825	0.305	0.002			0.570	0.936	1.281	1.509	1.728	2.010	2.221

Summer Rainfall

| Region | Parameters | | | | | Non-exceedance probability F(return period) | | | | | | |
	ξ	α	κ	γ	δ	0.10 1 year	0.50 2 year	0.80 5 year	0.90 10 year	0.95 20 year	0.98 50 year	0.99 100 year
Salmon Arm A	0.932	0.199	-0.198			0.578	0.932	1.249	1.479	1.727	2.097	2.421
Kelowna A	0.809	0.309	-0.042			0.556	0.923	1.286	1.537	1.785	2.117	2.374

Winter Snowfall

| Region | Parameters | | | Non-exceedance probability F(return period) | | | | | | |
	ξ	α	κ	0.10 1 year	0.50 2 year	0.80 5 year	0.90 10 year	0.95 20 year	0.98 50 year	0.99 100 year
Princeton A	0.901	0.386	-0.485	0.532	0.901	1.302	1.587	1.873	2.261	2.566
Kamloops A	0.892	0.430	-0.476	0.479	0.892	1.337	1.652	1.966	2.391	2.724
Penticton A	0.888	0.247	-0.256	0.472	0.888	1.299	1.616	1.973	2.536	3.051
Kelowna A	0.921	0.213	-0.214	0.547	0.921	1.265	1.519	1.795	2.216	2.587
Cache Creek 16 Mile	0.879	0.231	-0.288	0.504	0.879	1.272	1.586	1.949	2.535	3.087
Vernon	0.902	0.220	-0.252	0.531	0.902	1.267	1.547	1.861	2.355	2.806
Salmon Arm A	0.922	0.209	-0.215	0.556	0.922	1.259	1.509	1.780	2.193	2.559
Knouff Lake	0.940	0.209	-0.169	0.557	0.940	1.266	1.496	1.737	2.089	2.390

APPENDIX 1.C. Site quantile estimates, $\hat{Q}(F)$ corresponding to different non-exceedance probabilities (recurrence periods) of select seasonal maximum daily rainfall (mm) / snowfall (cm) data sets. Root mean square error (RMSE) is associated with each site quantile estimate. Method: RFA = regional frequency analysis, AS = at-site analysis using same fitted distribution as RFA.

Fall Rainfall

	Non-exceedance probability F (return period)													
	0.10		0.50		0.80		0.90		0.95		0.98		0.99	
Station	1 year		2 year		5 year		10 year		20 year		50 year		100 year	
	$\hat{Q}(F)$	RMSE	$\hat{Q}(F)$	RMSE	$\hat{Q}(F)$	RMSE	$\hat{Q}(F)$	RMSE	$\hat{Q}(F)$	RMSE	$\hat{Q}(F)$	RMSE	$\hat{Q}(F)$	RMSE
Princeton A (RFA)	6.5	0.3	11.8	0.2	17.3	0.2	21.2	0.5	25.2	1.0	30.7	1.9	35.0	2.8
Princeton A (AS)	6.0	0.5	11.4	0.8	17.4	1.3	22.0	2.0	26.9	3.1	34.1	5.5	40.3	8.2
Westwold (RFA)	5.9	0.4	11.0	0.4	16.7	0.3	20.6	0.8	24.3	1.3	28.9	2.2	32.3	2.9
Westwold (AS)	6.2	0.4	11.2	0.7	16.5	0.9	20.0	1.3	23.3	1.8	29.4	2.5	30.4	3.1
Kelowna (RFA)	7.1	0.4	13.1	0.2	18.8	0.3	22.5	0.5	26.0	0.9	30.4	1.6	33.8	2.2
Kelowna (AS)	6.8	0.7	13.2	0.8	19.0	1.2	22.7	1.6	26.2	2.2	30.7	3.3	34.0	4.2
Penticton A (RFA)	5.5	0.2	10.9	0.2	16.7	0.2	20.7	0.4	24.6	0.7	30.0	1.3	34.2	1.8
Penticton A (AS)	5.4	0.5	10.5	0.8	16.6	1.3	21.2	2.0	26.0	3.1	32.7	5.1	38.2	7.1
Ashcroft 1912-1970 (RFA)	5.4	0.4	9.5	0.2	12.9	0.3	15.1	0.6	17.0	0.9	19.4	1.5	21.1	1.9
Ashcroft 1912-1970 (AS)	4.2	0.7	9.3	0.8	13.7	1.0	16.4	1.4	18.9	1.9	22.0	2.7	24.2	3.5
Merritt (RFA)	5.6	0.5	11.4	0.7	18.2	0.4	24.0	0.7	31.0	1.8	42.9	4.5	54.7	7.8
Merritt (AS)	5.2	0.8	11.1	1.2	18.2	2.2	24.4	3.9	32.0	6.9	45.1	14.2	58.3	23.9
Salmon Arm (RFA)	9.1	0.4	15.8	0.3	22.5	0.3	27.0	0.6	31.4	1.1	37.1	1.9	41.5	2.6
Salmon Arm (AS)	9.4	0.7	16.0	0.8	22.3	1.2	26.5	1.7	30.5	2.4	35.7	3.6	39.6	4.7

Fall Rainfall

| Station | Non-exceedance probability F (return period) | | | | | | | | | | | | | |
| | 0.10 1 year | | 0.50 2 year | | 0.80 5 year | | 0.90 10 year | | 0.95 20 year | | 0.98 50 year | | 0.99 100 year | |
	$\hat{Q}(F)$	RMSE	$\hat{Q}(F)$	RMSE	$\hat{Q}(F)$	RMSE	$\hat{Q}(F)$	RMSE	$\hat{Q}(F)$	RMSE	$\hat{Q}(F)$	RMSE	$\hat{Q}(F)$	RMSE
Kamloops (RFA)	5.7	0.3	10.0	0.2	14.2	0.2	17.1	0.3	20.1	0.7	24.0	1.3	27.1	1.9
Kamloops (AS)	5.7	0.3	9.2	0.5	13.7	1.0	17.5	1.6	21.9	2.7	29.0	5.4	35.6	8.7
Blue River A (RFA)	14.9	0.5	23.5	0.4	32.0	0.3	37.9	0.7	43.8	1.4	51.7	2.6	57.8	3.8
Blue River A (AS)	16.3	1.1	23.7	1.4	31.1	2.1	36.2	3.0	41.2	4.3	47.9	6.9	53.0	9.7

Spring Rainfall

| Station | Non-exceedance probability F (return period) | | | | | | | | | | | | | |
| | 0.10 1 year | | 0.50 2 year | | 0.80 5 year | | 0.90 10 year | | 0.95 20 year | | 0.98 50 year | | 0.99 100 year | |
	$\hat{Q}(F)$	RMSE	$\hat{Q}(F)$	RMSE	$\hat{Q}(F)$	RMSE	$\hat{Q}(F)$	RMSE	$\hat{Q}(F)$	RMSE	$\hat{Q}(F)$	RMSE	$\hat{Q}(F)$	RMSE
Princeton A (RFA)	5.3	0.4	10.4	0.2	14.8	0.2	17.9	0.5	21.1	0.9	25.9	1.7	30.0	2.5
Princeton A (AS)	4.7	0.6	9.9	0.7	15.0	1.1	18.8	1.7	23.1	2.8	29.8	5.1	35.8	7.8
Penticton A (RFA)	6.0	0.4	12.6	0.3	18.5	0.2	22.7	0.4	26.9	0.8	32.3	1.5	35.7	2.0
Penticton A (AS)	7.2	0.8	13.4	0.7	18.4	1.1	22.0	1.6	25.7	2.4	31.0	3.9	35.5	5.6
Kelowna (RFA)	6.1	0.3	10.3	0.2	14.6	0.2	17.6	0.4	20.5	0.7	24.3	1.2	27.3	1.7
Kelowna (AS)	5.6	0.4	9.9	0.7	14.9	1.1	18.5	1.6	22.2	2.4	27.4	3.9	31.5	5.4
Salmon Arm (RFA)	7.5	0.4	12.3	0.2	17.2	0.2	20.7	0.5	24.3	1.0	29.2	1.9	33.2	2.8
Salmon Arm (AS)	7.3	0.6	12.5	0.7	17.5	0.9	20.8	1.3	23.9	1.8	27.9	2.8	30.9	3.9
Blue River A (RFA)	10.3	0.4	16.6	0.2	22.4	0.2	26.1	0.5	29.5	0.8	33.9	1.4	37.1	1.9
Blue River A (AS)	11.7	0.9	17.0	0.9	21.4	1.2	24.2	1.5	26.6	2.0	29.6	3.0	31.7	4.0

Spring Rainfall

Station	Non-exceedance probability F (return period)													
	0.10 1 year		0.50 2 year		0.80 5 year		0.90 10 year		0.95 20 year		0.98 50 year		0.99 100 year	
	$\hat{Q}(F)$	RMSE	$\hat{Q}(F)$	RMSE	$\hat{Q}(F)$	RMSE	$\hat{Q}(F)$	RMSE	$\hat{Q}(F)$	RMSE	$\hat{Q}(F)$	RMSE	$\hat{Q}(F)$	RMSE
Vavenby (RFA)	6.6	0.3	10.8	0.3	14.9	0.2	17.9	0.5	21.3	1.0	26.6	2.0	31.3	3.2
Vavenby (AS)	6.8	0.4	10.9	0.5	14.8	0.7	17.7	1.2	21.0	2.0	26.2	3.6	30.8	5.4
Ashcroft 1912-1970 (RFA)	3.6	0.4	8.5	0.3	13.6	0.3	17.2	0.6	20.9	1.2	25.9	2.3	29.9	3.5
Ashcroft 1912-1970 (AS)	3.5	0.7	8.5	0.9	13.7	1.4	17.3	2.0	21.0	3.0	26.1	4.9	30.1	7.0
One Hundred Mile House (RFA)	7.5	0.6	13.1	0.4	18.2	0.3	21.9	0.7	25.8	1.4	31.8	2.7	37.1	4.2
One Hundred Mile House (AS)	6.4	1.0	12.0	1.3	18.3	2.4	23.5	3.9	29.7	6.6	40.0	12.9	49.9	21.0
Kamloops (RFA)	4.2	0.4	9.1	0.3	13.5	0.3	16.7	0.5	20.1	1.0	25.3	2.1	29.8	3.2
Kamloops (AS)	4.6	0.6	9.5	0.5	13.4	0.8	16.0	1.1	18.7	1.6	22.6	2.6	25.7	3.7

Summer Rainfall

Station	Non-exceedance probability F (return period)													
	0.10 1 year		0.50 2 year		0.80 5 year		0.90 10 year		0.95 20 year		0.98 50 year		0.99 100 year	
	$\hat{Q}(F)$	RMSE	$\hat{Q}(F)$	RMSE	$\hat{Q}(F)$	RMSE	$\hat{Q}(F)$	RMSE	$\hat{Q}(F)$	RMSE	$\hat{Q}(F)$	RMSE	$\hat{Q}(F)$	RMSE
One Hundred Mile House (RFA)	12.9	0.8	20.2	0.6	28.0	0.5	33.8	1.1	39.8	2.3	48.4	4.8	55.5	7.3
One Hundred Mile House (AS)	12.4	1.3	20.1	1.6	28.4	2.6	34.4	3.9	40.8	5.9	49.7	10.2	57.0	15.0
Penticton A (RFA)	8.7	0.4	16.6	0.2	24.1	0.3	29.0	0.5	33.7	1.0	39.8	1.7	44.3	2.4
Penticton A (AS)	9.5	0.9	17.3	0.9	23.7	1.2	27.5	1.5	30.8	1.9	34.8	2.8	37.5	3.7

Summer Rainfall

Station	Non-exceedance probability F (return period)													
	0.10 1 year		0.50 2 year		0.80 5 year		0.90 10 year		0.95 20 year		0.98 50 year		0.99 100 year	
	$\hat{Q}(F)$	RMSE	$\hat{Q}(F)$	RMSE	$\hat{Q}(F)$	RMSE	$\hat{Q}(F)$	RMSE	$\hat{Q}(F)$	RMSE	$\hat{Q}(F)$	RMSE	$\hat{Q}(F)$	RMSE
Vernon (RFA)	9.8	0.4	17.1	0.3	23.9	0.3	28.1	0.7	32.0	1.1	36.8	1.7	40.2	2.2
Vernon (AS)	10.1	0.9	17.0	1.2	23.7	1.7	28.1	2.3	32.1	3.1	37.1	4.3	40.7	5.3
Ashcroft 1912-1970 (RFA)	7.2	0.4	13.3	0.3	19.2	0.3	22.9	0.6	26.3	1.1	30.6	1.7	33.6	2.1
Ashcroft 1912-1970 (AS)	6.6	0.9	13.4	1.1	19.5	1.5	23.3	1.9	26.8	2.6	31.0	3.6	34.0	4.4
Princeton A (RFA)	8.5	0.6	16.2	0.4	21.5	0.5	25.7	0.7	30.4	1.4	37.6	2.8	43.8	4.7
Princeton A (AS)	8.7	0.9	16.3	0.8	21.8	1.3	25.9	1.9	30.1	2.7	35.9	4.3	40.4	6.2
Kamloops (RFA)	8.0	0.4	15.0	0.3	21.6	0.3	26.0	0.6	30.3	1.1	35.8	1.9	40.0	2.8
Kamloops (AS)	7.1	0.8	14.8	0.9	22.1	1.4	27.1	1.9	31.9	2.7	38.2	4.3	43.0	5.9
Vavenby (RFA)	10.3	0.4	16.9	0.2	23.2	0.3	27.3	0.6	31.3	1.0	36.4	1.8	40.2	2.5
Vavenby (AS)	10.6	0.6	16.8	0.7	22.9	1.1	27.1	1.5	31.3	2.2	36.8	3.5	41.0	4.9
Salmon Arm (RFA)	10.9	0.5	17.6	0.3	23.6	0.3	27.9	0.6	32.6	1.2	39.6	2.3	45.7	3.5
Salmon Arm (AS)	11.1	0.9	18.0	0.8	23.6	1.1	27.4	1.6	31.3	2.4	36.8	3.9	41.4	5.5
Kelowna (RFA)	8.5	0.3	14.1	0.2	19.6	0.2	23.4	0.4	27.2	0.8	32.3	1.6	36.2	2.3
Kelowna (AS)	7.5	0.6	13.4	0.9	20.0	1.4	24.9	2.2	30.2	3.4	37.8	6.0	44.2	8.9

Winter Snowfall

Station	Non-exceedance probability F (return period)													
	0.10 1 year		0.50 2 year		0.80 5 year		0.90 10 year		0.95 20 year		0.98 50 year		0.99 100 year	
	$\hat{Q}(F)$	RMSE	$\hat{Q}(F)$	RMSE	$\hat{Q}(F)$	RMSE	$\hat{Q}(F)$	RMSE	$\hat{Q}(F)$	RMSE	$\hat{Q}(F)$	RMSE	$\hat{Q}(F)$	RMSE
Princeton A (RFA)	10.3	0.5	17.4	0.4	25.2	0.3	30.7	0.7	36.2	1.4	43.8	2.6	49.7	3.6
Princeton A (AS)	9.3	0.8	17.1	1.1	25.8	1.8	32.1	2.8	38.5	4.1	47.4	6.6	54.4	9.0

Winter Snowfall

Station	Non-exceedance probability F (return period)													
	0.10 1 year		0.50 2 year		0.80 5 year		0.90 10 year		0.95 20 year		0.98 50 year		0.99 100 year	
	$\hat{Q}(F)$	RMSE	$\hat{Q}(F)$	RMSE	$\hat{Q}(F)$	RMSE	$\hat{Q}(F)$	RMSE	$\hat{Q}(F)$	RMSE	$\hat{Q}(F)$	RMSE	$\hat{Q}(F)$	RMSE
Kamloops (RFA)	5.5	0.3	10.2	0.2	15.2	0.2	18.8	0.4	22.4	0.8	27.3	1.5	31.1	2.1
Kamloops (AS)	5.2	0.5	10.2	0.6	15.4	1.0	19.0	1.4	22.6	2.1	27.4	3.2	31.1	4.3
Penticton A (RFA)	5.1	0.3	9.6	0.2	14.0	0.1	17.5	0.3	21.3	0.8	27.4	1.6	33.0	2.6
Penticton A (AS)	5.6	0.5	9.9	0.6	13.9	0.9	16.8	1.3	19.9	2.1	24.6	3.7	28.7	5.5
Kelowna (RFA)	7.8	0.4	13.1	0.3	17.9	0.2	21.5	0.5	25.5	0.9	31.4	1.9	36.7	2.9
Kelowna (AS)	7.0	0.7	12.6	0.8	18.2	1.3	22.6	2.1	27.6	3.5	35.5	6.6	42.8	10.2
One Hundred Mile House (RFA)	7.6	0.5	13.3	0.5	19.2	0.3	23.9	0.6	29.4	1.5	38.2	3.2	46.5	5.2
One Hundred Mile House (AS)	9.7	0.5	12.9	0.9	17.3	1.8	21.4	3.1	26.8	5.6	36.7	11.9	47.2	20.6
Vernon (RFA)	9.8	0.5	16.6	0.4	23.3	0.3	28.5	0.7	34.3	1.5	43.3	3.2	51.6	5.0
Vernon (AS)	8.0	1.2	16.2	1.4	24.3	2.2	30.5	3.6	37.5	5.8	48.5	10.5	58.5	16.2
Blue River A (RFA)	16.4	0.7	27.2	0.5	37.1	0.4	44.5	1.0	52.5	1.9	64.7	3.8	75.4	5.9
Blue River A (AS)	18.7	1.5	27.9	1.6	35.9	2.3	41.7	3.5	47.8	5.4	57.0	9.3	64.8	13.7
Knouff Lake (RFA)	9.3	0.7	15.7	0.5	21.1	0.5	24.9	0.9	28.9	1.7	34.8	3.2	39.8	4.9
Knouff Lake (AS)	9.4	1.1	15.1	1.2	20.8	2.0	25.1	3.1	29.9	5.0	37.6	9.3	44.5	14.5

APPENDIX 2 (attached CD)

2.A   Description of MSC climate archive data flags.

2.B   Summary of MSC Thompson and Okanagan regions' surface weather stations.

2.C   Serial dependence analyses for seasonal maximum daily rainfall and snowfall.

2.D   Discordancy Measures for seasonal maximum daily rainfall and snowfall.

2.E   Lists of seasonal maximum daily rainfall and snowfall homogeneous regions' site characteristics and index-flood values.

2.F   Table of seasonal maximum daily rainfall and snowfall distribution fits.

2.G   Lists of regional growth curves and bounds for fall, summer and spring maximum daily rainfall, and winter maximum daily snowfall.

2.H   Spearman's rho matrices for seasonal maximum daily rainfall and snowfall homogeneous regions.

2.I   Comparison of select regional and at-site estimations